TATIANA FERNANDES ARAÚJO ALMEIDA

AVALIAÇÃO DOS EFEITOS DO BISFENOL A EM QUERATINÓCITOS E CÉLULAS DE NEOPLASIA DE CAVIDADE ORAL

Faculdade de Odontologia
Universidade Federal de Minas Gerais
Belo Horizonte
2020

Tatiana Fernandes Araújo Almeida

AVALIAÇÃO DOS EFEITOS DO BISFENOL A EM QUERATINÓCITOS E CÉLULAS DE NEOPLASIA DE CAVIDADE ORAL

Tese apresentada ao Colegiado de Pós-Graduação em Odontologia da Faculdade de Odontologia da Universidade Federal de Minhas Gerais como requisito parcial à obtenção do grau de Doutor em Odontologia – área de concentração em Patologia Bucal.

Orientador: Prof.(a) Tarcília Aparecida da Silva
Coorientador: Prof.(a) Ivana Márcia Alves Diniz

Belo Horizonte
2020

Ficha Catalográfica

A447a Almeida, Tatiana Fernandes Araújo.
2020 Avaliação dos efeitos do bisfenol A em queratinócitos e T células de neoplasia de cavidade oral / Tatiana Fernandes Araújo Almeida. -- 2020.

109 f. : il.

Orientadora: Tarcília Aparecida da Silva.
Coorientadora: Ivana Márcia Alves Diniz.

Tese (Doutorado) -- Universidade Federal de Minas Gerais, Faculdade de Odontologia.

1. Bis-fenol A-glicidil metacrilato. 2. Neoplasias bucais. 3. Técnicas de cultura de células. 4. Linhagem celular. 5. Receptores de estradiol. I. Silva, Tarcília Aparecida da . II. Diniz, Ivana Márcia Alves. III. Universidade Federal de Minas Gerais. Faculdade de Odontologia. IV. Título.

BLACK - D047

Elaborada por: Miriam Cândida de Jesus - CRB: 6/2727.

Biblioteca Faculdade de Odontologia - FAO UFMG

UNIVERSIDADE FEDERAL DE MINAS GERAIS

PROGRAMA DE PÓS-GRADUAÇÃO EM ODONTOLOGIA

FOLHA DE APROVAÇÃO

Avaliação dos efeitos do bisfenol A em queratinócitos e células de neoplasia de cavidade oral

TATIANA FERNANDES ARAÚJO ALMEIDA

Tese submetida à Banca Examinadora designada pelo Colegiado do Programa de Pós-Graduação em Odontologia, como requisito para obtenção do grau de Doutor, área de concentração Patologia Bucal.

Aprovada em 18 de março de 2020, pela banca constituída pelos membros:

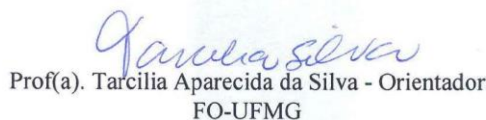

Prof(a). Tarcilia Aparecida da Silva - Orientador
FO-UFMG

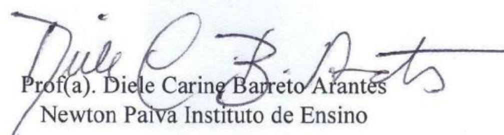

Prof(a). Diele Carine Barreto Arantes
Newton Paiva Instituto de Ensino

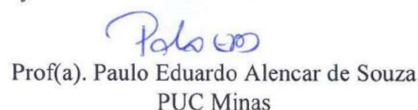

Prof(a). Paulo Eduardo Alencar de Souza
PUC Minas

Prof(a). Maria Cassia Ferreira de Aguiar
FO-UFMG

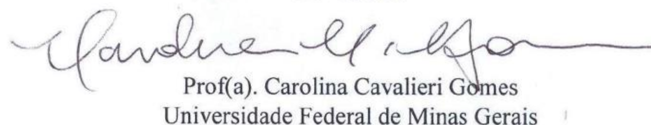

Prof(a). Carolina Cavalieri Gomes
Universidade Federal de Minas Gerais

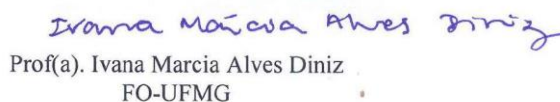

Prof(a). Ivana Marcia Alves Diniz
FO-UFMG

Belo Horizonte, 18 de março de 2020.

Dedico este trabalho ao meu marido, pais e irmãos que incentivam incondicionalmente o meu crescimento profissional e intelectual.

AGRADECIMENTO

À Deus, por instigar em mim a vontade de aprender sempre mais, por me conceder a possibilidade de ter ao meu lado pessoas incríveis e por me iluminar na conclusão de mais uma etapa.

Ao meu marido Nerimar, meu primeiro e único amor, que transformou os meus planos em nossos planos, quem me faz querer melhorar cada vez mais. Muito obrigada por me fazer sempre feliz com a certeza de que tudo dará certo.

Aos meus pais Tânia e Raimundo, meus maiores mestres. Muito obrigada pela imensurável dedicação, amor e carinho, por aceitarem minhas escolhas e caminharem sempre ao meu lado.

Aos meus irmãos Tássia e Rainan, meus grandes parceiros, muito obrigada por todo apoio e conforto.

Aos meus sogros Aparecida e Neri e ao meu cunhado Marcus Vinícius, pela torcida e confiança.

Agradeço em especial a minha orientadora, Profª. Tarcília Aparecida da Silva, primeiramente pela confiança ao me receber como orientanda, por todo o incentivo, dedicação, pelos ensinamentos transmitidos e por contribuir para o meu crescimento pessoal e profissional.

Muito obrigada à minha co-orientadora, Profª. Ivana Márcia Alves Diniz, pela amizade, dedicação e incentivos.

À Profª. Andréia Machado Leopoldino, por aceitar participar desta parceria, por toda atenção e por prontamente me receber no doutorado sanduíche na Faculdade de Ciências Farmacêuticas da USP em Ribeirão Preto (FCFRP/USP).

Aos colegas de laboratório da faculdade de odontologia da UFMG (FO/UFMG), Janine, Letícia, Amanda, Ana Laura, Sicília, Mariana, Isabella, Bianca e Lívia, muito obrigada pelo companheirismo, amizade e por compartilharem ideias e conhecimentos. Desejo muito sucesso a todas vocês.

Aos colegas de laboratório da FCFRP/USP Cristiane, Laís, Andrea, Tálita, Raquel, Lucas e Gabriel pela acolhida, ajuda e todo apoio durante o meu período longe de casa.

Aos professores Zenilda de Lourdes Cardeal; Helvécio Costa Menezes; Cleida Aparecida Oliveira; Soraia Macari; Gustavo Pompermaier Garlet e Fernanda

Rachid Campos Lobato de Almeida, pela parceria para o desenvolvimento deste trabalho.

Ao Prof. Armando da Silva Cunha Júnior, ao Prof. Rafael Escorsim Szawka e ao Prof. Fabio Daumas Nunes por nos atender prontamente no auxílio a este trabalho.

A todos os professores e técnicos das áreas de patologia bucal e estomatologia da FO/UFMG, que através de pequenos gestos e grandes ensinamentos fazem de mim uma pessoa melhor e mais sábia a cada momento.

Agradeço ao colegiado de pós graduação da FO/UFMG em nome da coordenadora Profª. Isabela Almeida Pordeus.

Finalmente agradeço à Coordenação de Pessoal de Nível Superior (CAPES), à Fundação de Amparo à Pesquisa do Estado de Minas Gerais (FAPEMIG) e ao Conselho Nacional de Desenvolvimento Científico e Tecnológico (CNPq) pelo apoio financeiro.

“Por vezes sentimos que aquilo que fazemos não é senão uma gota de água no mar. Mas o mar seria menor se lhe faltasse uma gota.”

Santa Teresa de Calcutá

RESUMO

O Bisfenol A (BPA) é um monômero utilizado na produção de garrafas plásticas, embalagens alimentícias, resinas odontológicas e vários outros materiais. Este monômero age como um desregulador do sistema endócrino e seus efeitos estão associados a cânceres em diferentes órgão e tecidos, como mama, próstata e tireóide. O BPA já foi detectado em fluidos humanos, incluindo saliva, mas os seus efeitos na mucosa bucal e em células orais neoplásicas não foram investigados. Os **objetivos** do presente trabalho foram 1) verificar os efeitos da exposição crônica ao BPA em glândulas salivares e mucosa bucal *in vivo* e 2) avaliar os efeitos do BPA *in vitro* em células de neoplasias bucais e queratinócitos; **Para atender ao objetivo 1**, camundongos machos e fêmeas receberam BPA (200 mg/mL) na água de beber durante 6 semanas. As mucosas orais (palato, língua e mucosa jugal) e as glândulas submandibulares foram avaliadas. **Para atender ao objetivo 2**, a resposta ao BPA foi examinada nas linhagens NOK-SI (queratinócito), HN12, HN13 (CCE de cavidade oral), UM HMC1 e UM HMC3a (neoplasia de glândula salivar). Os seguintes parâmetros foram avaliados: viabilidade, proliferação, invasão, angiogênese, produção de citocinas e fatores de crescimento e possíveis mecanismos de ação do BPA. **Resultados**. A exposição de camundongos ao BPA resultou em alterações microscópicas caracterizadas pelo aumento da espessura do epitélio da mucosa oral (palato, língua e mucosa jugal) e uma redução no número de ácinos das glândulas submandibulares. Foi observado também um acúmulo de BPA nos tecidos orais. *In vitro*, nas linhagens de CCE, o BPA aumentou a proliferação, invasão celular e os níveis da proteína vimentina, e ainda induziu a secreção de citocinas e fatores de crescimento, e a acetilação de histonas H3. Em queratinócitos orais, o BPA aumentou a proliferação celular e induziu a secreção de fatores de crescimento e a expressão de receptores de estrógeno (ER) α e β. Os efeitos do BPA foram revertidos na presença do antagonista puro do ER. Nas linhagens de neoplasias de glândula o BPA não alterou a proliferação e induziu a expressão de p63. Em conclusão, o BPA induz alterações morfológicas nos tecidos bucais e alterações moleculares nos queratinócitos e nas células de CCE de cavidade oral. Os mecanismos pelos quais o BPA induz estas alterações são dependentes da interação BPA-ER e da acetilação de histonas.

Palavras-chave: Bis-fenol A-glicidil metacrilato. Câncer de boca. Técnicas de cultura de células. Linhagem celular. Receptores de estradiol.

ABSTRACT

Evaluation of bisphenol A effects in keratinocytes and oral cavity neoplasia cells

Bisphenol A (BPA) is a monomer used to product plastic bottles, food packaging, inner coating of food cans, thermal papers, medical devices, dental resins and various other materials. Due to its chemical structure, this monomer acts as a deregulator of the endocrine system and its effects are associated with cancers in different organs and tissues such as breast, endometrium, ovary, prostate, testis and thyroid. BPA has been detected in several human fluids, including saliva, however its effects on the normal oral mucosa and neoplastic oral cells have not been investigated yet. Thus, the **objectives** of the present study were 1) to verify the effects of chronic exposure to BPA in salivary glands and oral mucosa in vivo and 2) to evaluate the effects of BPA in vitro on oral tumor cells and keratinocytes. **To meet objective 1**, male and female mice received BPA (200 mg / mL) in drinking water for 6 weeks. The oral mucosa (palate, tongue and buccal mucosa) and submandibular salivary glands were evaluated microscopically. **To meet objective 2**, the response to BPA was examined in immortalized cell lines NOK SI (keratinocyte); HN12, HN13 (OSCC), UM HMC1 and UM HMC3a (salivary gland tumor). The following parameters were evaluated: viability, proliferation, invasion, angiogenesis, cytokine and growth factors production. **Results**. Exposure of mice to BPA resulted in microscopic changes characterized by increased thickness of the oral mucosa epithelium (palate, tongue and buccal mucosa) and a reduction in the number of submandibular salivary glands acini. There was also an accumulation of BPA in the oral tissues. In vitro, in OSCC cells, BPA increased cell proliferation and invasion, vimentin expression, induced secretion of cytokines and growth factors, and induced histone H3 acetylation. In oral keratinocytes, BPA increased cell proliferation and induced secretion of growth factors and estrogen receptor (ER) α and β expression. The effects of BPA were reversed in the presence of the pure ER antagonist. In salivary gland tumor cell lines, BPA did not alter the proliferation and induced the expression of p63. BPA mechanism of action involves its interaction with ER, since the effects were reverted in the presence of pure receptor antagonist. In conclusion, BPA induces morphological changes in oral tissues and molecular changes in keratinocytes and OSCC cells. The mechanisms which BPA induces these changes are dependent to the BPA-ER interaction and histone acetylation.

Keywords: Bisphenol A-glycidyl methacrylate. Mouth neoplasms. Cell culture techniques. Cell line. Receptors, estradiol.

LISTA DE ABREVIATURAS E SIGLAS

ANVISA - Agência Nacional de Vigilância Sanitária
AR - Receptor de Andrógeno
BPA - Bisfenol A
CAM - Membrana Corioalantóica
CCE - Carcinoma de Células Escamosas
cDNA - Ácido Desoxirribonucleico Complementar
CEUA - Comissão de Ética no Uso de Animais
CT - Cycle Threshold
DNA - Ácido Desoxirribonucleico
DAB - Diaminobenzidina
DMEM - Dulbecco's Modified Eagle Medium
DMSO - Dimetilsulfóxido
EDC - Endocrine Disrupting Chemical
EFSA - European Food Safety Authority
EGF - Fator de Crescimento Epidérmico
ELISA - Enzyme-Linked Immunosorbent Assay
EMT - Transição Epitélio Mesênquima
ER - Receptor de Estrógeno
ERRγ - Receptor de Estrogênio Gama
FBS - Soro Fetal Bovino
FDA - Food and Drug Administration
GC / MS - Gas Chromatography–Mass Spectrometry
GCT - Granulated Convoluted Tubes
GPER - Receptor de Estrogênio Acoplado à Proteína G
HE - Hematoxilina e Eosina
HUVEC - Human Umbilical Vein Endothelial Cells
ICB – Instituto de Ciências Biológicas
IGF-1R - Receptor do fator de crescimento semelhante à insulina tipo 1
IL10 - Interleucina 10
INCA - Instituto Nacional do Câncer
MMP2 - Metaloproteinase 2
MMP9 - Metaloproteinase 9

mRNA - Ácido Ribonucleico Mensageiro
NIEHS - National Institute of Environmental Health Sciences
NOAEL - Nível Sem Efeito Adverso Observado Assumido
OSCC - Oral Squamous Cell Carcinoma
PBS – Solução Fosfato Salina
PIN - Neoplasia Intraepitelial Prostática
PVDF - Fluoreto de Polivinilideno
qRT PCR - Reação em Cadeia da Polimerase em Tempo Real
RNA - Ácido Ribonucleico
SDS-PAGE - Dodecilsulfato de Poliacrilamida de Sódio
SIM – Selected Ion Monitoring
TGF-β - Fator Transformador de Crescimento Beta
UFMG - Universidade Federal de Minas Gerais
VEGF - Fator de Crescimento Vascular

SUMÁRIO

1 INTRODUÇÃO 13

2 REVISÃO DA LITERATURA 16

2.1 Bisfenol A...16

2.1.1 O Bisfenol A e sua relação com tumores malignos...17

2.2 Carcinoma de células escamosas (CCE) de cavidade oral.........................19

2.2.1 Aspectos gerais e epidemiológicos...19

2.2.2 Características clínicas e histopatológicas do CCE de cavidade oral..............20

2.3 Neoplasias malignos de glândulas salivares...21

2.3.1 Aspectos gerais e epidemiológicos...21

2.3.2 Carcinoma mucoepidermóide..22

2.3.3 Carcinoma adenóide cístico...23

2.3.4 Adenocarcinoma...24

3 OBJETIVOS 25

3.1 Objetivo geral...25

3.2 Objetivos específicos...25

4 METODOLOGIA...26

4.1 Estudo in vivo – modelo experimental de exposição crônica ao BPA.......26

4.1.2 Análise microscópica...27

4.1.3 Histologia epitelial..27

4.1.4 Análise imunoistoquímica..27

4.1.5 Concentração de BPA nos tecidos de camundongos....................................28

4.1.5.1 Método de extração..28

4.1.5.2 Sistema cromatográfico..29

4.2 Estudo *in vitro*...29

4.2.1 Ensaio de viabilidade celular por resazurina...30

4.2.2 Ensaio clonogênico...30

4.2.3 Ensaio de imunocitoquímica..31

4.2.4 Tratamento com o antagonista do Receptor de Estrógeno.............................32

4.2.5 Análise de imunofluorescência..32

4.2.6 Extração de mRNA e qRT-PCR....32
4.2.7 Ensaio de Invasão Celular....33
4.2.8 ELISA - Enzyme-linked Immunosorbent Assay....34
4.2.9 Análise zimográfica de metaloproteinases da matriz....34
4.2.10 Western blotting....35
4.2.11 Ensaio de angiogênese....36
4.3 Avaliação de efeitos da pró-angiogênicos em modelo de membranas corioalantóicas....36

5 ARTIGO CIENTÍFICO....38

6 CONCLUSÕES....98

7 CONSIDERAÇÕES FINAIS....99

REFERÊNCIAS....101

1 INTRODUÇÃO

O Bisfenol A (BPA) é um plastificante de origem sintética disponível comercialmente desde 1957. É usado como material para a produção de resinas fenólicas, poliacrilatos e poliésteres e principalmente para a produção de resinas epóxi e plásticos de policarbonato (KANG; KONDO; KATAYAMA, 2006). Devido ao seu amplo espectro de utilização é um dos produtos químicos mais sintetizados mundialmente (MICHALOWICZ, 2014).

A exposição humana ao BPA é um fenômeno generalizado. A presença de BPA já foi relatada em diferentes fluidos humanos, como leite materno (ALTAMIRANO; MUNOZ-DE-TORO; LUQUE; GOMEZ *et al.*, 2015), líquido amniótico, fluidos placentários, urina (FERGUSON; MCELRATH; CANTONWINE; MUKHERJEE *et al.*, 2015) e saliva (KANUGA, 2014). A ingestão de alimentos contaminados é a principal forma de exposição ao BPA (KANG; KONDO; KATAYAMA, 2006), no entanto, o monômero também é detectado em águas residuais, água potável, ar e partículas de poeira (VANDENBERG; HAUSER; MARCUS; OLEA *et al.*, 2007).

O nível sem efeito adverso observado (NOAEL) do BPA, considerado pela *Food and Drug Administration* (FDA) é de 5 mg/kg de massa corporal por dia, já a recomendação da *European Food Safety Authority* (EFSA) para a exposição humana ao BPA é de 4 µg/kg de massa corporal por dia. No Brasil, a Agência Nacional de Vigilância Sanitária (ANVISA) segue as recomendações da FDA e proíbe a fabricação, importação e comercialização de mamadeiras com BPA no país desde 2011. É difícil estimar com precisão se esses níveis de BPA podem causar efeitos endócrinos ou tóxicos em humanos, bem como a dose precisa de exposição diária devido às inúmeras fontes de contaminação. No entanto, vários estudos relataram efeitos adversos endócrinos ou disruptivos do BPA em modelos animais em doses inferiores às recomendações internacionais (AYYANAN; LARIBI; SCHUEPBACH-MALLEPELL; SCHRICK *et al.*, 2011; NANJAPPA; SIMON; AKINGBEMI, 2012; NEWBOLD; JEFFERSON; PADILLA-BANKS, 2009).

O BPA atua como desregulador do sistema endócrino mimetizando as ligações hormonais aos receptores de estrógeno α e β (ERα e ERβ) (HWANG; PARK; KANG; YI *et al.*, 2013) receptor de andrógeno (AR) (WETHERILL; FISHER; STAUBACH; DANIELSEN *et al.*, 2005), receptor de estrógeno acoplado à proteína G (GPER) (PUPO; PISANO; LAPPANO; SANTOLLA *et al.*, 2012), , e receptor de estrógeno gama

(ERRγ) (ZHANG, K. S.; CHEN, H. Q.; CHEN, Y. S.; QIU, K. F. *et al.*, 2014). Estudos experimentais em animais e humanos demonstraram a capacidade deste plastificante de ativar as vias induzidas pelo estrógeno, por meio da ligação ao receptor e resultar em danos celulares (SHEELER; DUDLEY; KHAN, 2000). Neste contexto, o BPA está associado ao risco de desenvolver tumores em órgãos como em mama, endométrio, ovário, próstata, testículo e tireoide (MALLOZZI; LEONE; MANURITA; BELLATI *et al.*, 2017; MORIYAMA; TAGAMI; AKAMIZU; USUI *et al.*, 2002; SHAFEI; RAMZY; HEGAZY; HUSSENY *et al.*, 2018; TARAPORE; YING; OUYANG; BURKE *et al.*, 2014). Existe forte evidência científica de que a exposição ao BPA no início da vida de roedores os tornam mais susceptíveis ao desenvolvimento de câncer de mama ou próstata, sugerindo que o BPA também deva ser considerado como um carcinógeno para estes tipos de cânceres humanos (SEACHRIST; BONK; HO; PRINS *et al.*, 2016).

A exposição ao BPA pode alterar o reconhecimento e o reparo do dano oxidativo ao DNA por meio da estrutura da cromatina ou alteração da resposta e reparo do dano ao DNA. O mecanismo citotóxico do BPA pode ser gerado através da supressão da produção de energia mitocondrial e da disfunção mitocondrial e a indução do estresse oxidativo e da resposta inflamatória pelo BPA envolve a ativação das vias NF-κB, MAPKs e PI3K / AKT (GE; CHEN; LIU; ZHANG *et al.*, 2014; MURATA; KANG, 2018). A regulação positiva destas vias tem sido associada a uma maior proliferação celular, aumento da síntese de proteínas pró-sobrevivência e potencial metastático em células colorretais, da próstata, da mama e do ovário (EMFIETZOGLOU; SPYROU; MANTZOROS; DALAMAGA, 2019; GASSMAN, 2017).

A cavidade bucal representa o primeiro sítio de exposição ao BPA após ingestão. O monômero pode ser absorvido de maneira eficiente e rápida através da mucosa oral (GAYRARD; LACROIX; COLLET; VIGUIÉ *et al.*, 2013), contudo até o momento, não existem trabalhos que investigaram a relação do BPA com possíveis alterações na cavidade oral.

As neoplasias de glândulas salivares formam um grupo diverso de tumores que afetam as glândulas salivares maiores e menores. Representam cerca de 5% das neoplasias de cabeça e pescoço (BARNES; EVERSON; REICHART; SIDRANSKY, 2005). A raridade da doença dificulta o estudo da sua história natural, taxa de sobrevida e opções de tratamento. Estas lesões podem acometer indivíduos de diferentes idades, como crianças de 8 meses a idosos com idade superior a 80 anos (GAO; HAO; HUANG; MA *et al.*, 2016). O fato de as células neoplásicas em glândulas

salivares apresentarem receptores de estrógeno (KOLUDE; ADISA; ADEYEMI; LAWAL, 2013) juntamente à etiologia desconhecida para o desenvolvimento das neoplasias de glândulas salivares, bem como a similaridade morfológica com as neoplasias de mama (para os quais os efeitos do BPA já foram demonstrados) (LUZ; SILVA, 2016; PISAPIA; DEL POZZO; BARBA; CAPUTO *et al.*, 2012) pode indicar uma possível participação do BPA na patogênese destas neoplasias.

O CCE de cavidade oral é uma neoplasia maligna com origem no epitélio de revestimento oral (NEVILLE, 2009) e representa cerca de 90% das neoplasias de cabeça e pescoço (CURADO; HASHIBE, 2009). É mais frequente em pacientes adultos e idosos, com idade superior a 45 anos (CHATURVEDI; ENGELS; ANDERSON; GILLISON, 2008), mas alguns estudos têm demonstrado um aumento na incidência da doença em adultos jovens com idade entre 18 e 45 anos (CHATURVEDI; ENGELS; ANDERSON; GILLISON, 2008; GOLAS, 2007). Os queratinócitos da mucosa oral (VÄLIMAA; SAVOLAINEN; SOUKKA; SILVONIEMI *et al.*, 2004) e as células neoplásicas também apresentam receptores de estrógeno (CHANG; HSU; WU; HUANG *et al.*, 2014; COLELLA; IZZO; CARINCI; CAMPISI *et al.*, 2011) o que poderia indicar a responsividade ao BPA. Além disso o número de casos de CCE de cavidade oral aumenta a cada ano. Os dados do GLOBOCAN 2018 revelaram 354.864 mil novos casos de CCE na cavidade oral e em lábios em todo o mundo (BRAY; FERLAY; SOERJOMATARAM; SIEGEL *et al.*, 2018) e paralelamente a isso a produção e o consumo do BPA crescem diariamente.

Desta forma, os objetivos do presente trabalho foram verificar *in vivo* os efeitos da exposição ao BPA na cavidade oral e avaliar *in vitro* os efeitos do BPA em células neoplásicas e queratinócitos de boca.

2 REVISÃO DE LITERATURA

2.1 Bisfenol A

O BPA é um monômero plástico policarbonato (2,2-bis(4-hidroxifenil)propano), composto estruturalmente por dois anéis fenólicos (Figura 1), que foi desenvolvido pela primeira vez em 1890. Na década de 30, as propriedades biológicas de vários bisfenóis foram estudadas e, por conseguinte, detectada a atividade estrogênica do BPA (DODDS; LAWSON, 1938).

Devido à sua estabilidade, flexibilidade e resistência, este monômero é amplamente utilizado na indústria com a finalidade de fabricação de polímeros, como policarbonatos e resina epóxi, sendo utilizado na produção de garrafas plásticas, papéis térmicos, dispositivos médicos, painéis de carro, produtos eletroeletrônicos, revestimento interno de latas de alimentos, embalagens plásticas, resinas de uso odontológico e diversos outros materiais (GEENS; AERTS; BERTHOT; BOURGUIGNON *et al.*, 2012; GEENS; GOEYENS; COVACI, 2011). Em consequência do amplo espectro de utilização, o BPA é um dos produtos químicos mais sintetizados mundialmente, com mais de 3,8 milhões de toneladas produzidas anualmente (MICHALOWICZ, 2014).

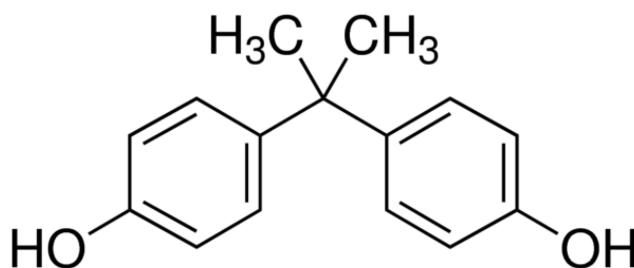

Figura 1 - Estrutura química do Bisfenol A.

Diversas condições possibilitam a transferência do BPA do plástico para o ambiente ou alimentos, dentre elas está elevação de temperatura que hidrolisam as ligações do polímero e liberam o BPA em maiores quantidades (COOPER; KENDIG; BELCHER, 2011). O ser humano pode se expor ao BPA por meio do ar, solo ou contato com a pele, mas a principal forma de exposição é a ingestão oral (KANG; KONDO; KATAYAMA, 2006). Após ingerido, o BPA é absorvido pelo trato

gastrointestinal e conjugado ao ácido glicurônico no fígado e então secretado na urina (DEKANT; VOLKEL, 2008). A presença do BPA já foi relatada em diferentes fluidos humanos, como leite materno (ALTAMIRANO; MUNOZ-DE-TORO; LUQUE; GOMEZ *et al.*, 2015), líquido amniótico, fluidos da placenta, urina (FERGUSON; MCELRATH; CANTONWINE; MUKHERJEE *et al.*, 2015) e saliva (KANUGA, 2014).

O BPA é capaz de se ligar a vários tipos de receptores, incluindo os receptores de estrógeno (ou estradiol) e andrógeno, sendo portanto também conhecido como xenoestrógeno ou desregulador endócrino (WETHERILL; FISHER; STAUBACH; DANIELSEN *et al.*, 2005; ZIV-GAL; CRAIG; WANG; FLAWS, 2013) e ao mimetizar o estradiol, o BPA é capaz de se ligar tanto aos ERα e ERβ (ROUTLEDGE; WHITE; PARKER; SUMPTER, 2000), bem como aos receptores de andrógeno (AR) (WETHERILL; FISHER; STAUBACH; DANIELSEN *et al.*, 2005), receptores de estrógenos acoplado à proteína G (GPER) (PUPO; PISANO; LAPPANO; SANTOLLA *et al.*, 2012) e receptores relacionados ao estrógeno γ (ERRγ) (ZHANG, K.-S.; CHEN, H.-Q.; CHEN, Y.-S.; QIU, K.-F. *et al.*, 2014). O termo desregulador endócrino conferido ao BPA, por sua vez refere-se aos efeitos desta substância interferindo no funcionamento normal do sistema endócrino (PISAPIA; DEL POZZO; BARBA; CAPUTO *et al.*, 2012).

O contato do BPA com humanos e animais pode induzir efeitos hepatotóxicos, mutagênicos e carcinogênicos em virtude do seu potencial oxidativo e mutagênico (HASSAN; ELOBEID; VIRK; OMER *et al.*, 2012; KERI; HO; HUNT; KNUDSEN *et al.*, 2007; RICHTER; BIRNBAUM; FARABOLLINI; NEWBOLD *et al.*, 2007; ZIV-GAL; CRAIG; WANG; FLAWS, 2013).

2.1.1 O BPA e sua relação com os tumores malignos

Por tratar-se de um desregulador endócrino extensamente utilizado em âmbito mundial, o potencial carcinogênico do BPA vem sendo amplamente estudado nos últimos anos (GAO; YANG; LI; FENG *et al.*, 2015; GIULIVO; LOPEZ DE ALDA; CAPRI; BARCELO, 2016). Seu potencial carcinogênico tem sido associado ao risco de câncer, principalmente sensíveis a hormônios, como câncer de mama, próstata, endométrio, ovário, testículos e tireoide. Mas também, já foi relacionado a tumores não sensíveis a hormônios, como câncer cervical, de pulmão e fígado (MURATA; KANG, 2018; SEACHRIST; BONK; HO; PRINS *et al.*, 2016).

Diversos efeitos deletérios têm sido associados ao BPA em diferentes sistemas, principalmente a sua interação com o sistema reprodutivo (FERGUSON; MCELRATH; CANTONWINE; MUKHERJEE *et al.*, 2015; TAKAHASHI; OISHI, 2000). Em roedores o BPA foi capaz de atravessar a placenta e estar presente no fluido folicular e amniótico (TAKAHASHI; OISHI, 2000; ZALKO; SOTO; DOLO; DORIO *et al.*, 2003). Em humanos a presença do BPA em plasma, fluido folicular, líquido amniótico e soro fetal de gestantes já foi confirmada (FERGUSON; MCELRATH; CANTONWINE; MUKHERJEE *et al.*, 2015; IKEZUKI; TSUTSUMI; TAKAI; KAMEI *et al.*, 2002).

O papel potencial do BPA na patogênese do câncer de mama vem sendo amplamente discutido. Estudos realizados *in vitro* têm demonstrado que a exposição ao BPA aumenta a proliferação de linhagens de células de câncer de mama (LUZ; SILVA, 2016; PISAPIA; DEL POZZO; BARBA; CAPUTO *et al.*, 2012). Em modelos murinos a exposição perinatal ao BPA levou a hiperplasias ductais, carcinoma ductal *in situ* e tumores malignos (ACEVEDO; DAVIS; SCHAEBERLE; SONNENSCHEIN *et al.*, 2013). Em mulheres após a menopausa, níveis séricos elevados de BPA foram relacionados com uma maior densidade do tecido da mama observada em mamografias, sendo este um fator de risco ao câncer de mama (SPRAGUE; TRENTHAM-DIETZ; HEDMAN; WANG *et al.*, 2013).

Em células epiteliais de mama não transformadas, o tratamento de longa duração com BPA, induziu um fenótipo invasivo, compactação da cromatina e outras alterações nucleares, bem como o aumento da transição epitélio mesênquima (EMT), diminuição das características epiteliais e uma maior migração celular (LUZ; SILVA, 2016). Em linhagens de células neoplásicas de mama, o BPA induziu a proliferação e EMT (LUZ; SILVA, 2016).

A exposição crônica ao BPA altera a expressão de proteínas nas glândulas mamárias de ratos, como vimentina; p-AKT e Fator transformador do crescimento-β (TGF-β) aumentando o risco de câncer de mama (BETANCOURT; MOBLEY; RUSSO; LAMARTINIERE, 2010).

O BPA também pode ser um dos fatores que contribuem para o desenvolvimento de câncer da próstata. Em murinos, a exposição crônica ao BPA induz a proliferação do lobo dorsolateral prostático, EMT (HUANG; ZHENG; PAN; WU *et al.*, 2018) e aumenta a incidência de neoplasia intraepitelial prostática (PIN) (PRINS; YE; BIRCH; HO *et al.*, 2011). Em homens com câncer de próstata foi observada uma

concentração mais elevada de BPA na urina, quando comparado a um grupo controle (TARAPORE; YING; OUYANG; BURKE *et al.*, 2014).

Alterações na tireoide também já foram relatadas em decorrência da exposição ao BPA, que inibe significativamente a ação dos hormônios produzidos por esta glândula, sugerindo que este composto pode afetar o desenvolvimento infantil devido a alteração na sinalização do hormônio da tireoide (MORIYAMA; TAGAMI; AKAMIZU; USUI *et al.*, 2002; ZOELLER, 2005).

Efeitos deletérios da exposição oral ao BPA como ressecamento da mucosa, espessamento do tecido epitelial e alterações morfológicas dos ácinos glandulares (menor quantidade e maior volume) foram evidenciados em ratos, comprovando a relação deste plastificante na desregulação da homeostase oral (FOLIA; BOUDALIA; MENETRIER; DECOCQ *et al.*, 2013).

Embora o CCE de cavidade oral não seja considerado uma neoplasia hormônio-sensível, suas células podem expressar receptores hormonais com significância prognóstica (GRSIC; OPACIC; SITIC; MILKOVIC PERISA *et al.*, 2016). Em CCE de cavidade oral a presença de receptores de estrógeno, principalmente do tipo α foi identificada (CHANG; HSU; WU; HUANG *et al.*, 2014; COLELLA; IZZO; CARINCI; CAMPISI *et al.*, 2011), indicando que as células neoplásicas poderiam ser responsivas ao BPA. Já em neoplasia de glândulas salivares a hormonioterapia já vem sendo investigada (MURASE; SUMIDA; ISHIKAWA; MURASE *et al.*, 2011).
O BPA pode estar ligado à etiopatogênese de câncer de boca e neoplasias de glândula salivar através de uma infinidade de mecanismos envolvendo alterações genéticas, epigenéticas, inflamatórias, imunológicas, metabólicas e hormonais (EMFIETZOGLOU; SPYROU; MANTZOROS; DALAMAGA, 2019), entretanto, nenhum estudo prévio verificou a possível associação do BPA com estes tumores.

2.2 Carcinoma de células escamosas (CCE) de cavidade oral

2.2.1 Aspectos gerais e epidemiológicos

A incidência e a mortalidade por câncer crescem rapidamente em todo o mundo. As razões são complexas, mas refletem tanto o envelhecimento quanto o crescimento da população, assim como mudanças na prevalência e distribuição dos fatores de risco para o câncer (BRAY; FERLAY; SOERJOMATARAM; SIEGEL *et al.*,

2018). O CCE de cavidade oral representa a sexta malignidade mais frequente (ALAM; BHATE; GANGADARAN; SAWANT *et al.*, 2012), e aproximadamente 3% de todos os novos casos de câncer diagnosticados (SCULLY; BAGAN, 2009).

Segundo dados do Instituto Nacional do Câncer (INCA) estima-se, para o Brasil, para cada ano do triênio 2020-2022, 11.180 novos casos de câncer da cavidade oral em homens, ocupando a quinta posição e 4.010 em mulheres, sendo o décimo terceiro mais frequente entre todos os cânceres. Tais valores correspondem a um risco estimado de 10,69 novos casos a cada 100 mil homens e 3,71 a cada 100 mil mulheres (BRASIL, 2019). Foram consideradas como câncer da cavidade oral as neoplasias com localização primária em lábios, cavidade oral, glândulas salivares e orofaringe.

Sem considerar os tumores de pele não melanoma, o câncer da cavidade oral em homens é o quinto mais frequente na região Sudeste (13,58/100 mil). Nordeste (7,65/100 mil) e Centro-Oeste (8,94/100 mil). Nas regiões Sul (13,32/100 mil) e Norte (3,80/100 mil) ocupa a sexta posição. Para as mulheres, é o décimo primeiro mais frequente na região nordeste (3,75/100 mil) e o décimo segundo na região Norte (1,69/100 mil). Nas regiões Centro-Oeste (2,90/100 mil) e Sudeste (4,12/100 mil) é o décimo terceiro mais frequente. Na região Sul (4,08/100 mil), ocupa a décima quarta posição (BRASIL, 2019).

2.2.2 Características clínicas e histopatológicas do CCE de cavidade oral

Clinicamente, a lesão mais comumente encontrada é de característica nodular constituída por úlcera persistente com endurecimento e infiltração periférica, podendo ou não estar associada a vegetações, manchas avermelhadas ou esbranquiçadas (MAJCHRZAK; SZYBIAK; WEGNER; PIENKOWSKI *et al.*, 2014). A localização predominante é a borda lateral de língua e o assoalho bucal (GERVÁSIO; DUTRA; TARTAGLIA; VASCONCELLOS *et al.*, 2001).

Microscopicamente, o CCE de cavidade oral é caracterizado pela presença de ilhas e cordões de células epiteliais com diferentes graus de pleomorfismo celular e nuclear invadindo o tecido conjuntivo (NEVILLE; DAMM; ALLEN; BOUQUOT, 2009). O tumor surge a partir de um epitélio de superfície displásico no qual a ceratinização de células epiteliais escamosas com a formação variável de pérolas de ceratina

associados a um padrão de crescimento invasivo são pré-requisitos para a gradação tumoral. Os tumores bem diferenciados apresentam queratinócitos volumosos semelhantes ao epitélio escamoso normal e produzem abundante ceratina, pouca atipia celular e escassa atividade mitótica. Os tumores moderadamente diferenciados geralmente apresentam menos ceratinização e marcante pleomorfismo nuclear com maior atividade mitótica e mitoses aberrantes, enquanto o CCE de cavidade oral pobremente diferenciado apresenta predominantemente células indiferenciadas com numerosas mitoses atípicas e ceratinização mínima ou ausente (EL-NAGGAR; CHAN; GRANDIS; TAKATA *et al.*, 2017).

2.3 Neoplasias malignas de glândulas salivares

2.3.1 Aspectos gerais e epidemiológicos

As glândulas salivares são órgãos exócrinos responsáveis pela produção e secreção de saliva. Compreendem os três pares de glândulas salivares maiores: parótida, submandibular e sublingual. As glândulas salivares menores encontram-se distribuídas em toda a cavidade bucal e orofaringe (ARANA; KATCHBURIAN, 2012; BARNES; EVERSON; REICHART; SIDRANSKY, 2005).

De acordo com o Instituto Nacional do Câncer (INCA), 95% dos nódulos palpáveis da glândula parótida são de origem tumoral. Com relação aos tumores de glândulas salivares menores, o palato é o sítio mais acometido. Os tumores malignos correspondem a 25% das neoplasias da parótida, 50% das neoplasias da glândula submandibular e 81% das neoplasias das glândulas salivares menores (INCA, 2002).

Os tumores malignos das glândulas salivares compreendem um grupo heterogêneo de tumores que envolvem 24 subtipos distintos de cânceres (Tabela 1) (BARNES; EVERSON; REICHART; SIDRANSKY, 2005). São tumores relativamente raros correspondendo a 20% dos tumores de glândulas salivares e 5% dos tumores malignos de cabeça e pescoço (BARNES; EVERSON; REICHART; SIDRANSKY, 2005).

Dentre as neoplasias malignas das glândulas salivares, o carcinoma mucoepidermóide, carcinoma adenoide cístico e adenocarcinoma são as mais prevalentes (GAO; HAO; HUANG; MA *et al.*, 2016; SPIRO, 1986), representando mais de 60% dos tumores malignos (GAO; HAO; HUANG; MA *et al.*, 2016).

Tabela 1 - Classificação histológica dos tumores malignos das glândulas salivares de acordo com a Organização Mundial de Saúde, 2017.

Classificação histológica dos tumores malignos das glândulas salivares	ICD-O
Carcinoma mucoepidermóide	8430/3
Carcinoma adenoide cístico	8200/3
Carcinoma de células acinares	8550/3
Adenocarcinoma polimorfo	8525/3
Carcinoma de células claras	8310/3
Adenocarcinoma de células basais	8147/3
Carcinoma intraductal	8500/3
Adenocarcinoma, sem especificação	8140/3
Carcinoma do ducto salivar	8500/3
Carcinoma mioepitelial	8982/3
Carcinoma epitelial mioepitelial	8562/3
Carcinoma ex adenoma pleomórfico	8941/3
Carcinoma secretor	8502/3
Carcinoma sebáceo	8410/3
Carcinossarcoma	8980/3
Carcinoma pobremente diferenciado	
Carcinoma indiferenciado	8020/3
Carcinoma neuroendócrino de células grandes	8013/3
Carcinoma neuroendócrino de células pequenas	8041/3
Carcinoma linfoepitelial	8082/3
Carcinoma de células escamosas	8070/3
Carcinoma oncocítico	8290/3
Sialoblastoma	8974/1

ICD-O - Código de Morfologia da Classificação Internacional de Doenças para Oncologia. 1 para tumores de comportamento incerto e 3 para tumores malignos. Adaptado de Barnes *et al.*, 2017.

2.3.2 Carcinoma mucoepidermóide

O carcinoma mucoepidermóide é o tumor maligno mais comum das glândulas salivares, representando cerca de 30-35% dos tumores malignos de glândulas salivares (GAO; HAO; HUANG; MA *et al.*, 2016; SPIRO, 1986). Esta neoplasia é observada principalmente em adultos maiores de 45 anos (SULTAN; RODRIGUEZ-GALINDO; AL-SHARABATI; GUZZO *et al.*, 2011). Com relação à localização anatômica, nas glândulas salivares maiores, esta neoplasia é mais frequente nas glândulas parótida e submandibular (GOODE; AUCLAIR; ELLIS, 1998). Em glândulas salivares menores, o sítio mais afetado é o palato (EVERSOLE, 1970; GAO; HAO; HUANG; MA *et al.*, 2016).

Os carcinomas mucoepidermóides são tumores epiteliais produtores de mucina, apresentam comportamento biológico que varia de baixo a alto grau e principalmente as lesões de comportamento local invasivo podem causar metástase (SIMPSON; SKALOVA; DI PALMA; LEIVO, 2014; TRIANTAFILLIDOU; DIMITRAKOPOULOS; IORDANIDIS; KOUFOGIANNIS, 2006). Usualmente o carcinoma mucoepidermóide apresenta-se clinicamente como um aumento de volume assintomático, em glândulas salivares maiores. Em glândulas salivares menores a neoplasia também se apresenta como aumento de volume indolor, algumas vezes flutuantes, com coloração azulada ou avermelhada (NEVILLE, 2009; TRIANTAFILLIDOU; DIMITRAKOPOULOS; IORDANIDIS; KOUFOGIANNIS, 2006).

Microscopicamente são observadas células mucosas, epidermóides e intermediárias. Tipicamente apresentam-se como uma infiltração lobular do tecido adjacente. Nos tumores de baixo grau são observadas numerosas células mucosas dispostas ao redor de estruturas microcísticas e poucas células epidermóides. Os carcinomas de alto grau são caracterizados pela predominante presença de células neoplásicas epidermóides em arranjo predominantemente sólido com poucos espaços císticos (BARNES; EVERSON; REICHART; SIDRANSKY, 2005; REGEZI; SCIUBBA; JORDAN, 2012).

2.3.3 Carcinoma adenóide cístico

O carcinoma adenoide cístico é o segundo tumor maligno mais frequente, representando 10-15% dos tumores das glândulas salivares (GAO; HAO; HUANG; MA *et al.*, 2016; SPIRO, 1986). Pode acometer glândulas salivares maiores e menores, e a sua origem sugerida é a partir de células do ducto intercalar (AKRISH; PELED; BEN-IZHAK; NAGLER, 2009).

Clinicamente, o carcinoma adenoide cístico, manifesta-se como um aumento de volume comumente sintomático. Em parótida podem ocasionar paralisia do nervo facial e em palato podem apresentar superfície lisa ou ulcerada (BARNES; EVERSON; REICHART; SIDRANSKY, 2005; JASO; MALHOTRA, 2011).

Os achados histopatológicos para o carcinoma adenoide cístico mostram uma mistura de células mioepiteliais e ductais em arranjos variados, que correspondem a três principais padrões: cribiforme, tubular e sólido (JASO; MALHOTRA, 2011). O padrão cribiforme é caracterizado pela presença de ilhas de

células basalóides contendo espaços cilíndricos que armazenam mucina. O padrão tubular é composto por ilhas menores de células com estrutura ductiforme inseridas em estroma hialinizado. A variante sólida mostra pouca formação de ductos, e apresentam ilhas maiores de células com núcleos pequenos e intensamente corados (JASO; MALHOTRA, 2011).

2.3.4 Adenocarcinoma

O adenocarcinoma sem outra especificação representa o terceiro mais frequente tumor maligno de glândula salivar (GAO; HAO; HUANG; MA *et al.*, 2016; SPIRO, 1986). O adenocarcinoma representa um grupo diverso de neoplasias, mais comuns em parótida, seguido das glândulas salivares menores e glândula submandibular (NEVILLE, 2009). Clinicamente podem manifestar-se como lesões nodulares ou tumorais, sintomáticas ou não. Também podem causar paralisia do nervo facial quando localizados em parótida. As características microscópicas são variadas, mas o padrão de malignidade é bem visualizado com a presença de células pleomórficas e crescimento infiltrativo. Variam de bem diferenciados a pobremente diferenciados (BARNES; EVERSON; REICHART; SIDRANSKY, 2005; MICHAL; SKALOVA; SIMPSON; RASLAN *et al.*, 1999).

O tratamento para os tumores malignos de glândulas salivares consiste na excisão cirúrgica, associada ou não à radioterapia (VANDER POORTEN; HUNT; BRADLEY; HAIGENTZ *et al.*, 2014).

3 OBJETIVOS

3.1 Objetivo geral

Avaliar os efeitos do BPA *in vitro* e *in vivo* e verificar a possível associação com neoplasias de cavidade oral.

3.2 Objetivos específicos

1) Verificar os efeitos da exposição ao BPA em glândulas salivares e mucosa bucal utilizando modelo experimental em camundongos;

2) Avaliar *in vitro* os efeitos do BPA em células neoplásicas derivadas de neoplasias bucais e queratinócitos;

4 METODOLOGIA

O presente estudo foi aprovado pelo Comitê de ética do Uso de Animais (CEUA) da Universidade Federal de Minas Gerais (UFMG) (protocolo 387/2016).

4.1 Estudo *in vivo* – modelo experimental de exposição crônica ao BPA

Fizeram parte deste experimento um total de 60 camundongos C57BL/6, 30 machos e 30 fêmeas com aproximadamente 4 semanas, realizados em momentos distintos em grupos experimentais separados. Os camundongos foram obtidos no Biotério Central da UFMG e mantidos no biotério do Laboratório de Imunofarmacologia do ICB-UFMG.

Os animais foram mantidos sob condições controladas de iluminação e temperatura, dieta padrão para camundongo, água ad libitum e pesados semanalmente. Machos e fêmeas foram divididos em três grupos: controle não tratado (n=10), controle de veículo (dimetilsulfoxido-DMSO) (n=10) e BPA (200 mg/L) (FOLIA; BOUDALIA; MENETRIER; DECOCQ *et al.*, 2013). Semanalmente, alíquotas de BPA (Sigma, St. Louis, MO, USA) foram diluídas na água de beber dos animais e acondicionadas em garrafas de vidro. A mesma concentração de DMSO foi diluída na água do grupo veículo. No grupo controle não tratado ficou disponível para os animais água filtrada, a mesma utilizada para a diluição do BPA e DMSO.

Os camundongos receberam as doses de BPA, veículo ou apenas água, durante seis semanas, com uma ingestão média diária de 5 mL. Após este período, os animais foram eutanasiados com sobredose de anestésico, que consistiu em solução de quetamina (100 mg/mL) e xilazina (20 mg/mL) nas doses de 180 mg/kg e 25 mg/kg, respectivamente, por via intraperitoneal, procedendo então à coleta dos seguintes órgãos/tecidos: glândulas salivares maiores, língua, mucosa jugal, palato, glândulas mamárias das fêmeas e próstata dos machos. Após a dissecação das peças, as mesmas foram identificadas para análise macroscópica.

4.1.2 Análise microscópica

Todos os tecidos coletados citados previamente, foram fixados em solução tamponada de formaldeído a 10%, e processados por técnicas de rotina. As línguas, glândula submandibular esquerda e próstatas foram cortadas no sentido ântero-posterior, e a metade incluída segundo a orientação da secção desejada. A mucosa bucal esquerda foi removida e incluída sem corte à macroscopia e realizado pelo mesmo operador. Cortes de 4 µm de espessura foram obtidos para coloração com hematoxilina e eosina (HE).

4.1.3 Histologia epitelial

Dez campos em cada lâmina foram fotografados em microscópio optico (20x) (Leica DM500) para análise morfométrica com o auxílio do softwere Image J (Scion Corporation, EUA).

Nas mucosas orais, a espessura do epitélio e do estrato córneo foi medida em milímetros em dez campos em cada lâmina. Na glândula salivar submandibular, foram quantificados ácinos e túbulos granulares convolutos (GCT) por milímetros quadrados.

Os lobos prostáticos foram separados (anterior, dorsolateral e ventral) e analisados quanto à presença de hiperplasia intraepitelial prostática (PIN) e proliferação. As glândulas mamárias das fêmeas foram avaliadas qualitativamente quanto à presença de hiperplasia glandular.

4.1.4 Análise imunoistoquímica

Cortes na espessura de 3µm foram obtidos da língua e palato e montados em lâminas com carga positiva. Para a reação de imunoistoquímica os cortes foram hidratados e tratados com peróxido de hidrogênio (3%). A recuperação antigênica foi realizada a 95ºC em banho-maria, com solução de ácido cítrico 10mM, pH 6,0 por 20 minutos. Posteriormente os cortes foram incubados com anticorpo primário durante 18 horas (Ki67 policlonal, diluição 1:250; *rabbit anti mouse ki67*, Abcam, Cambridge, MA).

Em seguida as lâminas foram incubadas com anticorpo secundário biotinilado LINK universal (LSAB + *System-HRP*, *Mouse/Rabbit*, Dako) por 30 minutos a 37°C, seguido de 3 lavagens em solução salina tamponada com fosfato (PBS). Após esta etapa, as lâminas foram incubadas com *Streptavidin-HRP* (LSAB) por mais 30 minutos, e reveladas com 20 µL do substrato DAB-*Cromogen* (3,3 diaminobenzidina, solução–DAB, Dako), diluído em 1 mL de substrato buffer (*Imidazole* HCL buffer, pH 7,5) por 3 a 5 minutos a 37°C, seguida por lavagens em água corrente. As lâminas foram contra coradas com hematoxilina e lavadas em água corrente. Os cortes foram desidratados em 3 banhos de álcool absoluto, diafanizados em 3 banhos de xilol e montados com lamínulas e resina sintética (*Entellan*, Merck).

Um controle negativo, do mesmo tecido analisado, foi incluído em cada série de reações imunoistoquímicas, com a omissão do anticorpo primário.

Os cortes foram analisadas por um microscópio óptico (Axioskop 40 Zeiss, Carl Zeiss, Göttingen, Alemanha) com ampliação original de 400x usando retículo de integração acoplada (Carl Zeiss - Axiostar 1122-100) e contado em 20 campos consecutivos. Os resultados foram expressos em número de células positivas por milímetro quadrado.

4.1.5 Concentração de BPA nos tecidos de camundongos

Uma hemissecção da língua e a glândula salivar direita dos camundongos machos (n = 5) foram usadas para analisar a presença de BPA. Os tecidos foram congelados imediatamente após a coleta com nitrogênio líquido e armazenados a -80ºC. Para a análise os tecidos foram preparados com β-glucuronidase (E. coli) para desconjugação enzimática (FREDERIKSEN; JORGENSEN; ANDERSSON, 2010).

A extração e derivatização do analito foram realizadas e, em seguida, analisadas com cromatografia gasosa-espectrometria de massa (GC / MS) (ThermoScientific) quanto à presença de BPA.

4.1.5.1 Método de extração

Para a extração dos analitos foi utilizado o método de microextração em fase líquida (LPME) com duas fases, conforme previamente descrito por Moreira *et al.*, (2015). O procedimento de extração consistiu de 35 µL de octanol introduzidos em

uma fibra oca de 10 cm, previamente embebida em octanol por 10 segundos. A fibra oca contendo o octanol foi colocada dentro do frasco contendo 9 mL água ultra pura e 100 µL de acetona UV/HPLC juntamente com o fragmento de tecido do animal e uma barra magnética para a agitação por um período de 70 min em temperatura ambiente. Posteriormente, a fibra foi retirada do frasco de extração e o octanol contendo os analitos foi transferido para um frasco de 2 mL, contendo um *insert*, com o auxílio de uma seringa. Uma alíquota de 13 µL do octanol foi transferida para outro frasco de 2 mL, contendo 25 µL de N,O-Bis(trimethylsilyl)trifluoroacetamide (BSTFA) e 5 µL de acetonitrila. O frasco foi agitado por 30 segundos e em seguida, deixado em repouso por 5 min. Após o término da derivatização a amostra foi analisada por cromatografia gasosa acoplada à espectometria de massas (CG / MS).

4.1.5.2 Sistema cromatográfico

As análises do BPA foram realizadas em um cromatográfo a gás (Agilent - 7890 C) acoplado a um espectrômetro de massas com analisador do tipo quadrupolo (Agilent - 5975 C). A análise cromatográfica foi realizada com injeção no modo *splitless* por 2 minutos utilizando uma coluna 5% fenilpolidimetilsiloxilana DB-5MS Agilent (60 m x 250 µm x 0,25 µm) com uma temperatura do injetor de 250ºC e fluxo de hélio de 1,5mL min^{-1}. Foi realizada uma rampa de temperatura com início em 120ºC, com aumento para 220ºC a 5ºC, mantida por 1 min, aumento para 270ºC a 3ºC e aumento para 320ºC a 20ºC, mantida por 5 min. O tempo total de corrida foi de 45,2 minutos. A análise foi realizada no modo SIM (*Selected Ion Monitoring*) com ionização por elétrons e energia de 70eV.

4.2 Estudo *in vitro*

Foram utilizadas linhagens de células imortalizadas, são elas: NOK SI (queratinócitos orais humanos, não tumoral), HN12 (CCE oral humano metastático), HN13 (CCE oral humano), UM HMC1, UM HMC3a (WARNER; ADAMS; BERNARDI; NOR *et al.*, 2013) (carcinoma mucoepidermóide de glândula salivar humano), HaCat (queratinócitos humanos, não tumorigênicos) e SCC25 (CCE oral humano).

As linhagens NOK SI, HN12 e HN13 foram cultivadas em Meio Essencial Modificado de Dulbecco (DMEM, Sigma-Aldrich, Munique, Alemanha) sem indicador

de pH, suplementado com soro fetal bovino a 2% (FBS, GIBCO, Carlsbad, CA, EUA) e penicilina-estreptomicina (Sigma-Aldrich).

As linhagens UM HMC1 e UM HMC3a foram cultivadas em DMEM, suplementado com penicilina-estreptomicina, L-glutamina (Invitrogen), 2% de SFB (Invitrogen), 20 ng / ml de fator de crescimento epidérmico (EGF; Sigma-Aldrich, St.Louis, MO, EUA), 400 ng / ml hidrocortisona (SigmaAldrich) e 5 µg / ml de insulina (Sigma-Aldrich).

As linhagens HaCat e SCC25 foram testadas quanto à proliferação (experimentos complementares) cultivadas em DMEM, suplementadas com 2% de SFB e penicilina-estreptomicina.

As células foram cultivadas à 37ºC em atmosfera úmida de ar com 5% CO_2. Os ensaios foram realizados antes das células atingirem 80% de confluência. O meio foi substituído a cada dois dias.

4.2.1 Ensaio de viabilidade celular por resazurina

O teste de viabilidade foi baseado no uso de resazurina (Alamar Blue) cuja redução está relacionada à viabilidade celular. As células, HN12, HN13, NOK SI, UM HMC1 e UM HMC3a, foram plaqueadas a uma densidade celular de $4x10^3$ células / por poço em microplacas de 96 poços e incubadas em atmosfera umidificada de 5% de CO_2 a 37 °C durante a noite. O BPA em diferentes concentrações (1 nM, 10 nM, 50 nM, 100 nM, 500 nM, 1 µM, 10 µM) foram testados e comparados ao grupo controle do veículo, DMSO 0,05%. As células foram avaliadas em 48, 72 e 120 horas. A resazurina foi preparada a 0,01 mg / mL em DMEM e adicionada às células. As placas foram mantidas protegidas da luz e incubadas em atmosfera umidificada a 95% contendo CO_2 a 5%, a 37 °C, por 4 horas. A absorbância foi medida no fluorímetro do leitor de microplacas multimodal Synergy 2 (Biotek, Winooski, VT, EUA) com excitação 530/25 nm e emissão 590/35 nm. Um poço contendo apenas meio sem indicador de pH e resazurina foi utilizado como controle branco da reação.

4.2.2 Ensaio clonogênico

NOK-SI (400 células), HN12 (400 células) e HN13 (200 células) foram cultivadas por 15, 12 e 8 dias, respectivamente, em microplacas de 12 poços em

triplicata. As células foram incubadas com veículo DMSO (0,05%) ou BPA a 10 nM, 500 nM e 1 µM. O meio de cultura foi substituído a cada dois dias. Posteriormente, as células foram fixadas em formalina tamponada neutra a 10% e coradas com solução cristal de violeta 1%. As colônias contendo pelo menos 50 células foram contadas como positivas usando o software Image J.

4.2.3 Ensaio de imunocitoquímica

As células HaCat e SCC25 foram plaqueadas a uma densidade celular de $1x10^3$ / por poço em microplacas de 96 poços e incubadas em uma atmosfera umidificada a 95% contendo CO_2 a 5% a 37 °C durante 18 horas. As células foram tratadas com BPA nas doses de 1 µM e 10 µM por sete dias. O meio de cultura foi substituído a cada dois dias. Um grupo controle (controle não tratado) e um veículo (DMSO 0,05%) também foram testados. Após sete dias de cultura, as células foram fixadas com metanol gelado. A análise imunocitoquímica foi realizada em duplicata em todos os grupos com a técnica do complexo estreptavidina-biotina-peroxidase. Os anticorpos primários utilizados e suas diluições foram: anti-Ki67 (clone MIB-1, 1: 400, Dako Cytomation, Glostrup, Dinamarca) e anti-Caspase-3 (clone 3CSPO3, 1:50, ThermoFisher, Rockford, EUA). A revelação foi realizada com DAB-Cromigen e a contra coloração com hematoxilina. A quantificação das células Ki67 e Caspase-3 positivas foi realizada por aquisição de imagem usando o leitor multimodo Cytation 5 Cell (Biotek) e contadas com os softwere Image J.

As linhagens UM HMC1 e UM HMC3a foram plaqueadas a uma densidade celular de $4x10^5$ / por poço em microplacas de 12 poços em uma lamínula de vidro e incubadas em uma atmosfera umidificada a 95% contendo CO_2 a 5% a 37 ° C por 18 horas. As células foram tratadas com BPA a 50nM e veículo (DMSO 0,05%) por 48 horas. A análise imunocitoquímica foi realizada como descrito anteriormente em triplicata. O anticorpo primário utilizado foi anti-p63 (MC0221, 1:50, Medaysis, Livermore, EUA). A quantificação de células positivas foi realizada por aquisição de imagem em microscópio óptico (Opticam O600R), ampliação original de 200x usando softwere integrado (OPTHD) e contada em 10 campos consecutivos com softwere Image J.

4.2.4 Tratamento com o antagonista do Receptor de Estrógeno

O ensaio clonogênico, como descrito anteriormente (4.2.2), também foi realizado com HN12 e NOK-SI na presença do antagonista puro do receptor de estrógeno (ER) ICI 182, 780 (Sigma-Aldrich) na concentração de 10^{-5} M. Os tratamentos foram renovados a cada dois dias, durante 12 dias em HN12 e 15 dias em NOK-SI.

4.2.5 Análise de imunofluorescência

A proliferação celular por ki67 foi avaliada nas linhagens celulares NOK SI, UM HMC1 e UM HMC3a através de imunofluorescência. As células foram plaqueadas a uma densidade celular de $4x10^3$ / por poço em quadruplicatas e cultivadas por 96 horas em microplacas de 96 poços. Foram analisados grupo veículo (DMSO 0,05%) e BPA, nas doses de 10 nM e 1 µM para NOK SI e 50 nM para UM HMC1 e UM HMC3a. As células foram fixadas com metanol gelado, incubadas com peróxido de hidrogênio a 0,3% e com o anticorpo primário anti-Ki67 (15580, 1: 200, Abcam, Cambridge, Inglaterra), 4 ° C, por 18 horas. O anticorpo secundário foi anti-*rabbit*-Alexa 488 (Invitrogen). O DAPI (4′,6-diamidino-2-phenylindole) foi utilizado para coloração nuclear de DNA (azul) (Sigma-Aldrich). As células foram analisadas com o Sistema de Análise de Alto Conteúdo de Campo Largo ImageXpress Micro XLS (Molecular Devices) com ampliação original de 200x e contadas em vinte campos por poço.

4.2.6 Extração de mRNA e qRT-PCR

Para a análise de PCR em tempo real (qRT-PCR), as células NOK-SI, HN12 e HN13 foram plaqueadas a uma densidade celular de $3x10^5$ / por poço e cultivadas por 72 horas em microplacas de 6 poços em duplicata, com os grupos controle não tratado, veículo (DMSO 0,05%) e BPA a 10 nM.

O mRNA total foi extraído usando Trizol. Em seguida foi realizada a purificação em coluna (RNeasy Mini Kit, Qiagen Inc., Valencia, CA, EUA). A integridade das amostras de mRNA foi verificada através da análise de 1 µL do mRNA total no Bioanalyzer 2100 (Agilent Technologies, Santa Clara, CA, EUA), de acordo

com as instruções do fabricante. Após a extração do mRNA, o DNA complementar (cDNA) foi sintetizado a partir de 2 mL de RNA usando uma reação de transcrição reversa de alta capacidade (Kit de transcrição reversa de cDNA) (Applied Biosystems).

Os genes alvo analisados foram ERα (NM_001122742.1; F: atgagagctgccaacctttg; R: ggttggtcagtaagcccatc), ERβ (NM_001291723; F: tggagtctggtcgtgtgaag; R: acttcaccattcccacttcg) e GAPDH (NM_001289745.2; F: gaaggtgaaggtcggagtcaac; R: cagagttaaaagcagccctggt). As sequências dos iniciadores genéticos foram projetadas com base nas sequências nucleotídicas nas bases de dados Ensemble e NCBI.

Os níveis de mRNA foram medidos por qRT-PCR usando o SYBR Green PCR Master Mix. O protocolo de termociclagem consistiu em uma etapa inicial de pré-incubação a 95°C por 10 minutos, 45 ciclos de amplificação começando em 95 °C por 10 s, 60 °C por 30 s e 72 °C por 1 s, seguidos por um único passo de resfriamento a 40 °C por 10 s. Os dados foram analisados usando o software Light Cycler® 480. A expressão de cada gene foi normalizada pela expressão média de GAPDH, e quantificada usando o método de *cycle threshold* (Ct) e cálculo de $2^{-\Delta\Delta Ct}$.

Também foi realizada uma reação de qRT-PCR array (GLOWACKI; YOSHIZAWA; JHUNJHUNWALA; VIEIRA *et al.*, 2013) em um instrumento Viia7 (LifeTechnologies, Carlsbad, CA) usando um painel personalizado contendo alvos para criação de perfil de expressão gênica. Os dados da qRT-PCR array foram analisados pelo software RT^2 PCR Data Analysis online software (SABiosciences, Frederick, MD) como descrito anteriormente (GARLET; HORWAT; RAY; GARLET *et al.*, 2012).

4.2.7 Ensaio de Invasão Celular

O ensaio de invasão celular foi realizado com a linhagem HN12, utilizando câmaras bipartidas. Para isso, insertos contendo uma membrana de policarbonato de poros de 8 µm (Boyden modificada) foram colocadas em microplacas de 24 poços, dividindo-as em compartimentos superior e inferior. Previamente ao plaqueamento das células, a fim de cobrir a superfície de cada membrana, foi aplicada uma camada de Matrigel (Cat. 35423C, BD Biosciences, Bedford, MA) diluída em DMEM sem SFB na proporção de 1: 1.

Em seguida, as células foram plaqueadas no compartimento superior do inserto, a uma densidade celular de $1x10^4$ / por poço e tratadas com BPA (10 nM e 1 µM) ou com o veículo (DMSO 0,05%). As células foram mantidas em cultura por 72 horas e, em seguida, fixadas em solução de formaldeído a 10% por 15 minutos. As células com capacidade de invasão, ficaram aderidas no fundo da membrana, então foram coradas com DAPI (Sigma-Aldrich).

Cinco campos de cada poço foram fotografados com a ampliação original de 200x usando um microscópio invertido (Zeiss Axiovert 40) e as imagens analisadas pelo AxioVision Rel. 4.8.2 software (Carl Zeiss). As células com capacidade de invasão foram então contadas usando o software Image J e os resultados expressos em média de células / campo.

4.2.8 ELISA - Enzyme-linked Immunosorbent Assay

Para avaliar a presença de interleucina 10 (IL-10), TGF-β, metaloproteinase da matriz 9 (MMP9), fator de crescimento epidermal (EGF) e fator de crescimento vascular (VEGF) as linhagens NOK SI, HN12 e HN13 foram plaqueadas em placas de cultivo de 24-poços na densidade de $2,5x10^3$ / por poço.

O tratamento das células foi realizado com BPA (Sigma-Aldrich) nas doses de 10 nM, 500 nM e 1 µM por 24, 48 e 72 horas. Um grupo veículo (DMSO 0,05%) também foi testado. O meio foi trocado a cada 2 dias e o BPA reposto. No último dia de cultura o sobrenadante foi coletado e utilizado para o ensaio de ELISA. As concentrações de citocinas foram medidas usando kits comercialmente disponíveis, de acordo com as instruções do fabricante (R & D Systems, Minneapolis, EUA) e os resultados expressos em picogramas de citocinas por mililitro (± Desvio Padrão – SD).

4.2.9 Análise zimográfica de metaloproteinases da matriz

As células HN12 e HN13 foram plaqueadas a uma densidade celular de $3x10^5$ / poço em uma microplaca de 6 poços em triplicata. O tratamento com BPA (10 nM, 500 nM e 1 µM) foi realizado durante 24 horas. Vinte microlitros do sobrenadante foram separados em gel de eletroforese dodecilsulfato de poliacrilamida de sódio (SDS-PAGE) 8% contendo 1 mg / mL de gelatina.

Após a corrida o gel foi lavado com Triton X-100 a 2% por 40 min e incubado em um tampão contendo Tris-HCl (10 mM), pH 8,0 e $CaCl_2$ (5 mM) por 16 horas a 37 °C. O gel foi então corado com azul de Coomassie a 0,25%. Após a remoção do corante, as bandas negativas que representam a atividade de MMP2 e MMP9 foram visualizadas.

A análise foi semiquantitativa utilizando densitometria no software Image J. A atividade de MMP2 e MMP9 foi apresentada como densidade óptica (DO) × mm^2, representando a área de varredura sob as curvas, que considera o brilho e a largura da zona de lise do substrato.

4.2.10 Western blotting

As células HN12, HN13, NOK SI, UM HMC1 e UM HMC3a foram plaqueadas a uma densidade de 3×10^6 células / poço em uma microplaca de 6 poços e tratadas com BPA (10 nM, 500 nM e 1 µM para HN12, HN13 e NOK SI; 50 nM para UM HMC1 e UM HMC3a) durante 2 e 24 horas.

Os extratos de proteína celular foram obtidos utilizando o Reagente *CelLytic Mammalian Cell Lysis/Extraction* (Sigma-Aldrich) com coquetéis de protease e inibidores de fosfatase (Sigma-Aldrich). A concentração de proteína foi determinada usando o ensaio de proteína de Bradford (Bio-Rad Laboratories, Hercules, CA, EUA). Trinta microgramas de proteína foram separados por eletroforese 10% SDS-PAGE e transferidos para uma membrana de fluoreto de polivinilideno (PVDF) (GE HealthCare, Freiburg, Alemanha). As membranas foram bloqueadas com leite sem gordura a 5% em solução salina tamponada com Tris contendo 10% de Tween 20.

Foram utilizados anticorpos contra ERK1 / 2 (M 5670; Sigma-Aldrich), fosfo-p44 / 42 MAPK ERK1 / 2 (pERK1 / 2 ; # 4377; Cell Signaling), AKT (# 9272 Cell Signaling), fosfo AKT (# 4056, Cell Signaling), NF-κB (# 8242, Cell Signaling), fosfo NF-κB (# 3033, Cell Signaling), STAT3 (# 9139, Cell Signaling), fosfo STAT3 (# 3270, Cell Signaling), c-myc (# 5605, Cell Signaling), histona H3 (# 4499, Cell Signaling), acetil-histona H3 (# 8173 , Cell Signaling), Vimentina (# 5741, Cell Signaling), β-actina (# 3700, Cell Signaling) e GAPDH (# 5174, Cell Signaling).

As reações foram desenvolvidas usando o sistema de transferência quimioluminescente ECL Western (GE Health-Care). A análise densitométrica foi

realizada usando o software Image J. β-actina e GAPDH foram utilizados como controle de carregamento.

4.2.11 Ensaio de angiogênese

Para avaliar os efeitos dos fatores liberados por células neoplásicas, HN12, tratadas com BPA, sobre a formação de estrutura semelhante a vasos sanguíneos, foi realizado ensaio *in vitro* de formação de tubos endoteliais (PYRIOCHOU; TSIGKOS; VASSILAKOPOULOS; COTTIN *et al.*, 2007). Para isso, os poços de uma placa de 96 poços foram revestidos por 45 µl de Matrigel (BD Biosciences, EUA) e mantidos por 1 h a 37 ºC. Após polimerização, 1 x 10^4 células endoteliais do cordão umbilical humano (HUVEC) foram semeadas na matriz e incubadas na presença de 75 µL do meio condicionado para 1 x 10^5 células HN12 previamente tratadas com BPA (10nM e 1 µM) e veículo (DMSO 0,05%).

Após 16 horas de tratamento, as estruturas tipo vaso foram incubadas com solução de cálcio AM e homodímero de etídio (2 µM de calceína AM e 4 µM de EthD-1) em PBS, de acordo com o protocolo de coloração do fabricante por 30 minutos. Os poços foram lavadas com PBS, para remoção do excesso de corante.

As análises foram realizadas através de imagens adquididas usando o Microscópio Estéreo Modular Leica para Imagem Fluorescente (MZ10 F) na ampliação original de 40x. O número de segmentos e o número de nós foram quantificados usando o *pluguin* analisador de angiogênese no software ImageJ.

4.3 Avaliação de efeitos da pró-angiogênicos em modelo de membranas corioalantóicas

A membrana corioalantóica (CAM) de ovos de galinha fertilizados foi utilizada para dois testes. No primeiro ensaio, o BPA foi testado diluído em PBS nas doses 10 nM e 1 µM. O controle negativo foi PBS 1x e o controle positivo foi VEGF (2000 pg / mL). No segundo ensaio, as amostras avaliadas foram o sobrenadante de 48 horas de células HN12 cultivadas com o tratamento de BPA (10 nM e 1 µM) ou veículo (DMSO 0,05%). Neste ensaio, o controle negativo foi DMEM e o controle positivo foi VEGF (2000 pg / mL). Oito ovos foram utilizados para cada amostra avaliada.

Utilizou-se o método descrito anteriormente por Nowak-Sliwinska et al. (NOWAK-SLIWINSKA; BALLINI; WAGNIERES; VAN DEN BERGH, 2010). Os ovos de galinha, três dias após a fertilização, foram colocados em uma incubadora. Um orifício de aproximadamente 1 cm de diâmetro foi aberto na casca do ovo para fornecer acesso à CAM. Cinco dias após a fertilização, as amostras foram aplicadas sobre a superfície da CAM e reaplicadas seis dias após a fertilização. Sete dias após a fertilização, as CAMs foram analisadas com um microscópio óptico (Leica, modelo DM4000B, Alemanha) acoplado a uma câmera digital CCD Leica modelo DFC 280 (Software Leica Application Suite V 3.3.0, Alemanha). As imagens obtidas foram utilizadas para quantificação das características capilares, utilizando o software Image J. Os vasos sanguíneos foram expressos como densidade óptica (DO) × mm^2.

5 ARTIGO CIENTÍFICO

Effects of bisphenol A on the oral mucosa and salivary glands: Is there a link between environmental pollutants and oral cancer?

Tatiana Fernandes Araujo Almeida[1]; Sicília Rezende Oliveira[1]; Janine Mayra da Silva[1]; Ana Laura Fernandes de Oliveira[1]; Zenilda de Lourdes Cardeal[2]; Helvécio Costa Menezes[2]; José Messias Gomes[2]; Gabriel Henrique Campolina-Silva[3]; Cleida Aparecida Oliveira[3]; Soraia Macari[4]; Gustavo Pompermaier Garlet[5]; Ivana Márcia Alves Diniz[4]; Andréia Machado Leopoldino[6+]; Tarcília Aparecida da Silva[1+]

[1] Department of Oral Surgery and Pathology, School of Dentistry, Universidade Federal de Minas Gerais, Belo Horizonte, Brazil.

[2] Department of Chemistry, Institute of Exact Sciences, Universidade Federal de Minas Gerais, Belo Horizonte, Brazil.

[3] Department of Morphology, Institute of Biological Sciences, Universidade Federal de Minas Gerais, Belo Horizonte, Brazil.

[4] Department of Restorative Dentistry, School of Dentistry, Universidade Federal de Minas Gerais, Belo Horizonte, Brazil.

[5] Department of Biological Sciences, School of Dentistry, Universidade de São Paulo, Bauru, Brazil.

[6] Department of Clinical Analyses, Toxicology and Food Sciences, School of Pharmaceutical Sciences of Ribeirão Preto, University of São Paulo, Ribeirão Preto, Brazil.

[+]Senior authors equally contributed to the study

*Corresponding author: Tarcília Aparecida da Silva. Department of Oral Surgery and Pathology, School of Dentistry, Universidade Federal de Minas Gerais. Av. Antônio Carlos, 6627, Pampulha, Belo Horizonte, MG, Brazil. CEP: 31.270-901. E-mail: silva.tarcilia@gmail.com.

ABSTRACT

Background: Bisphenol A (BPA) is a synthetic plastic monomer widely used in water pipes, food packages, and dental materials. BPA is an endocrine disruptor that is detectable in different human fluids, including saliva, and is associated with endocrine cancers.

Objectives: To evaluate the impact of chronic *in vivo* exposure to BPA and its *in vitro* effects on neoplastic and non-neoplastic oral cells.

Methods: We evaluated the oral mucosa and salivary glands of mice chronically exposed to BPA (200 mg/L). The response of keratinocytes (NOK SI) and Head and Neck (HN) Squamous Cell Carcinoma (SCC), HN12 and HN13 cell lines to BPA was examined.

Results: *In vivo*, BPA accumulates in oral tissues and causes increases in epithelial proliferative activity and atrophic changes in the salivary glands. *In vitro*, BPA targets intracellular signals through estrogen receptor binding. BPA disrupts the function of keratinocytes by altering pro-survival and proliferative pathways and the secretion of cytokines and growth factors. In tumor cells, BPA induces proliferative, invasive, pro-angiogenic, and epigenetic events.

Discussion: Our data highlight the harmful effects of BPA in oral tissues. BPA may be a modifier of oral cancer cell behavior by prompting a functional shift to a more aggressive phenotype.

Keywords: Bisphenol A-Glycidyl Methacrylate. Mouth Neoplasms. Cell Culture Techniques. Histone Acetylation. Receptors, Estradiol

INTRODUCTION

Bisphenol A (BPA) is a synthetic plastic monomer widely used in polycarbonates and epoxy resins found in plastic bottles, food packages, the inner coat of food cans, thermal papers, dental resins, and other materials. This compound has recently emerged as a new environmental pollutant[1]. Exposure to BPA is considered a wide phenomenon once it can occur through air, soil, or skin contact, although oral ingestion is the primary exposure route[2]. BPA has been detected in different human fluids such as breast milk[3], amniotic fluid, placental fluids, urine[4], and saliva[5].

BPA is an endocrine-disrupting chemical that exerts its effects on tissues by mimicking endogenous hormones via binding to estrogen receptors α and β (ERα and ERβ)[6], androgen receptor (AR)[7], G protein-coupled estrogen receptor (GPER)[8], insulin-like growth factor-1 receptor (IGF-1R)[6], and estrogen-related receptor gamma (ERRγ)[9], thereby inducing cell proliferation, migration, invasion, and epithelial-mesenchymal transition (EMT)[10, 11]. BPA has been implicated in the development of breast, endometrial, ovary, prostate, testis, and thyroid cancer[12, 13].

In vivo studies using different animal species have confirmed the carcinogenic potential of BPA. In rats, perinatal exposure to this monomer induced mammary ductal hyperplasia and *in situ* ductal carcinoma[14]. In rhesus monkeys, BPA altered the female mammary glands' development by increasing the density of mammary buds[15]. In mice, contribute to brain and behavioural change, even at doses below what regulatory agencies regard as "safe" for humans[16]. Also induced the formation of ovarian cysts and cystadenomas[17] and increased the incidence of prostatic intraepithelial neoplasia (PIN)[18] and hepatic preneoplastic and neoplastic lesions[19]. In line with these findings, high serum levels of BPA were correlated with

augmented mammographic breast density – a marker of breast cancer risk in postmenopausal women[20]. In men, increased urinary concentrations of BPA were found in prostate cancer patients[12].

Recent studies reported a high concentration of BPA in the oral cavity and oropharyngeal space[5]. These findings have alerted to its possible correlation with the pathogenesis of oral and oropharyngeal cancers[11], mainly because the oral cavity is the first site of contact with BPA and the use of some dental materials has been shown to increase the salivary concentration of BPA by more than 20 times[5]. The incidence of oral cancer is growing worldwide[21], just as BPA's production rate and use are expanding[22]. However, there is little information about the disturbance of oral tissue homeostasis by chronic BPA exposure[23]. Herein, we investigate whether BPA disturbs the epithelium and salivary glands using *in vivo* and *in vitro* approaches, and the potential mechanisms involved.

METHODS

Ethical standards

All animal procedures were performed in accordance with relevant guidelines and regulations. All experimental protocols were approved by a named institutional/licencing committee, The Animal Care and Use Committee of the Universidade Federal de Minas Gerais (UFMG) (Protocol number 387/2016).

Recommendations for experimental design were adopted according to the Animals in Research: Reporting in Vivo Experiments (the ARRIVE guidelines 2.0).

Experimental model of BPA chronic exposure

In order to evaluate the effects of chronic *in vivo* exposure to BPA a total of sixty four-six weeks male (n=30) and female (n=30) C57BL/6 mice, weighting 15-25g, were used to the in vivo experiments. The animals were kept at the same rack under the controlled cycle of 12 hours light/dark and temperature conditions. Animals received a standard diet and water ad libitum and were weighed weekly. The animals would be excluded if it died prematurely.

Male and female mice were randomized using a computer based random order generator and divided into three groups: untreated (n=10, control), vehicle (dimethyl sulfoxide-DMSO) (n=10), and BPA (200 mg / L) (n=10) (Sigma-Aldrich)[23]. The sample size calculation was performed according to the difference between two averages using the standard deviation obtained in the literature[23]. The power of the experiment was 80%. The treatment was diluted, always in the morning, in drinking water and filled into glass bottles, with an average daily consumption of 6 mL and weekly replenishment.

After six weeks of BPA treatment, the animals were euthanized and the oral mucosa (buccal mucosa, tongue, palate), left submandibular salivary gland, female mammary gland and male prostate organs were collected and immediately fixed in formalin 10%. After 48 hours, tissues were processed, embedded in paraffin, sectioned at 4 μm, and prepared for routine hematoxylin and eosin (HE) staining, by an operator blinded to the groups. During all data analysis the operator was blinded. Ten fields on each slide were photographed under light microscopy (Leica DM500; magnification 20x) for morphometric analysis by using the Image J Software (Scion Corporation, U.S.A.). In the oral mucosa, the thickness of the epithelium and stratum corneum was measured in millimeters. In the submandibular salivary gland, acini and granulated convoluted tubules (GCT) were quantified per squared millimeters (n=10 per group). The prostatic lobes were separated (anterior, dorsolateral and ventral) and analyzed for the presence of intraepithelial hyperplasia and proliferation. Female mammary glands were evaluated qualitatively for the presence of glandular hyperplasia (n=10 per group).

Tongue and palate sections were analyzed by immunohistochemistry (n=5). The tissues slides were deparaffinized, rehydrated and rinsed in distilled water, followed by incubation with 0.3% hydrogen peroxide and Avidin/Biotin blocking system (Dako, Carpinteria, CA, USA). Sections were then incubated with a monoclonal mouse anti-human Ki-67 (15580 Abcam, 1:2000), 4 °C, overnight. Negative controls were obtained by the omission of the primary antibody, which was replaced by 1% phosphate buffered solution- bovine serum albumin (PBS-BSA). The cells were analyzed by a light microscope (Axioskop 40 Zeiss, Carl Zeiss, Gottingen, Germany) at 400x original magnification using coupled integration lattice (Carl Zeiss - Axiostar

1122-100). and counted in 20 consecutive fields. The results were expressed as the number of positive cells per squared millimeters.

BPA concentration in mice tissues

A hemi section of the tongue and the right salivary gland of the male mice (n=5) were used to analyze for the presence of BPA. The tissues were immediately frozen after collection with liquid nitrogen and stored at -80ºC. The tissues were weighted and placed into a flask containing 9 mL of ultra-pure water and 100 µL of acetone UV/HPLC. Analyte extraction and concentration were performed using hollow fiber liquid-phase microextraction technique (HF-LPME). A hollow fiber contains 15.0 µL of solvent mixture octanol and ethyl octanoate (1:1) was immersed in the flask and the system was kept under agitating for 55 min. After extraction, 8.0 µL of the solvent mixture contain the analyte was transferred to a vial in which 15.4 µL of N,O-Bis(trimethylsilyl)trifluoroacetamide containing 1% TMCS and 3.0 µL of acetonitrile were added and stirred for 30 seconds.

Afterward, the analysis was performed using a gas chromatography system coupled with a mass spectrometry equipped with an ion trap mass analyzer (Thermo Scientific Finigan Trace DSQ single quadrupole GC / MS). An HP-5MS Agilent column (30 m x 250 µm x 0.25 µm) was used with helium as a carrier gas at a flow rate of 1.3 mL/min. The temperature of the injector was 250 ˚C and the injection performed at splitless mode for 1.2 min. The column temperature program was set as follows: initially, 120 ˚C, increasing to 190 ˚C at a rate of 5 ˚C/min, followed by a heating to 210 ˚C at a rate of 15 ˚C/min. The temperature was then increased to 230 ˚C at a rate of 5 ˚C/min and maintained for 2 min, further increased to 250 ˚C at a rate of 30 ˚C/min and finally maintained for 5 min. The total run time was 27 min. The transfer line

temperature was set at 250 ˚C and the analysis was conducted in a segment scan mode with the ion source temperature at 240 ˚C with electron ionization (EI) at 70 eV.

Statistical analysis was performed using the GraphPad Prism software, version 5.0. All variables analyzed in the in vivo experiment were continuous quantitative. All data are shown as mean ± s.d. (*): $p < 0.05$. Mann Whitney test was used to determine statistical significance between groups. A nonparametric test was used, which does not require the assumption of normality.

Cell culture

The human non-tumor oral keratinocyte spontaneously immortalizes cell line NOK SI and human OSCC cell lines, HN12 (tumorigenic and metastatic) and HN13 (tongue squamous carcinoma) were cultured in Dulbecco's Modified Essential Medium (DMEM, Sigma-Aldrich, Munich, Germany) without phenol red, supplemented with 2% fetal bovine serum (FBS, GIBCO, Carlsbad, CA, USA), and penicillin-streptomycin (Sigma-Aldrich) in a humidified atmosphere containing 5% CO2, at 37°C. We also evaluated the effect of BPA on mucoepidermoid carcinoma cell lines, UM HMC1 and UM HMC3a. cultured in DMEM, supplemented with penicillin/streptomycin, L-glutamine (Invitrogen), 10% FBS, 20 ng/mL epidermal growth factor (EGF; Sigma-Aldrich, St. Louis, MO, USA), 400 ng/mL hydrocortisone (Sigma-Aldrich), and 5 µg/mL insulin (Sigma-Aldrich). Cells were passaged using 0.05% trypsin/EDTA (Invitrogen). The medium was refreshed every other day.

The spontaneously transformed human epithelial cell line from adult skin cell line (HaCat) and the tongue squamous carcinoma cells - SCC25 (human, tumorigenic) (American Type Culture Collection, USA) were also tested for proliferation and apoptosis (supplementary experiments) and cultured in DMEM, supplemented

with 10% FBS and penicillin-streptomycin. (all from GIBCO). In the SCC25 cell culture medium 500 ng/ml of hydrocortisone was added (Sigma-Aldrich).

Resazurin cell viability assay

The viability test was based on the use of resazurin (Alamar Blue, Thermo), whose reduction is related to cell viability. Cells, HN12, HN13, NOK SI, UM HMC1 and UM HMC3a, were plated in quadruplicate and 2 independent biological replicates at a cell density of $4x10^3$ cells/per well in 96-well microplates and incubated in a humidified atmosphere of 5% CO_2 at 37°C overnight. BPA at different concentrations (1 nM, 10 nM, 50 nM, 100 nM, 500 nM, 1 µM, 10 µM) were tested, and compared to the vehicle control group, DMSO 0.05%. Cells were evaluated after 48, 72 and 120 hours by addition of resazurin (0.01 mg/mL) in DMEM. The plates were kept protected from light and incubated for 4 hours in a 95% humidified atmosphere containing CO_2 5%, at 37°C. The absorbance was measured in the fluorimeter of Synergy 2 Multi-mode Microplate Reader (Biotek, Winooski, VT, USA) with excitation 530 / 25 nm and emission 590 / 35 nm. A well containing medium without resazurin was used as a reaction blank control.

Clonogenic assay

NOK-SI (400 cells/well), HN12 (400 cells/well) and HN13 (200 cells/well) were cultured for 15, 12 and 8 days, respectively, in 12 wells microplates in triplicate and 3 independent biological replicates. Cells were incubated with vehicle DMSO (0.05%) or BPA at 10 nM, 500 nM and 1 µM. The media with treatments were refreshed every two days. Subsequently, the cells were fixed in 10% neutral buffered formalin

and stained with 1% crystal violet solution (Sigma-Aldrich). Colonies containing at least 50 cells were automatically counted by using the Image J Software.

Immunocytochemistry assay

HaCat and SCC25 cells were plated in quadruplicate at a cell density of $1x10^3$/per well in 96-well microplates and incubated in a 95% humidified atmosphere containing 5% CO_2 at 37°C overnight. Cells were incubated with BPA at the doses of 1 µM and 10 µM for seven days. The medium with treatments were refreshed every two days. One control (untreated control) and one vehicle (DMSO 0.05%) group were also tested. After seven days of culture, cells were fixed with cold methanol. Immunocytochemistry analysis was performed in duplicate in all groups with the streptavidin-biotin-peroxidase complex technique. The primary antibodies and their dilutions were as follows, anti Ki67 (clone MIB-1, 1: 400, Dako Cytomation, Glostrup, Denmark) revelated with diaminobenzidine (DAB, Dako) and stained with Mayer's hematoxylin. Quantification of Ki67 positive cells was performed by image acquisition using the Cytation 5 Cell (Biotek) multimode reader and counted with Image J software.

The UM HMC1 and UM HMC3a cell lines were plated at a cell density of $4x10^5$/per well in 12-well microplates on a glass cover slip and incubated in a 95% humidified atmosphere containing CO_2 5% at 37°C overnight. Cells were incubated with BPA at 50nM and vehicle (DMSO 0.05%) for 48 hours. Immunocytochemistry analysis was performed in triplicate. The primary antibody used was anti p63 (MC0221, 1:50, Medaysis, Livermore, USA). Quantification of p63 positive cells was performed by image acquisition at light microscope (Opticam O600R) 200x original magnification using the integrated software (OPTHD) and counted in 10 consecutive fields with Image J software.

Estrogen Receptor antagonist treatment

The clonogenic assay, as described earlier, was also performed with HN12 and NOK-SI in the presence of pure antagonist of Estrogen Receptor (ER) ICI 182, 780 (Sigma-Aldrich) at a concentration of 10^{-5} M and 2 independent biological replicates. The media with compounds treatments were refreshed every two days for 12 days in HN12 and for 15 days in NOK SI.

Immunofluorescence analysis

The cellular proliferation was assessed in the NOK SI, UM HMC1 and UM HMC3a cell lines by immunofluorescence. Cells were plated at a cell density of $4x10^3$/per well in quadruplicate and 3 independent biological replicates and cultured for 96 hours in 96-well microplates. Vehicle group (DMSO 0.05%) and BPA (10 nM and 1 µM for NOK SI and 50 nM for UM HMC1 and HM HMC3a) were analyzed. Cells were fixed with methanol, incubated with 0.3% hydrogen peroxide, and with the primary antibody anti-Ki67 (15580, 1: 200, Abcam, Cambridge, England), at 4°C, overnight. The secondary antibody was anti-rabbit-Alexa 488 (Invitrogen). DAPI was used for nuclear DNA staining (blue) (Sigma-Aldrich). Cells were analyzed with the ImageXpress Micro XLS Widefield High-Content Analysis System (Molecular Devices) at original magnification 200x and counted in twenty random fields per well.

mRNA extraction, quantitative real-time PCR (qRT-PCR) and PCR array reactions

For qRT-PCR analysis, the cells NOK-SI, HN12 and HN13 were plated at a cell density of $3x10^5$/per well and cultured for 72 hours in 6-well microplates in

duplicate. Three groups were performed: standard condition, vehicle (DMSO 0.05%), and BPA at 10 nM.

Total mRNA was extracted by using Trizol reagent (Thermo) followed by column purification (RNeasy Mini Kit, Qiagen Inc., Valencia, CA, USA). The quality and integrity of mRNA samples were checked by analyzing 1 µL of total mRNA on the 2100 Bioanalyzer (Agilent Technologies, Santa Clara, CA, USA), according to the manufacturer's instructions. The complementary DNA (cDNA) was synthesized from 2 µg of RNA by using a reverse transcription reaction High-Capacity cDNA Reverse Transcription Kit (Applied Biosystems).

The target genes analyzed by quantitative real-time PCR (qRT-PCR*)* were Erα (NM_001122742.1; F: atgagagctgccaacctttg; R: ggttggtcagtaagcccatc), Erβ (NM_001291723; F: tggagtctggtcgtgtgaag; R: acttcaccattcccacttcg) and GAPDH (NM_001289745.2; F: gaaggtgaaggtcggagtcaac; R: cagagttaaaagcagccctggt). The qRT-PCR reactions were performed using SYBR Green PCR Master Mix (Thermo). The thermocycling protocol consisted of an initial pre-incubation step at 95 °C for 10 minutes, 45 amplification cycles starting at 95 °C for 10 s, 60 °C for 30 s, and 72 °C for 1 s, followed by a single cooling step at 40 °C for 10 s. Data were analyzed by using the Light Cycler® 480 software. The relative expression of each gene was normalized by the mean expression of one housekeeping gene, GAPDH, and quantified using the cycle threshold (Ct) and $2^{-\Delta\Delta Ct}$ calculation.

The RealTimePCR array reactions were performed as previously described[24] in a Viia7 instrument (LifeTechnologies, Carlsbad, CA) using a customized panel containing targets for gene expression profiling (including BPA-related receptors, proliferation, apoptosis, extracellular matrix remodeling, histones deacetylases and EMT markers). RealTimePCR array data were analyzed by the RT^2

profiler PCR Array Data Analysis online software (SABiosciences, Frederick, MD) by normalizing the initial geometric mean of three constitutive genes (GAPDH, ACTB, Hprt1) and subsequently normalized by the control group, results are reported as fold change relative to the control group.

Cell Invasion Assay

The cell invasion assay was performed with the HN12 cell lines using bipartite chambers. HN12 cells ($1x10^4$/per well) were plated in triplicate in the upper compartment of the insert covered by Matrigel (Cat. 35423C, BD Biosciences, Bedford, MA) and incubated with BPA (at 10 nM and 1 μM), or with the vehicle (DMSO 0.05%). Cells were kept in culture for 72 hours, and then fixed in 10% formaldehyde solution for 15 minutes. Cells that migrated, invaded and attached on the downside of the membrane were stained with DAPI (Sigma-Aldrich).

Five random fields from each membrane were photographed at the original magnification 200x by using an inverted microscope (Zeiss Axiovert 40) and the images analyzed by AxioVision Rel. 4.8.2 software (Carl Zeiss). Cells that were capable of transmigrating through the membrane pores were then counted by using the Image J software and the results presented as the mean of cells/field.

ELISA – Enzyme-linked Immunosorbent Assay

To evaluate the presence of the cytokines: interleukin 10 (IL-10), transforming growth factor beta (TGF-β), matrix metalloproteinase 9 (MMP9), epidermal growth factors (EGF) and vascular growth factors (VEGF) the NOK SI, HN12 and HN13 cell lines were plated at a cell density of $2.5x10^3$/per well and cultured in 24-well microplates.

Treatment was carried out with BPA at 10 nM, 500 nM and 1 μM for 24, 48 and 72 hours. A vehicle group (DMSO 0.05%) was also tested. On the last day of culture, the supernatant was collected and analyzed by using commercial ELISA assays. according to the manufacturer instructions (R & D Systems, Minneapolis, MN, USA).

Zymography analysis of matrix metalloproteinases

Cells HN12 e HN13 were plated at a cell density of 3×10^5/well in triplicate and 3 independent biological replicates in a 6-well microplate and incubated with BPA (10 nM, 500 nM and 1 μM) for 24 hours. Twenty microliters of the supernatant were collected and resolved by 8% sodium dodecyl sulfate-polyacrylamide gel electrophoresis (SDS-PAGE) containing 1 mg / mL gelatin. The gel was then washed with 2% Triton X-100 for 40 min and incubated in a reaction buffer containing 10 mM Tris–HCl, pH 8.0, and 5 mM $CaCl_2$ 5 mM for 16 hours at 37°C. The gel was then stained with Coomassie blue 0.25% (Thermo). After removing the stain, the negative bands representing the MMP2 and MMP9 activity could be visualized. Semiquantitative analysis using densitometry was performed with the Image J software. The MMP activity was presented as optical density (OD) × mm^2, representing the scanning area under the curves, which considers both brightness and width of the substrate lysis zone.

Western blotting

Cells HN12, HN13, NOK SI, UM HMC1 and UM HMC3a, were plated at a cell density of 3×10^6/well in a 6-well microplate and incubated with BPA (10 nM, 500 nM and 1 μM for HN12, HN13, NOK SI and 50 nM for UM HMC1 and UM HMC3a) for

2 and 24 hours, performed in biological triplicate. Cell protein extracts were obtained using the CelLytic Mammalian Cell Lysis/Extraction Reagent (Sigma-Aldrich) with protease and phosphatase inhibitor cocktails (Sigma-Aldrich). Protein concentration was determined by using the Bradford protein assay (Bio-Rad Laboratories, Hercules, CA, USA). Thirty micrograms of protein were separated by 10% SDS-PAGE and transferred to a PVDF membrane (GE HealthCare, Freiburg, Germany). A prestained protein ladder (Thermo) was loaded in all SDS-PAGE. The membranes were blocked in 5% non-fat dry milk in Tris-buffered saline containing 10% Tween 20. Antibodies against ERK1/2 (M 5670; Sigma-Aldrich), phospho-p44/42 MAPK ERK1/2 (pERK1/2; #4377; Cell Signaling), AKT (#9272, Cell Signaling), phospho AKT (Thr308) (#4056, Cell Signaling), NF-κB (#8242, Cell Signaling), phospho NF-κB (#3033, Cell Signaling), STAT3 (#9139, Cell Signaling), phospho STAT3 (#3270, Cell Signaling), c-myc (#5605, Cell Signaling), histone H3 (#4499, Cell Signaling), acetyl-histone H3 (#8173, Cell Signaling), Vimentin (#5741, Cell Signaling), β-actin (#3700, Cell Signaling) and GAPDH (#5174, Cell Signaling) were used. The reactions were developed using the chemiluminescent ECL Western blotting system (GE Health-Care). Densitometric analysis was performed using the Image J software. B-actin and GAPDH were used as the loading controls.

Angiogenesis assay

To evaluate the effects of factors secreted by neoplastic cells, incubated with BPA, on the formation of blood vessels, an in vitro assay was performed by using the human umbilical cord endothelial cells (HUVEC). For this, 96-well plate were coated with Matrigel (BD Biosciences, USA), as recommended by the company. After Matrigel polymerization, 1 x 10^4 HUVEC cells were plated in quadruplicate and added of the

conditioned medium that was obtained from HN12 cells previously cultured for 48 hours with BPA (10nM and 1μM) and vehicle (DMSO 0.05%) in 3 independent biological replicates. The vessel-like structures were analyzed after 16 hs by using calcium AM and ethidium homodimer solution (2 μM calcein AM and 4 μM EthD-1, Thermo) to stain, according to manufacturer protocol. Cells were washed with fresh phosphate buffered saline (PBS), and Images were taken using a Modular Stereo Microscope for Fluorescent Imaging Leica (MZ10 F) at the 40x original magnification. The number of segments and nodes were quantified using the angiogenesis analyzer plugin on the ImageJ software.

Evaluation of the pro-angiogenesis effects in a model of chorioallantoic membranes

The chorioallantoic membrane (CAM) from fertilized chicken eggs was used for two different tests. In the first assay, the BPA was tested diluted in PBS at the doses of 10 nM and 1 μM. The negative control was PBS 1x and the positive control was VEGF (2000 pg / mL). In the second assay, the evaluated samples were the HN12 supernatant at the 48 hour time interval. The tested groups were: vehicle (DMSO 0.05%), BPA 10 nM and 1 μM. In this assay, the negative control was DMEM and the positive control was VEGF (2000 pg / mL). Eight eggs were used for each evaluated sample.

The fertilized chicken eggs were placed in a hatching incubator and three days after fertilization, a hole of approximately 1 cm in diameter was opened in the eggshell to provide access to the CAM. Five days after fertilization, samples were applied over the CAM surface in a well-defined part, and then reapplied six days after fertilization. After 24 hours the CAMs were analyzed with a light microscope (Leica,

model DM4000B, Germany) coupled to a Leica digital CCD camera model DFC 280 (Software Leica Application Suite V 3.3.0, Germany). The images obtained were used for the quantification of the capillary features by using the Image J software. Blood vessels were expressed as optical density (OD) × mm^2.

RESULTS

Chronic BPA exposure causes morphological changes in the oral mucosa and salivary glands

We first evaluated the effects of chronic BPA exposure on male and female C57BL/6 mice's oral mucosa. We observed thickening of the buccal mucosa, tongue, and palate in the groups receiving drinking water spiked with BPA (200 mg/L) compared to the untreated (control) and vehicle (DMSO) groups (Fig. 1a and 1b). This increase in epithelial thickness at the three different oral mucosa sites analyzed (buccal mucosa, tongue, and palate) was identified in both male and female mice. Likewise, there was an increase in the stratum corneum's thickness in the BPA group compared to vehicle control (Fig. 1c – 1f). No differences at any of the mucosal sites evaluated were observed between the untreated control and vehicle in either male or female animals (data not shown).

Next, we determined whether the epithelial thickening is related to an increase in epithelial proliferative activity. The number of cells positive for Ki67, a proliferation marker, was higher in BPA-treated animals. Besides, the labeling intensity was higher when compared to the controls in both male (Fig. 1g and 1h) and female (Fig. 1i and 1j) animals.

Exposure to BPA also caused disturbances in the submandibular salivary glands. Figures 2a and 2b show the histological features observed in the male and female BPA groups. There was a reduction in the number of acini and an increase of granulated convoluted tubules (GCT) in male (Fig. 2c and 2d) and female (Fig. 2e and 2f) animals. The submandibular salivary gland's weight was similar between groups (untreated control: 124.8 ± 7.1 mg; vehicle: 132.5 ± 15.1 mg, and BPA: 123.8 ± 15.3 mg).

Considering the well-established effects of BPA on the prostate and mammary glands[14, 18], we obtained samples from these tissues for histological analysis. A comparison of all groups showed no alterations in the histopathological score (Supplementary fig. 1a) or the mammary glands' weight. In contrast, BPA induced a significant number of prostate epithelial lesions ranging from benign lesions (atrophy and hyperplasia) to pre-malignant prostate intraepithelial neoplasia (PIN) (Supplementary fig. 1b). It was also observed thickening of the muscle layer involving acini with lesions, mainly of the PIN type (Supplementary fig. 1c). The weights of the prostate complex, seminal vesicle, and testicles were similar between groups, with no significant differences (data not shown).

Chronic BPA exposure results in the accumulation of the chemical in the oral mucosa and salivary glands

Considering BPA's effects on the oral epithelium and salivary gland morphology, we then analyzed tissue samples by mass spectrometry to quantify BPA at these sites. We observed a significant accumulation of BPA in the tongue (Fig. 3a) and salivary glands (Fig. 3b).

BPA induces cell proliferation and invasion *in vitro*

We next evaluated the response of non-tumor oral keratinocytes spontaneously immortalized (NOK-SI) cell line to BPA. The *in vitro* assays also included the neoplastic oral squamous cell carcinoma (OSCC) cell lines HN12 and HN13 and neoplastic salivary gland cells of mucoepidermoid carcinoma (UM HMC1 and UM HMC3a).

In the first experiments, we determined whether BPA induces cytotoxicity by the resazurin assay. The assays were performed at different concentrations of BPA

(1 nM, 10 nM, 50 nM, 100 nM, 500 nM, 1 μM, 10 μM) after 48, 72 and 120 hours of incubation. There was no reduction in cell viability at any of the concentrations tested. From these results, three concentrations from a nanomolar (10 nM), including an intermediate (500 nM) to a micromolar (1 μM) were selected for the subsequent experiments using the NOK-SI, HN12, and HN13 cell lines. The 50 nM concentration was used for the assays with the UM HMC1 and UM HMC3a cell lines (Supplementary fig. 2).

The clonogenic assay was performed using the NOK-SI, HN12, and HN13 cell lines to determine BPA's effects on colony-forming capacity. In the presence of BPA (10 nM), the NOK-SI (Fig. 4a), and HN12 (Fig. 4b) cell lines formed a larger number of colonies. No effect was detected for HN13 (Fig. 4c). In line with these results, BPA induced an increase in the proliferative response of NOK-SI cells (90% ± 4% of Ki67-positive cells in the BPA group versus 68% ± 12% in the vehicle group, $p<0.05$) (Fig. 4d-4f).

No change in cell proliferation was observed for the UM HMC1 or UM HMC3a cell line (Supplementary fig. 3a and 3b). However, staining of the tumor protein p63 was higher in the cells incubated with BPA than vehicle control (Supplementary fig. 3c-3e). We also analyzed BPA's effects on target proteins related to survival and proliferation pathways, e.g., pAKT, pERK and pNFκB. There were no differences in these proteins between groups, except for a lower level of pAKT (2 hours) and an apparent increase of pERK (24 hours) in the BPA-treated group compared to the vehicle control (Supplementary fig. 3f).

To confirm that BPA's effects were not restricted to a specific cell line, we additionally analyzed its effects on another keratinocyte cell line (HaCat) and an OSCC

cell line (SCC25). Consistent with the previous data, both cell lines exhibited higher Ki67 expression in the presence of BPA (Supplementary fig. 4a and 4b).

Considering the effects of BPA on clonogenicity and cell proliferation, we then tested whether BPA modifies neoplastic cells' behavior by changing their migration/invasion capacity and the production of pro-tumorigenic factors. Noteworthy, BPA induced an increase in HN12 cell invasion. At the nanomolar concentration, the number of invading cells was even higher than the micromolar concentration and the vehicle group (Fig. 4g - 4j). Since this invasion ability is linked to metalloproteinases[9], we evaluated if BPA modifies MMP-2 and MMP-9 activities. These enzymes were measured by zymography on gelatin-copolymerized gels. HN12 and HN13 cells were incubated with BPA for 24 hours, and the supernatant was analyzed. MMP-2 activity was increased in HN12 (Fig. 4k) but not in HN13 cells incubated with BPA (Fig 4m). MMP-9 activity was augmented in both the HN12 (Fig 4l) and the HN13 cell line (Fig. 4n). Consistently, MMP9 concentration, measured by ELISA in the culture supernatants, was higher in both HN12 (Fig. 4o) and HN13 (Fig. 4p) cells incubated with BPA.

BPA promotes angiogenesis and stimulates VEGF production of oral cancer cell line

Angiogenesis is an essential step in tumor growth and metastasis[25]. We analyzed BPA's effect on angiogenesis using two different models, chicken chorioallantoic membrane (CAM) and tubule formation using human umbilical cord endothelial cells (HUVEC). The conditioned medium from HN12 cells cultured in the presence of BPA (10 nM and 1 μM for 48 hours) was able to induce blood vessel formation similar to VEGF (positive control, 2000 pg/mL) (Fig. 5a and 5b). Accordingly, VEGF levels were increased in HN12 cells' supernatants incubated with BPA (Fig. 5e).

Also, the direct application of BPA (10 nM) to CAMs stimulated blood vessel formation when compared to the negative control (vehicle in phosphate-buffered solution) (Fig. 5c and 5d).

To confirm the potential of BPA to induce tumor angiogenesis, we investigated the formation of endothelial tubes using HUVEC cells. Consistent with the findings of the CAM assay, the number of segments (Fig. 5f) and nodes (Fig. 5g) of vessel-like structures was significantly increased in the presence of BPA (Fig 5h).

BPA modifies the production of cytokines and growth factors in cells

Cytokines and growth factors have essential roles in modulating neoplastic and non-neoplastic cell behavior. These molecules sustain proliferation and contribute to angiogenesis, invasion, and ultimately, metastasis[26]. The production of epidermal growth factor (EGF), transforming growth factor-β (TGF-β), and interleukin-10 (IL-10) were evaluated in the supernatants of NOK-SI and HN12 cell cultures exposed or not to BPA.

In NOK-SI cells, 10 nM, 500 nM, and one μM BPA increased EGF secretion after 48 and 72 hours (Fig. 6a – 6c). Furthermore, BPA increased the secretion of TGF-β after 48 and 72 hours of exposure to 10 nM and 500 nM (Fig. 6d – 6f) but did not alter IL-10 levels (Fig. 6g – 6i).

In the HN12 cell line, there was an increase in EGF after 24 hours (10 nM, 500 nM, and 1 μM), 48 hours (10 nM, and 1 μM), and 72 hours (1 μM) of BPA exposure (Fig. 6j – 6l). Analysis of TGF-β showed that BPA increased the secretion of this factor after 24 hours (10 nM, 500 nM, and 1 μM), 48 hours (10 nM, 500 nM, and 1 μM), and 72 hours (500 nM, and 1 μM) (Fig. 6m – 6o). In this neoplastic cell line, BPA also

increased the release of IL-10 after 24 hours (10 nM, 500 nM, and 1 μM), 48 hours (10 nM and 500 nM), and 72 hours (1 μM) (Fig. 6p – 6r).

BPA increases the protein levels of pAKT, pERK, pNFkB, pSTA3, c-Myc and vimentin

To better understand BPA's mechanism inducing cell proliferation, we analyzed the effects of BPA on target proteins of pathways involved in cell survival and proliferation (pAKT, pERK, pNFκB, pSTAT3, and c-Myc oncogene). The possible effect of BPA on EMT was also evaluated by analyzing vimentin expression [10]. Overall, BPA seems to activate all proteins related to the critical cell survival and proliferation pathways analyzed (Fig.7). The increased c-Myc protein, evidenced in the three cell lines, participates directly and indirectly in cell cycle regulation, cell growth, genomic instability, and immortality[27]. Nanomolar concentrations of BPA exerted remarkable effects on the proteins and signaling pathways (Fig. 7a-c). Moreover, in the metastatic OSCC cell line HN12, BPA augmented vimentin levels (Supplementary 5).

BPA induces acetylation of H3 histones

The acetylation of histones is related to less condensed chromatin and consequently increased gene transcription[28]. Genotoxic activities and epigenetic modifications caused by BPA exposure have been reported and may play important roles in carcinogenesis[29]. Interestingly, we observed that incubation with BPA for 2 hours reduced the acetylation of H3 histones in the HN12 (Fig. 7d) and HN13 (Fig. 7e) cell lines, while incubation for 24 hours increased acetylation. In line with these findings, we verified that BPA up-regulated mRNA expression of histone deacetylases (HDAC1, HDAC3, HDAC5, HDAC7) in all cell lines evaluated (NOK-SI, HN12, and HN13) (Fig. 8).

BPA up-regulates the expression of growth factors, extracellular matrix and remodeling proteins, BPA-related receptors and EMT markers in oral keratinocyte and neoplastic cell lines

Differential gene expression of several molecules involved in cell growth, apoptosis, EMT, angiogenesis, histone deacetylation, and BPA-related receptors were investigated in the untreated (control) vehicle BPA (10 nM) groups using the NOK-SI, HN12, and HN13 cell lines. First, an exploratory analysis was performed using pooled samples. The selected targets showing differential expression between the control and BPA groups were analyzed regarding their expression kinetics.

BPA up-regulated the expression of BPA-related receptors (EGFR, AR, IGF1R, ESRRG, and GPER1), factors involved in cell growth and proliferation (MAPK3, TGFB1, TP53, and EGF), EMT-related genes (SNAI1, SNAI2, SNAI3, and TWIST1), and extracellular matrix and remodeling proteins (BMP7, MMP2, MMP3, and MMP9) in all cell lines evaluated (Fig. 8). Furthermore, VEGF expression was significantly augmented by BPA (Fig. 8), thus confirming the results described above. On the other hand, exposure to BPA seems to down-regulate the expression of apoptosis markers (BCL2, CASP3, CASP8, CASP9, BAX, and BAD) (Fig. 8).

The effects of BPA are dependent on estrogen receptors

Since our findings showed that BPA modulates BPA-related receptors' expression, we also explored whether BPA exposure changes ERα and ERβ mRNA levels. We observed that those receptors' expression was significantly augmented in non-neoplastic keratinocytes stimulated with BPA compared to the vehicle (Fig. 9a). In

the HN12 cell lines, BPA did not change the expression of ERα but reduced ERβ (Fig. 9b).

Considering that the effect of BPA may be mediated by ER[10], we tested whether an ER antagonist (ICI 182,780) reverses BPA's effect on colony formation in the HN12 and NOK-SI cell lines. BPA-induced colony formation was significantly diminished in the presence of the ER antagonist (Fig. 9c and 9d). These results confirm that BPA's effects on oral keratinocytes and oral carcinoma cells are dependent on ER activation.

DISCUSSION

In the present study, we demonstrated that chronic exposure of mice to BPA disrupts the oral mucosa's microarchitecture by altering the epithelial proliferative index. Furthermore, submandibular salivary glands exhibited atrophic changes, as indicated by a reduction in the number of salivary glands acini. Accordingly, there was an accumulation of the BPA molecule in these tissues. *In vitro*, BPA induced cell proliferation, altered the production of cytokines, growth factors and metalloproteinases, and modified ER and other BPA-related receptors' expression. In the presence of BPA, the invasiveness, production of cytokines and growth factors and angiogenesis-inductive properties of neoplastic cells were increased. BPA also induced the expression of EMT markers. Mechanistically, BPA activates intracellular pathways related to cell proliferation and survival, such as AKT, ERK, NFκB, STAT3, and c-Myc, and induces epigenetic modifications by histone H3 acetylation and deacetylation associated with HDAC1, HDAC3, HDAC5, and HDAC7. We further verified that BPA's effects are almost abolished in the presence of an ER antagonist, thus suggesting that these effects largely occur via these receptors.

It is believed that the ingestion of contaminated food and liquids contributes more than 90% to environmental exposure to BPA[1]. The transfer of BPA from its constituent products into the environment or food depends on several factors like temperature and pH[30]. Importantly, the oral cavity is the first site of contact with BPA, and the use of some dental materials may increase the concentration of BPA in saliva[5]. To evaluate the possible changes in healthy tissues due to chronic BPA exposure, we modeled an oral exposure scenario by administering BPA in drinking water to mice. Our findings show that BPA accumulates in tissues and disturbs oral

mucosa homeostasis. These effects occur at least in part through BPA interaction with ERs since buccal mucosa and salivary gland tissue express these receptors and are estrogen-responsive tissues[31]. Our data also demonstrated morphological alterations in acini and GCT of the submandibular salivary gland. Similar alterations have already been described in rats[23]. In rodents, GCT are hormone-sensitive secretory structures that stimulate EGF and TGF-β secretion and regulate the biology of healthy and malignant cells, and the maintenance of the oral epithelium. These growth factors are produced by GCT cells and secreted into the saliva. Salivary gland-derived growth factors may be directly involved in the protection and repair of the mucosal membranes. Serous acini are responsible for the exocrine secretion of salivary proteins[32]. Taken together, our results highlight the submandibular salivary glands and oral mucosa as targets of BPA. As expected, the changes induced by BPA in the prostate of mice validated our experimental model and confirmed the alterations described in previous studies[33].

The *in vivo* findings led us to investigate the effects of BPA in specific cell types. For salivary gland mucoepidermoid carcinoma cells, augmented p63 immunostaining was observed in the BPA group. Although protein p63 is commonly present in basal and myoepithelial cells from healthy human samples, its increase is useful for diagnosing mucoepidermoid carcinoma[34]. Actually, an oncogenic function has been suggested for p63, and its overexpression is associated with recurrence, metastasis, and poor prognosis in myoepithelial carcinoma patients[35].

For OSCC and non-tumor oral keratinocyte cell lines, we showed that a low concentration of BPA is sufficient to increase c-Myc, pAKT, pERK, pNFκB, and pSTAT3. All of these targets are involved in cell proliferation and survival. Similarly, BPA stimulated the growth and proliferation of ovarian and breast human cancer

cells[10] by activation of AKT and ERK1/2[36] and through EGF/EGFR/ERK signaling in endometrial cell cancer[37]. In the present work, we demonstrate that BPA's effects via alternative pathways contribute to change cellular homeostasis.

The influence of BPA on cancer cell migration and invasion has been identified in several types of malignant tumors such as ovarian[38], breast[39], endometrial[40], colorectal[41], and lung cancer cells[9]. Here, we showed that BPA increases the invasiveness of oral cancer cells and the secretion of MMPs. Previous studies have demonstrated the ability of BPA to induce the production of MMP2 and MMP9[9], to reduce epithelial cell junction proteins, and to increase mesenchymal markers like vimentin in ovarian[38] and prostate cancer cells[33]. Metalloproteinases may play critical roles in degrading extracellular matrices and promoting tumor invasion and metastasis[42]. EMT is another substantial alteration that interferes with the migration and metastasis of tumor cells through the loss of cell-cell adhesion and cell-matrix adhesion[43]. In our study, there was an increase of EMT markers such as vimentin, SNAI1, SNAI2, SNAI3, and TWIST in BPA-incubated OSCC cells. Accordingly, vimentin is particularly correlated with increased tumor growth and invasion and poor prognosis[44]. In OSCC models, cells expressing SNAI showed complete EMT phenotypes[45], while TWIST was associated with carcinogenesis and lymph node metastasis[46].

Exposure to BPA leads to the activation of inflammatory pathways in animals[47] and humans[48]. We observed that BPA exposure increased IL-10 production by OSCC cell lines and TGF-β and EGF expression in keratinocytes and OSCC cell lines. IL-10 is an immunomodulatory cytokine with an anti-inflammatory activity that exerts pro-angiogenic and pro-tumor effects through the modulation of STAT3 and cell proliferation[49]. TGF-β plays a pro-angiogenic role regulating the

spontaneous expression and activity of VEGF and stimulating EMT, invasion, and metastasis. Likewise, EGF is related to the clonal expansion and invasion of tumor cells[26]. Interestingly, in human macrophages, BPA treatment decreased the production of IL-10 and TGF-β[50], while it stimulated a Th2 response profile characterized by increased IL-10 expression in primary cultured mouse lymphocytes[51]. However, in cancer, IL-10 has an immunosuppressive effect in the tumor microenvironment, supporting tumor escape from the host immune response[49]. TGF-β levels are associated with immunosuppression and cancer cell proliferation and metastasis, thus contributing to tumor progression and invasiveness in more advanced stages of the disease[52] Taken together, our data support the role of BPA in the modulation of the tumor microenvironment and induction of cellular changes that favor cell migration and tumor progression.

The effects of BPA mainly occur via binding to ERs, both in the nuclear and plasma membrane. The BPA molecule has structural features that confer the ability to bind to ERα and ERβ but displays less affinity to the ERs than 17β-estradiol, the most active estrogen[53]. Once activated, ERs can further bind specific DNA sequences as a homodimer and modulate gene expression[54]. Many of these ER-regulated genes, including c-Myc, function as an oncogene in various other human tumors[55]. In the HN12 OSCC cell line, we found an increase in c-Myc protein levels due to BPA exposure. There is evidence that ERα activation is crucial for developing hormone-induced tumors in humans[56]. Therefore, the activation of ER by BPA may trigger the same cascades. Here, we demonstrated for the first time that ER activation is pivotal for some of the effects of BPA on both neoplastic and non-neoplastic oral keratinocytes. We also observed the up-regulation of ERα and ERβ induced by BPA in NOK-SI cells. A similar effect was reported previously in ovarian cancer cells[6]. On

the other hand, in oral cancer cells, BPA treatment did not change ERα but reduced ERβ. In line with these results, BPA attenuated ERβ expression in breast cancer cells[57]. The alteration of the ERα:ERβ ratio may pose a high risk of cancer progression. In truth, the levels of ERβ expression decrease in the following order: normal breast lobules, usual ductal hyperplasia, ductal carcinoma in situ, and invasive cancer[58]. Furthermore, under our experimental conditions, BPA was able to up-regulate all other BPA-related receptors, e.g., AR, GPER1, IGF1R and ESRRG, indicating potential BPA-binding sites on oral keratinocytes and tumor cells. Binding of BPA to these nuclear and membrane receptors activates cell growth, survival, proliferation, migration, invasion, and anticancer drug resistance through several signaling pathways[10].

Epigenetic modifications are hereditary and reversible changes that occur in response to environmental stimuli and are not caused by changes in the DNA sequence. The epigenetic modifications due to BPA exposure associated with histone acetylation remain poorly understood. Our results showed that a low concentration of BPA promotes an initial reduction in histone H3K9 acetylation levels followed by hyperacetylation after 24 hours. Interestingly, after 72 hours, up-regulation of HDAC1, HDAC3, HDAC5 and HDAC7 mRNA was observed in the OSCC cell lines. Other studies correlating BPA with these modifications reported that DNA methylation decreased at the genomic level[59], and the levels of H3K9 and H4K16 acetylation increased abnormally after treatment with BPA[60]. BPA's effects on histone modifications and HDAC activities need to be better studied; however, BPA may affect chromatin remodeling and consequently gene expression as suggested by the modifications induced by this monomer in oral cells observed in the present work.

The present study provides new experimental data supporting that BPA targets intracellular signals through binding to ERs on oral neoplastic and non-neoplastic keratinocytes. BPA disrupts keratinocytes' function by altering proliferation, pro-survival and proliferative intracellular pathways and the secretion of cytokines and growth factors. In tumor cells, BPA induces proliferative, invasive, proangiogenic and epigenetic events and augments the production of cytokines and pro-angiogenic factors and enzymes. The plethora of BPA effects on normal keratinocytes and neoplastic cells reinforces public measures' relevance to minimize exposure to BPA and opens up perspectives on monitoring BPA exposure in the population. Importantly, oral ingestion is the main route of exposure and the monomer accumulates in the oral mucosa and salivary glands resulting in harmful effects in these tissues. Furthermore, BPA may be a modifier of oral cancer cell behavior by prompting a shift to a more aggressive phenotype.

Acknowledgements: This study was supported by Coordenação de Aperfeiçoamento de Pessoal de Nível Superior (CAPES, Finance Code 001), Brazil. We would like to thank the Conselho Nacional de Desenvolvimento Científico e Tecnológico (CNPq), and the Fundação de Amparo à Pesquisa do Estado de São Paulo (FAPESP), Brazil. We also thank Prof. Armando da Silva Cunha Júnior, Prof. Rafael Escorsim Szawka, Prof. Fabio Daumas Nunes and Dr. Cristiana Bernadelli Garcia for promptly assisting us with this work.

Competing Financial Interests: The authors declare they have no actual or potential competing financial interests.

Author contributions statement

T.F.A.A. was the PhD student responsible for the research. Was involved in planning, conceived, and conducted the experiments, data collected, acuration and writing-original draft. Z.L.C., H.C.M., C.A.O., S.M., G.P.G. and I.M.A.D., verified the analytical methods, conceived and designed the analysis. S.R.O., J.M.S, A.L.F.O., J.M.G. and G.H.C.S., analysed the results and conducted part of the experiments. A.M.L. and T.A.S. conceived the original idea, supervised the project and were in charge of overall direction and planning. All authors discussed the results, contributed to the final manuscript and reviewed the manuscript.

REFERENCES

[1] Geens T, Aerts D, Berthot C, Bourguignon JP, Goeyens L, Lecomte P, et al. A review of dietary and non-dietary exposure to bisphenol-A. Food and chemical toxicology : an international journal published for the British Industrial Biological Research Association. 2012;50:3725-40.

[2] Kang JH, Kondo F, Katayama Y. Human exposure to bisphenol A. Toxicology. 2006;226:79-89.

[3] Altamirano GA, Munoz-de-Toro M, Luque EH, Gomez AL, Delconte MB, Kass L. Milk lipid composition is modified by perinatal exposure to bisphenol A. Molecular and cellular endocrinology. 2015;411:258-67.

[4] Ferguson KK, McElrath TF, Cantonwine DE, Mukherjee B, Meeker JD. Phthalate metabolites and bisphenol-A in association with circulating angiogenic biomarkers across pregnancy. Placenta. 2015;36:699-703.

[5] Lee J-H, Yi S-K, Kim S-Y, Kim J-S, Son S-A, Jeong S-H, et al. Salivary bisphenol A levels and their association with composite resin restoration. Chemosphere. 2017;172:46-51.

[6] Hwang KA, Park MA, Kang NH, Yi BR, Hyun SH, Jeung EB, et al. Anticancer effect of genistein on BG-1 ovarian cancer growth induced by 17 beta-estradiol or bisphenol A via the suppression of the crosstalk between estrogen receptor alpha and insulin-like growth factor-1 receptor signaling pathways. Toxicology and applied pharmacology. 2013;272:637-46.

[7] Wetherill YB, Fisher NL, Staubach A, Danielsen M, de Vere White RW, Knudsen KE. Xenoestrogen action in prostate cancer: pleiotropic effects dependent on androgen receptor status. Cancer research. 2005;65:54-65.

[8] Pupo M, Pisano A, Lappano R, Santolla MF, De Francesco EM, Abonante S, et al. Bisphenol A induces gene expression changes and proliferative effects through GPER in breast cancer cells and cancer-associated fibroblasts. Environ Health Perspect. 2012;120:1177-82.

[9] Zhang K-S, Chen H-Q, Chen Y-S, Qiu K-F, Zheng X-B, Li G-C, et al. Bisphenol A stimulates human lung cancer cell migration via upregulation of matrix metalloproteinases by GPER/EGFR/ERK1/2 signal pathway. Biomedicine & Pharmacotherapy. 2014;68:1037-43.

[10] Murata M, Kang JH. Bisphenol A (BPA) and cell signaling pathways. Biotechnology advances. 2018;36:311-27.

[11] Emfietzoglou R, Spyrou N, Mantzoros CS, Dalamaga M. Could the endocrine disruptor bisphenol-A be implicated in the pathogenesis of oral and oropharyngeal cancer? Metabolic considerations and future directions. Metabolism: clinical and experimental. 2019;91:61-9.

[12] Tarapore P, Ying J, Ouyang B, Burke B, Bracken B, Ho SM. Exposure to bisphenol A correlates with early-onset prostate cancer and promotes centrosome amplification and anchorage-independent growth in vitro. PloS one. 2014;9:e90332.

[13] Moriyama K, Tagami T, Akamizu T, Usui T, Saijo M, Kanamoto N, et al. Thyroid hormone action is disrupted by bisphenol A as an antagonist. The Journal of clinical endocrinology and metabolism. 2002;87:5185-90.

[14] Acevedo N, Davis B, Schaeberle CM, Sonnenschein C, Soto AM. Perinatally administered bisphenol a as a potential mammary gland carcinogen in rats. Environ Health Perspect. 2013;121:1040-6.

[15] Tharp AP, Maffini MV, Hunt PA, VandeVoort CA, Sonnenschein C, Soto AM. Bisphenol A alters the development of the rhesus monkey mammary gland. Proc Natl Acad Sci U S A. 2012;109:8190-5.

[16] Patisaul HB. Achieving CLARITY on bisphenol A, brain and behaviour. Journal of neuroendocrinology. 2020;32:e12730.

[17] Newbold RR, Jefferson WN, Padilla-Banks E. Prenatal exposure to bisphenol a at environmentally relevant doses adversely affects the murine female reproductive tract later in life. Environ Health Perspect. 2009;117:879-85.

[18] Prins GS, Hu WY, Shi GB, Hu DP, Majumdar S, Li G, et al. Bisphenol A promotes human prostate stem-progenitor cell self-renewal and increases in vivo carcinogenesis in human prostate epithelium. Endocrinology. 2014;155:805-17.

[19] Weinhouse C, Anderson OS, Bergin IL, Vandenbergh DJ, Gyekis JP, Dingman MA, et al. Dose-dependent incidence of hepatic tumors in adult mice following perinatal exposure to bisphenol A. Environ Health Perspect. 2014;122:485-91.

[20] Sprague BL, Trentham-Dietz A, Hedman CJ, Wang J, Hemming JD, Hampton JM, et al. Circulating serum xenoestrogens and mammographic breast density. Breast cancer research : BCR. 2013;15:R45.

[21] Bray F, Ferlay J, Soerjomataram I, Siegel RL, Torre LA, Jemal A. Global cancer statistics 2018: GLOBOCAN estimates of incidence and mortality worldwide for 36 cancers in 185 countries. CA: a cancer journal for clinicians. 2018;68:394-424.

[22] Dianin A. Condensation of Ketones with Phenols Zhurnal Russkago Fiziko-Khimicheskago Obshchestva. J Russ Phys Chem Soc St Petersburg. 1891;23:601-11.

[23] Folia M, Boudalia S, Menetrier F, Decocq L, Pasquis B, Schneider C, et al. Oral homeostasis disruption by medical plasticizer component bisphenol A in adult male rats. The Laryngoscope. 2013;123:1405-10.

[24] Glowacki AJ, Yoshizawa S, Jhunjhunwala S, Vieira AE, Garlet GP, Sfeir C, et al. Prevention of inflammation-mediated bone loss in murine and canine periodontal disease via recruitment of regulatory lymphocytes. Proc Natl Acad Sci U S A. 2013;110:18525-30.

[25] Nishida N, Yano H, Nishida T, Kamura T, Kojiro M. Angiogenesis in cancer. Vasc Health Risk Manag. 2006;2:213-9.

[26] Witsch E, Sela M, Yarden Y. Roles for growth factors in cancer progression. Physiology (Bethesda). 2010;25:85-101.

[27] Dang CV. c-Myc target genes involved in cell growth, apoptosis, and metabolism. Molecular and cellular biology. 1999;19:1-11.

[28] Di Martile M, Del Bufalo D, Trisciuoglio D. The multifaceted role of lysine acetylation in cancer: prognostic biomarker and therapeutic target. Oncotarget. 2016;7:55789-810.

[29] Ferreira LL, Couto R, Oliveira PJ. Bisphenol A as epigenetic modulator: setting the stage for carcinogenesis? European journal of clinical investigation. 2015;45 Suppl 1:32-6.

[30] Kang JH, Kito K, Kondo F. Factors influencing the migration of bisphenol A from cans. Journal of food protection. 2003;66:1444-7.

[31] Leimola-Virtanen R, Salo T, Toikkanen S, Pulkkinen J, Syrjanen S. Expression of estrogen receptor (ER) in oral mucosa and salivary glands. Maturitas. 2000;36:131-7.

[32] Amano O, Mizobe K, Bando Y, Sakiyama K. Anatomy and histology of rodent and human major salivary glands: -overview of the Japan salivary gland society-sponsored workshop. Acta histochemica et cytochemica. 2012;45:241-50.

[33] Huang D-Y, Zheng C-C, Pan Q, Wu S-S, Su X, Li L, et al. Oral exposure of low-dose bisphenol A promotes proliferation of dorsolateral prostate and induces epithelial-mesenchymal transition in aged rats. Scientific reports. 2018;8:490-.

[34] Sams RN, Gnepp DR. P63 expression can be used in differential diagnosis of salivary gland acinic cell and mucoepidermoid carcinomas. Head and neck pathology. 2013;7:64-8.

[35] Jiang YH, Cheng B, Ge MH, Zhang G. The prognostic significance of p63 and Ki-67 expression in myoepithelial carcinoma. Head & neck oncology. 2012;4:9.

[36] Cuomo D, Porreca I, Cobellis G, Tarallo R, Nassa G, Falco G, et al. Carcinogenic risk and Bisphenol A exposure: A focus on molecular aspects in endoderm derived glands. Molecular and cellular endocrinology. 2017;457:20-34.

[37] Yaguchi T. The endocrine disruptor bisphenol A promotes nuclear ERRgamma translocation, facilitating cell proliferation of Grade I endometrial cancer cells via EGF-dependent and EGF-independent pathways. Molecular and cellular biochemistry. 2019;452:41-50.

[38] Kim YS, Choi KC, Hwang KA. Genistein suppressed epithelial-mesenchymal transition and migration efficacies of BG-1 ovarian cancer cells activated by estrogenic chemicals via estrogen receptor pathway and downregulation of TGF-beta signaling pathway. Phytomedicine : international journal of phytotherapy and phytopharmacology. 2015;22:993-9.

[39] Castillo Sanchez R, Gomez R, Perez Salazar E. Bisphenol A Induces Migration through a GPER-, FAK-, Src-, and ERK2-Dependent Pathway in MDA-MB-231 Breast Cancer Cells. Chemical research in toxicology. 2016;29:285-95.

[40] Wang KH, Kao AP, Chang CC, Lin TC, Kuo TC. Bisphenol A-induced epithelial to mesenchymal transition is mediated by cyclooxygenase-2 up-regulation in human endometrial carcinoma cells. Reproductive toxicology (Elmsford, NY). 2015;58:229-33.

[41] Chen ZJ, Yang XL, Liu H, Wei W, Zhang KS, Huang HB, et al. Bisphenol A modulates colorectal cancer protein profile and promotes the metastasis via induction of epithelial to mesenchymal transitions. Archives of toxicology. 2015;89:1371-81.

[42] Li H, Qiu Z, Li F, Wang C. The relationship between MMP-2 and MMP-9 expression levels with breast cancer incidence and prognosis. Oncology letters. 2017;14:5865-70.

[43] Kalluri R, Weinberg RA. The basics of epithelial-mesenchymal transition. The Journal of clinical investigation. 2009;119:1420-8.

[44] Satelli A, Li S. Vimentin in cancer and its potential as a molecular target for cancer therapy. Cellular and molecular life sciences : CMLS. 2011;68:3033-46.

[45] Takkunen M, Grenman R, Hukkanen M, Korhonen M, García de Herreros A, Virtanen I. Snail-dependent and -independent epithelial-mesenchymal transition in oral squamous carcinoma cells. The journal of histochemistry and cytochemistry : official journal of the Histochemistry Society. 2006;54:1263-75.

[46] Seyedmajidi M, Seifi S, Moslemi D, Mozaffari SF, Gholinia H, Zolfaghari Z. Immunohistochemical expression of TWIST in oral squamous cell carcinoma and its

correlation with clinicopathologic factors. Journal of cancer research and therapeutics. 2018;14:964-9.

[47] Palacios-Arreola MI, Nava-Castro KE. A single neonatal administration of Bisphenol A induces higher tumour weight associated to changes in tumour microenvironment in the adulthood. 2017;7:10573.

[48] Watkins DJ, Ferguson KK, Anzalota Del Toro LV, Alshawabkeh AN, Cordero JF, Meeker JD. Associations between urinary phenol and paraben concentrations and markers of oxidative stress and inflammation among pregnant women in Puerto Rico. International journal of hygiene and environmental health. 2015;218:212-9.

[49] Acuner-Ozbabacan ES, Engin BH, Guven-Maiorov E, Kuzu G, Muratcioglu S, Baspinar A, et al. The structural network of Interleukin-10 and its implications in inflammation and cancer. BMC genomics. 2014;15 Suppl 4:S2-S.

[50] Chen Y, Xu HS, Guo TL. Modulation of cytokine/chemokine production in human macrophages by bisphenol A: A comparison to analogues and interactions with genistein. Journal of immunotoxicology. 2018;15:96-103.

[51] Lee J, Lim K-T. Plant-originated glycoprotein (36 kDa) suppresses interleukin-4 and -10 in bisphenol A–stimulated primary cultured mouse lymphocytes. Drug and chemical toxicology. 2010;33:421-9.

[52] Bellomo C, Caja L, Moustakas A. Transforming growth factor β as regulator of cancer stemness and metastasis. British Journal Of Cancer. 2016;115:761.

[53] Bolli A, Galluzzo P, Ascenzi P, Del Pozzo G, Manco I, Vietri MT, et al. Laccase treatment impairs bisphenol A-induced cancer cell proliferation affecting estrogen receptor alpha-dependent rapid signals. IUBMB life. 2008;60:843-52.

[54] Shanle EK, Xu W. Endocrine disrupting chemicals targeting estrogen receptor signaling: identification and mechanisms of action. Chemical research in toxicology. 2011;24:6-19.

[55] Wu C, Zhang H-F, Gupta N, Alshareef A, Wang Q, Huang Y-H, et al. A positive feedback loop involving the Wnt/β-catenin/MYC/Sox2 axis defines a highly tumorigenic cell subpopulation in ALK-positive anaplastic large cell lymphoma. Journal of hematology & oncology. 2016;9:120-.

[56] Hua H, Zhang H, Kong Q, Jiang Y. Mechanisms for estrogen receptor expression in human cancer. Experimental hematology & oncology. 2018;7:24-.

[57] Dairkee SH, Luciani-Torres MG, Moore DH, Goodson WH, 3rd. Bisphenol-A-induced inactivation of the p53 axis underlying deregulation of proliferation kinetics, and cell death in non-malignant human breast epithelial cells. Carcinogenesis. 2013;34:703-12.

[58] Shaaban AM, O'Neill PA, Davies MP, Sibson R, West CR, Smith PH, et al. Declining estrogen receptor-beta expression defines malignant progression of human breast neoplasia. The American journal of surgical pathology. 2003;27:1502-12.

[59] Kochmanski J, Marchlewicz EH, Savidge M, Montrose L, Faulk C, Dolinoy DC. Longitudinal effects of developmental bisphenol A and variable diet exposures on epigenetic drift in mice. Reproductive toxicology (Elmsford, NY). 2017;68:154-63.

[60] Liu B, Zhou S, Yang C, Chen P, Chen P, Xi D, et al. Bisphenol A deteriorates egg quality through HDAC7 suppression. Oncotarget. 2017;8:92359-65.

FIGURE CAPTIONS

Fig. 1: Effects of chronic exposure to Bisphenol A (BPA) in the microscopic architecture of the oral mucosa and in the proliferative index of oral keratinocytes. Representative images of the buccal mucosa, tongue and palate of male (a) and female (b) mice receiving BPA (200 mg / L) or vehicle (DMSO, 0.05%). The thickness of epithelium and stratum corneum of male (c, d) and female mice (e, f) from vehicle (n=10 male and n=10 female) and BPA (n=10 male and n=10 female) groups. Representative images and quantification of ki67 immunostained cells/mm2 in male (g, h) and female (i, j). There is a lower number of positive cells in the palate of mice receiving vehicle (DMSO, 200 mg / L/left side image) compared to the BPA group (200 mg/mL/right side image) in the drinking water (n=5 per group). All data are shown as mean ± s.d. (*): $p < 0.05$. Mann Whitney test was used to determine statistical significance between groups.

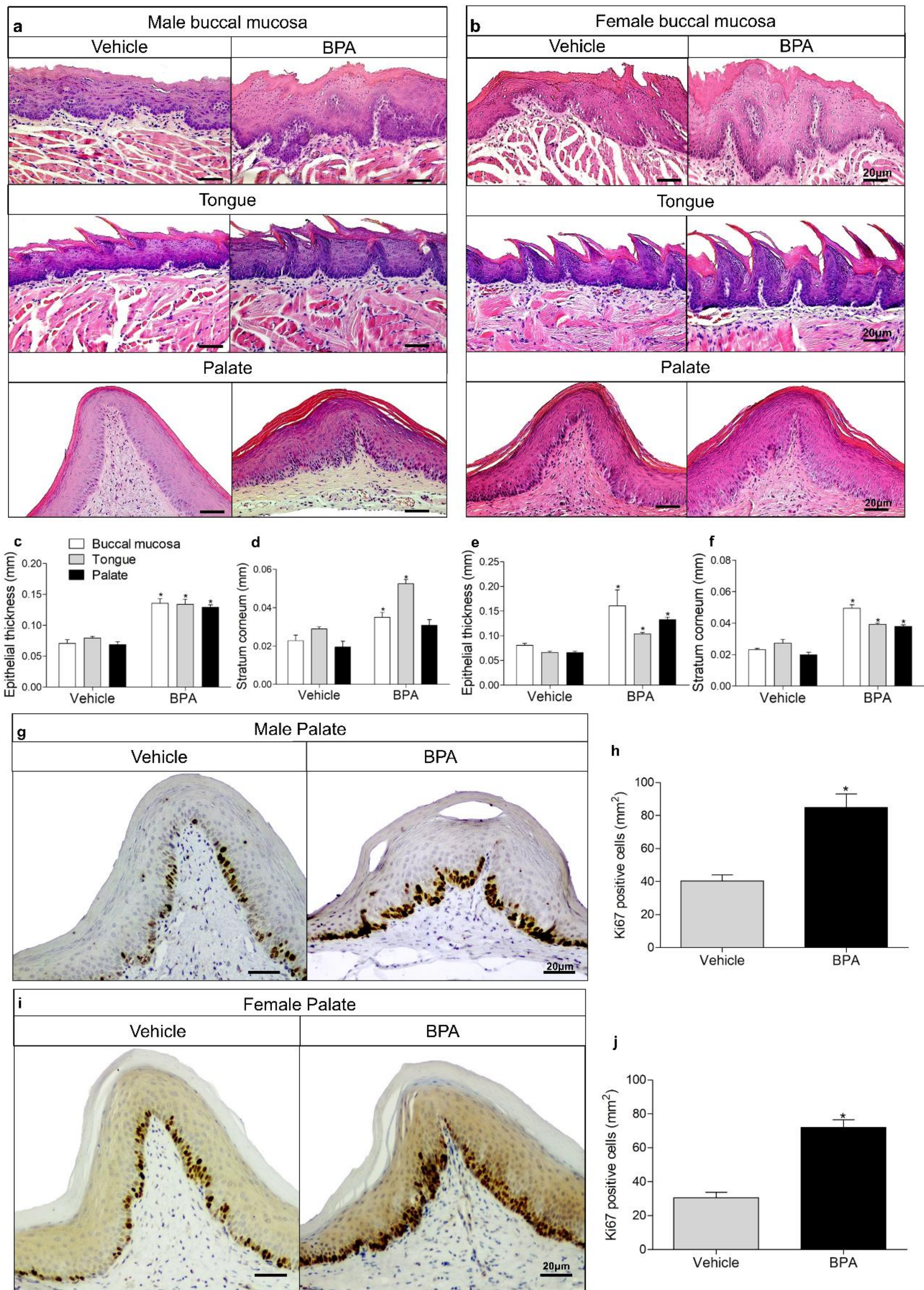
a
Male buccal mucosa
Vehicle
BPA
Tongue
Palate
b
Female buccal mucosa
Vehicle
BPA
20μm
Tongue
Palate
c
Buccal mucosa
Tongue
Palate
Epithelial thickness (mm)
Vehicle
BPA
d
Stratum corneum (mm)
e
Epithelial thickness (mm)
f
Stratum corneum (mm)
g
Male Palate
h
Ki67 positive cells (mm²)
i
Female Palate
j

Fig. 2: Effects of chronic exposure to Bisphenol A in the morphology of the submandibular salivary gland. Representative images of submandibular glands of male (a) and female (b) mice receiving vehicle (DMSO 200 mg / L) or BPA (200 mg / L). Histomorphometry of acini and GCT area of male (c, d) and female (e, f) mice. n=10 per group. (A) represents mice acinis and (G) represents GCT in histologic image. All data are shown as mean ± s.d. (*): $p < 0.05$. Mann Whitney test was used to determine statistical significance between groups. GCT: granulated convoluted tubes.

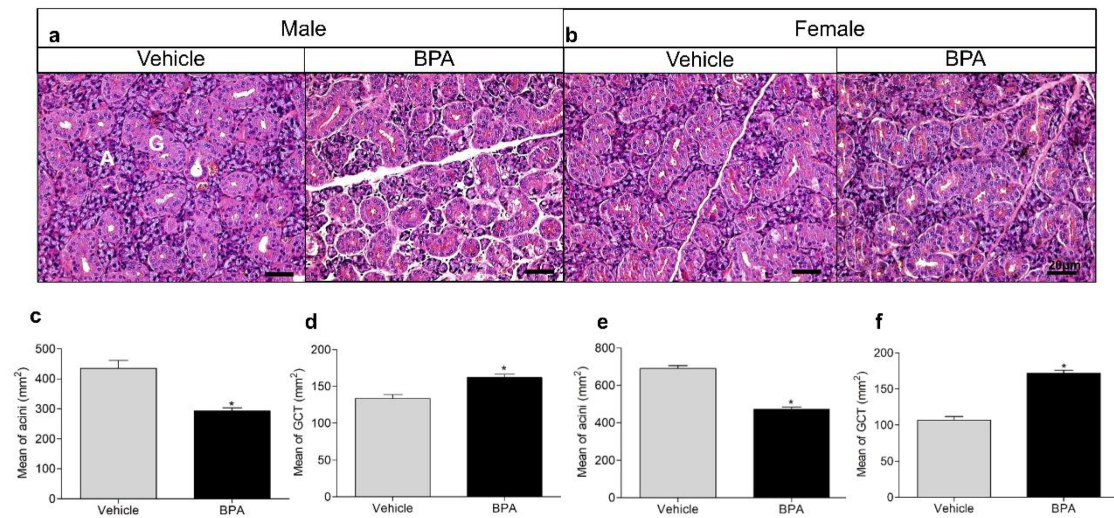

Fig. 3: BPA accumulates in tongue (a) and salivary gland (b) tissues from mice chronically exposed to BPA. The concentrations of BPA in the tongue and submandibular salivary gland of mice chronically exposed to BPA (200 mg / L) in drinking water were measured by gas chromatography-mass spectrometry. n=5 per group. All data are shown as mean ± s.d. (*) $p < 0.05$. Mann Whitney test was used to determine statistical significance between groups.

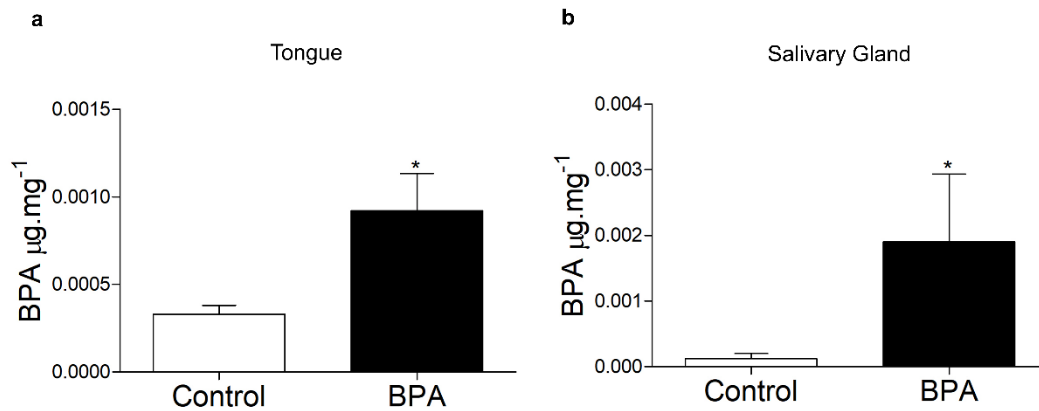

Fig. 4: BPA induces cell proliferation and invasion in oral keratinocytes and OSCC cells in vitro. Colony formation assay in NOK SI (a), HN12 (b) and HN13 (c) stimulated with BPA (10 nM, 500 nM and 1 μM) or vehicle (DMSO 0.05%). Relative ratio of positive / negative Ki67 NOK SI cells treated with BPA (10 nM and 1 μM) or vehicle (DMSO 0.05%) (d) and representative immunofluorescence images of vehicle (e) and BPA 10 nM (f) groups. Number of invaded HN12 cells treated with BPA (10 nM and 1 μM) and vehicle (DMSO 0.05%) (g) and representative images of DAPI stained cells of vehicle (h) BPA 10 nM (i) and BPA 1 μM (j) groups. MMP2 and MMP9 concentration obtained by zymography in HN12 (k, l) and HN13 (m, n) treated with BPA (10 nM, 500 nM and 1 μM) and vehicle (DMSO 0.05%) and respective representative gels. MMP9 levels detected by ELISA in supernatants of HN12 (o) and HN13 (p) cells treated with BPA (10 nM, 500 nM and 1 μM) and vehicle (DMSO 0.05%). All data are shown as mean ± s.e.m for n =3 independent biological replicates (*): $p < 0.05$. One-way Anova test followed by the Bonferroni post-hoc test was used to determine statistical significance among the groups. BPA: bisphenol A; DMSO: Dimethyl sulfoxide; HN12: Head and Neck 12; HN13: Head and Neck 13; MMP2: Matrix Metallopeptidase 2; MMP9: Matrix Metallopeptidase 9; NOK SI: Normal Oral Keratinocytes-Spontaneously Immortalized.

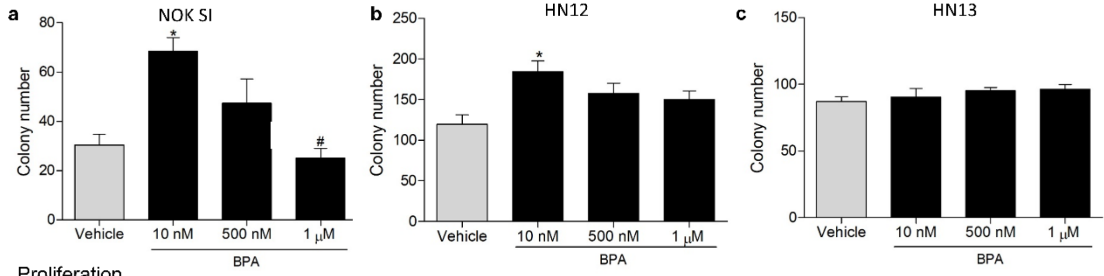
Colony assay
a
NOK SI
Colony number
Vehicle
10 nM
500 nM
1 μM
BPA
b
HN12
c
HN13

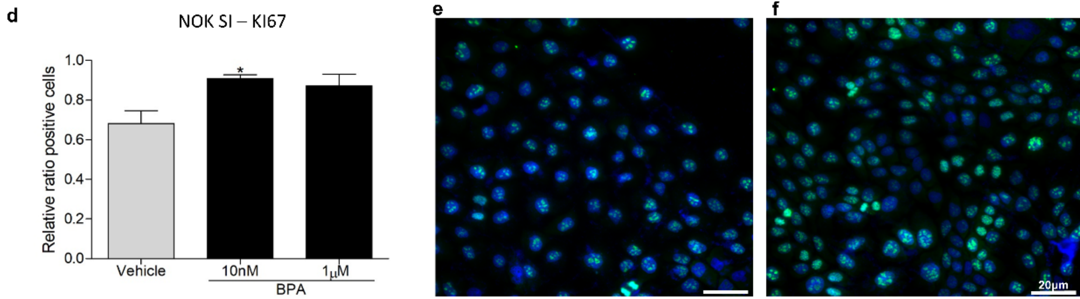
Proliferation
d
NOK SI – KI67
Relative ratio positive cells
Vehicle
10nM
1μM
BPA
e
f
20μm

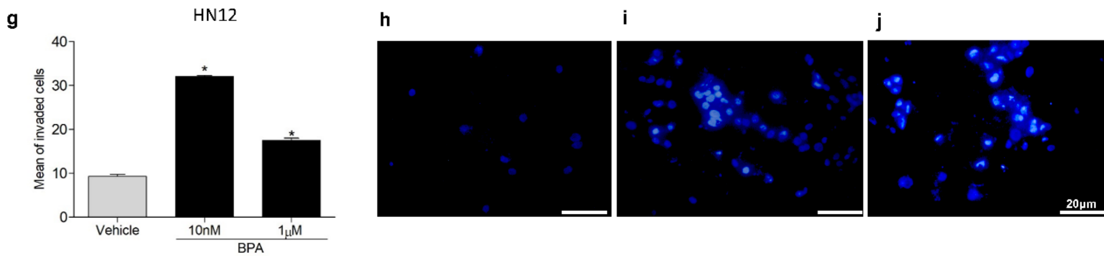
Invasion
g
HN12
Mean of invaded cells
Vehicle
10nM
1μM
BPA
h
i
j
20μm

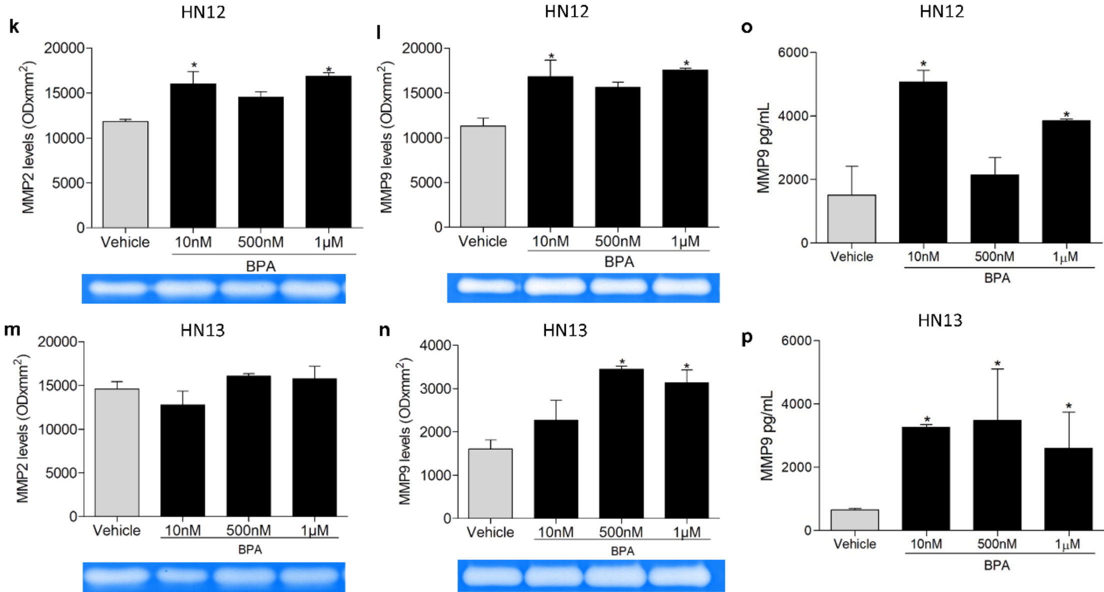
Metalloproteinases
k
HN12
MMP2 levels (ODxmm2)
l
MMP9 levels (ODxmm2)
o
MMP9 pg/mL
m
HN13
n
p
Vehicle
10nM
500nM
1μM
BPA

Fig. 5: BPA induces angiogenesis and VEGF production. The optical density of blood vessels in a model of CAM of chicken after application of supernatants (conditioned media) of HN12 incubated with BPA (10 nM and 1 μM); vehicle (DMSO 0.05%) or culture medium (control) (a, b). VEGF (2000 pg/mL) was used as a positive control. The optical density of blood vessels by using the model of CAM were determined after the application of BPA (10 nM and 1 μM), vehicle and VEGF (2000 pg/mL) in phosphate-buffered saline (PBS) (c, d). VEGF concentration in HN12 supernatants (e). CAM data were shown as optical density ± s.e.m. for n=2 independent biological replicates. Eight eggs were used for each condition. Vessel-like structures in HUVEC cultured with HN12 cell supernatants treated with BPA (10 nM and 1 μM) and vehicle (DMSO 0.05%) (f, g) and representative images (h). HUVEC data are shown as mean ± s.e.m for n=3 independent biological replicates. (*): $p < 0.05$. Mann Whitney test was used to determine statistical significance between groups. CAM: Chorioallantoic Membrane; HN12: Head and Neck 12; HUVEC: Human Umbilical Vein Endothelial Cells; VEGF: Vascular Endothelial Growth Factor.

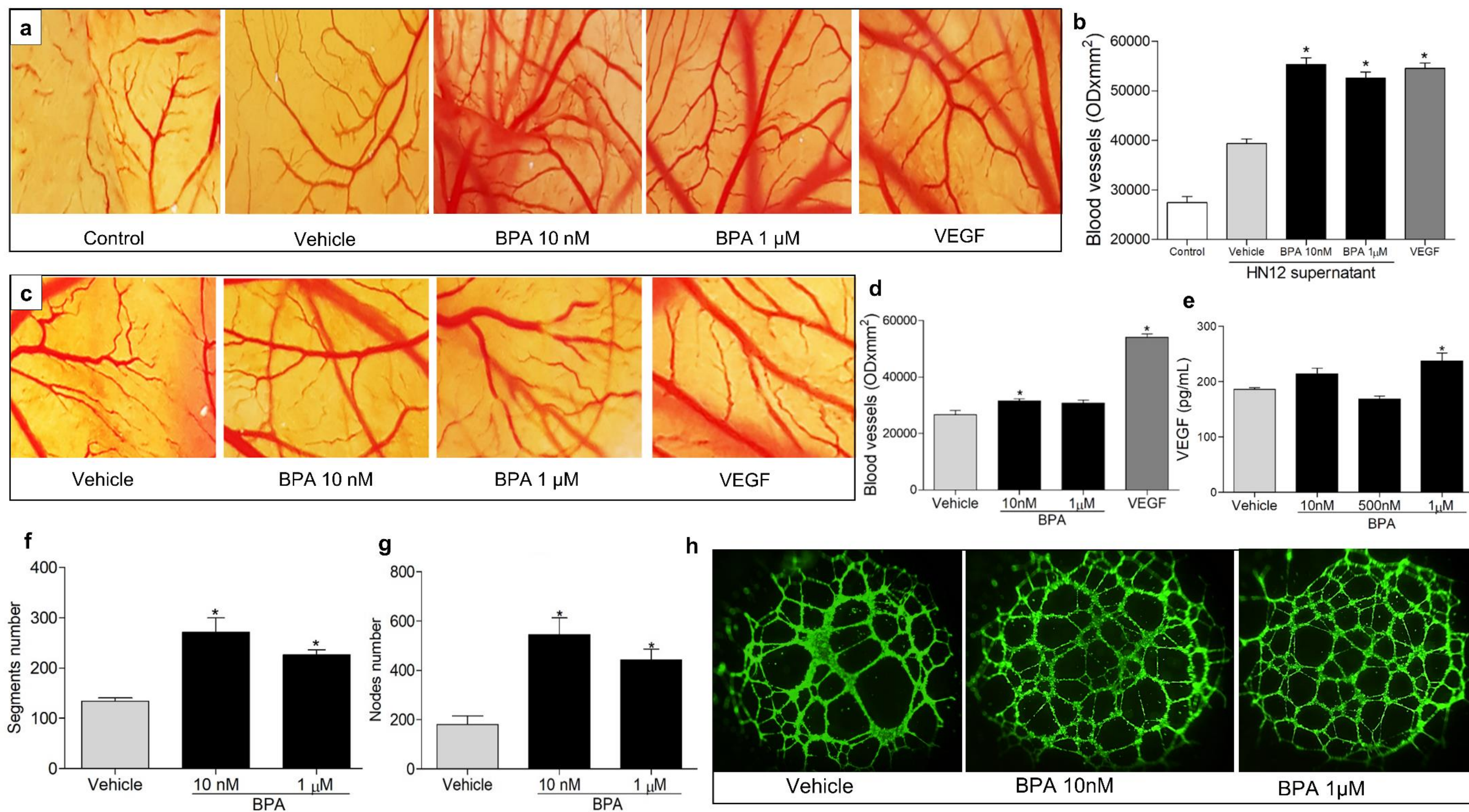
a
Control
Vehicle
BPA 10 nM
BPA 1 μM
VEGF
b
Blood vessels (ODxmm2)
60000
50000
40000
30000
20000
Control
Vehicle
BPA 10nM
BPA 1μM
VEGF
HN12 supernatant
c
Vehicle
BPA 10 nM
BPA 1 μM
VEGF
d
Blood vessels (ODxmm2)
60000
40000
20000
0
Vehicle
10nM
1μM
VEGF
BPA
e
VEGF (pg/mL)
300
200
100
0
Vehicle
10nM
500nM
1μM
BPA
f
Segments number
400
300
200
100
0
Vehicle
10 nM
1 μM
BPA
g
Nodes number
800
600
400
200
0
Vehicle
10 nM
1 μM
BPA
h
Vehicle
BPA 10nM
BPA 1μM

Fig. 6: BPA alters the production of cytokines and growth factors in NOK SI and HN12 cells. EGF, TGF-β and IL-10 production were assessed in NOK SI (a-i), and HN12 (j-r) supernatants after 24, 48 and 72 hours of BPA stimuli (10 nM, 500 nM and 1 μM). Mean of vehicle group is represented by the dotted line. All data are shown as means ± s.e.m for samples in duplicate. (*): $p < 0.05$. One-way ANOVA test followed by the Bonferroni posthoc test was used to determine statistical significance between groups. EGF: Epidermal Growth Factor; HN12: Head and Neck 12; IL-10: Interleukin 10; NOK SI: Normal Oral Keratinocytes-Spontaneously Immortalized; TGF- β: Transforming Growth Factor Beta.

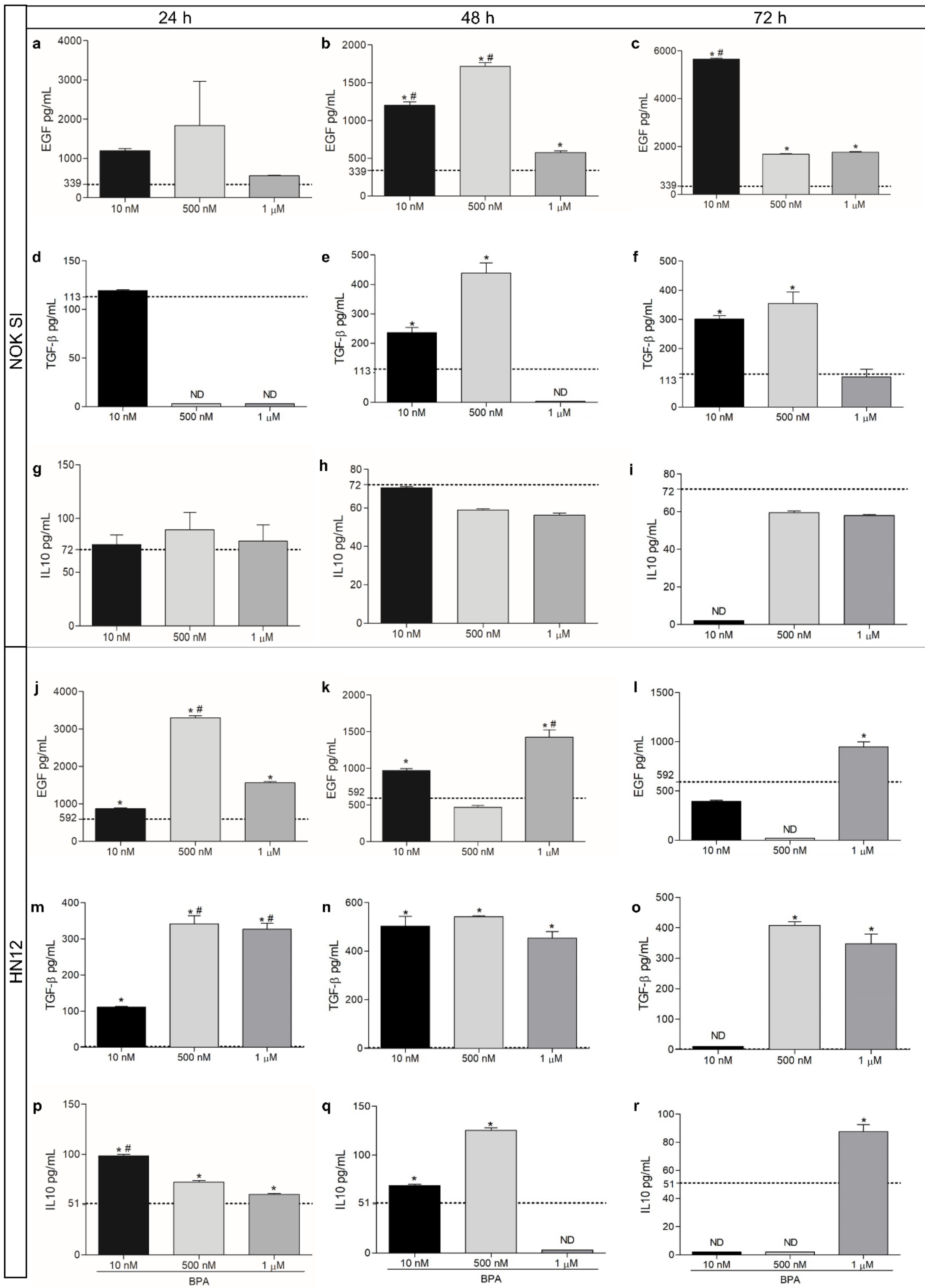

24 h
48 h
72 h
NOK SI
HN12
EGF pg/mL
TGF-β pg/mL
IL10 pg/mL
10 nM
500 nM
1 μM
BPA
ND

Fig. 7: BPA triggers signaling pathways involved with survival, proliferation and H3 histone acetylation. NOK SI (a), HN12 (b) and HN13 (c) cells were stimulated with BPA (10 nM, 500 nM and 1 μM) and collected after 2 and 24 hours. The following primary antibodies were used for: c-Myc; total and phosphorylated AKT, ERK, NF-κB and STAT3; total and acetylated H3 histone. GAPDH or β-actin were used as a loading control. Equal amounts of protein (30 μg) from each sample were subjected to SDS-PAGE and Western blot. AKT: Protein kinase B; NF-κB: Nuclear Factor kappa-light-chain-enhancer of Activated B cells; ERK: Extracellular Signal-Regulated Kinase; GAPDH: Glyceraldehyde 3-Phosphate Dehydrogenase; HN12: Head and Neck 12; HN13: Head and Neck 13; NOK SI: Normal Oral Keratinocytes-Spontaneously Immortalized; STAT3: Signal transducer and activator of transcription 3.

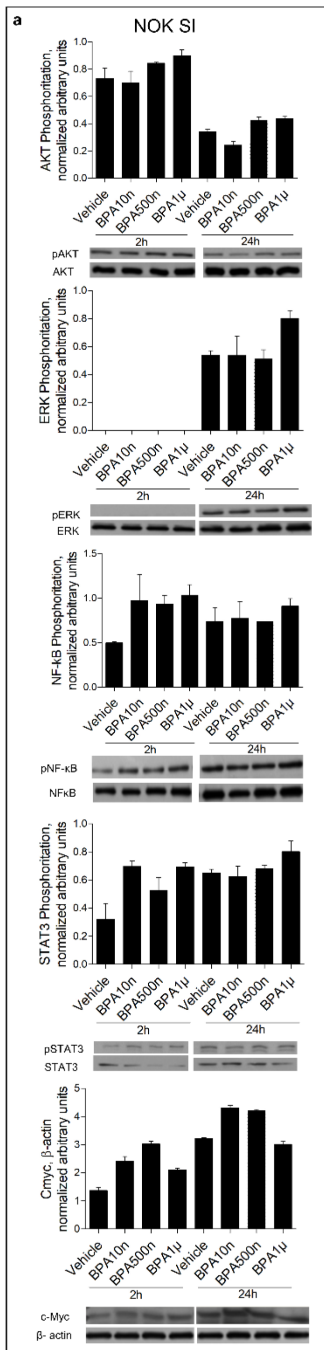

a
NOK SI
AKT Phosphoritation, normalized arbitrary units
Vehicle
BPA10n
BPA500n
BPA1μ
2h
24h
pAKT
AKT
ERK Phosphoritation, normalized arbitrary units
pERK
ERK
NF-κB Phosphoritation, normalized arbitrary units
pNF-κB
NFκB
STAT3 Phosphoritation, normalized arbitrary units
pSTAT3
STAT3
Cmyc, β-actin normalized arbitrary units
c-Myc
β- actin

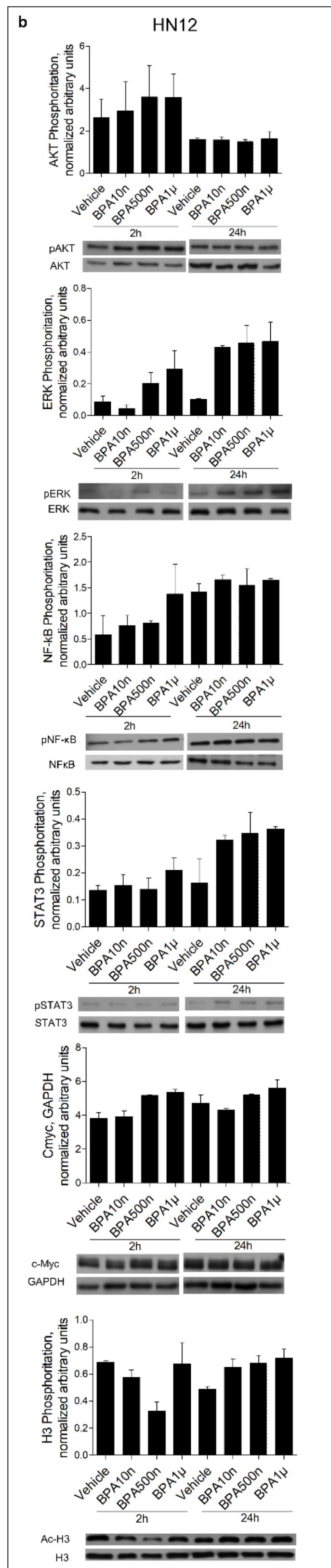

b
HN12
AKT Phosphoritation, normalized arbitrary units
Vehicle
BPA10n
BPA500n
BPA1μ
2h
24h
pAKT
AKT
ERK Phosphoritation, normalized arbitrary units
pERK
ERK
NF-kB Phosphoritation, normalized arbitrary units
pNF-κB
NFκB
STAT3 Phosphoritation, normalized arbitrary units
pSTAT3
STAT3
Cmyc, GAPDH normalized arbitrary units
c-Myc
GAPDH
H3 Phosphoritation, normalized arbitrary units
Ac-H3
H3

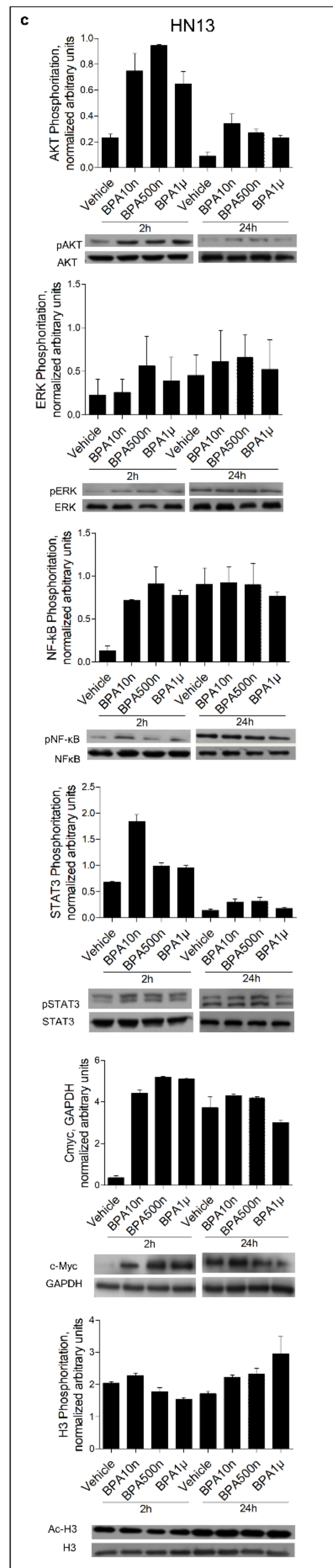

c
HN13
AKT Phosphoritation, normalized arbitrary units
Vehicle
BPA10n
BPA500n
BPA1μ
2h
24h
pAKT
AKT
ERK Phosphoritation, normalized arbitrary units
pERK
ERK
NF-kB Phosphoritation, normalized arbitrary units
pNF-κB
NFκB
STAT3 Phosphoritation, normalized arbitrary units
pSTAT3
STAT3
Cmyc, GAPDH normalized arbitrary units
c-Myc
GAPDH
H3 Phosphoritation, normalized arbitrary units
Ac-H3
H3

Fig. 8: Heat map of molecular pathways affected by BPA in the NOK SI, HN12 and HN13 cell lines. PCR array analysis of growth factors and markers of proliferation, apoptosis, EMT, angiogenesis, histone deacetylase and BPA-related receptors markers in the oral cell lines treated with BPA (10 nM), vehicle (DMSO, 0.05%) or untreated cells (control). Data were obtained when comparing the relative expression of the different groups normalized to the control. One-way ANOVA test followed by the Bonferroni post-hoc test was used to determine statistical significance between groups. (*): $p < 0.05$. AR: Androgen Receptor; BAD: BCL2 associated agonist of cell death; BAX: BCL2 associated X; BCL2: B-cell lymphoma protein 2; BMP7: bone morphogenetic protein 7; CASP3: Caspase 3; CASP8; Caspase 8; CASP9: Caspase 9; EGF: Epidermal Growth Factor; EGFR: Epidermal Growth Factor Receptor; EMT: Epithelial Mesenchymal Transition; ESRRG: Estrogen Related Receptor Gamma; HDAC1: Histone Deacetylase 1; HDAC3: Histone Deacetylase 3; HDAC5: Histone Deacetylase 5; HDAC7: Histone Deacetylase 7; HN12: Head and Neck 12; HN13: Head and Neck 13; IGF1R: Insulin Like Growth Factor 1 Receptor; MAPK3: Mitogen-Activated Protein Kinase 3; MMP2: Matrix Metallopeptidase 2; MMP3: Matrix Metallopeptidase 3; MMP9: Matrix Metallopeptidase 9; NOK SI: Normal Oral Keratinocytes-Spontaneously Immortalized; SNAI1: snail family transcriptional repressor 1; SNAI2: snail family transcriptional repressor 2; SNAI3: snail family transcriptional repressor 3; TWIST1: twist family bHLH transcription factor 1; TP53: tumor protein p53; TGFB1: transforming growth factor beta 1; VEGF: vascular endothelial growth factor B.

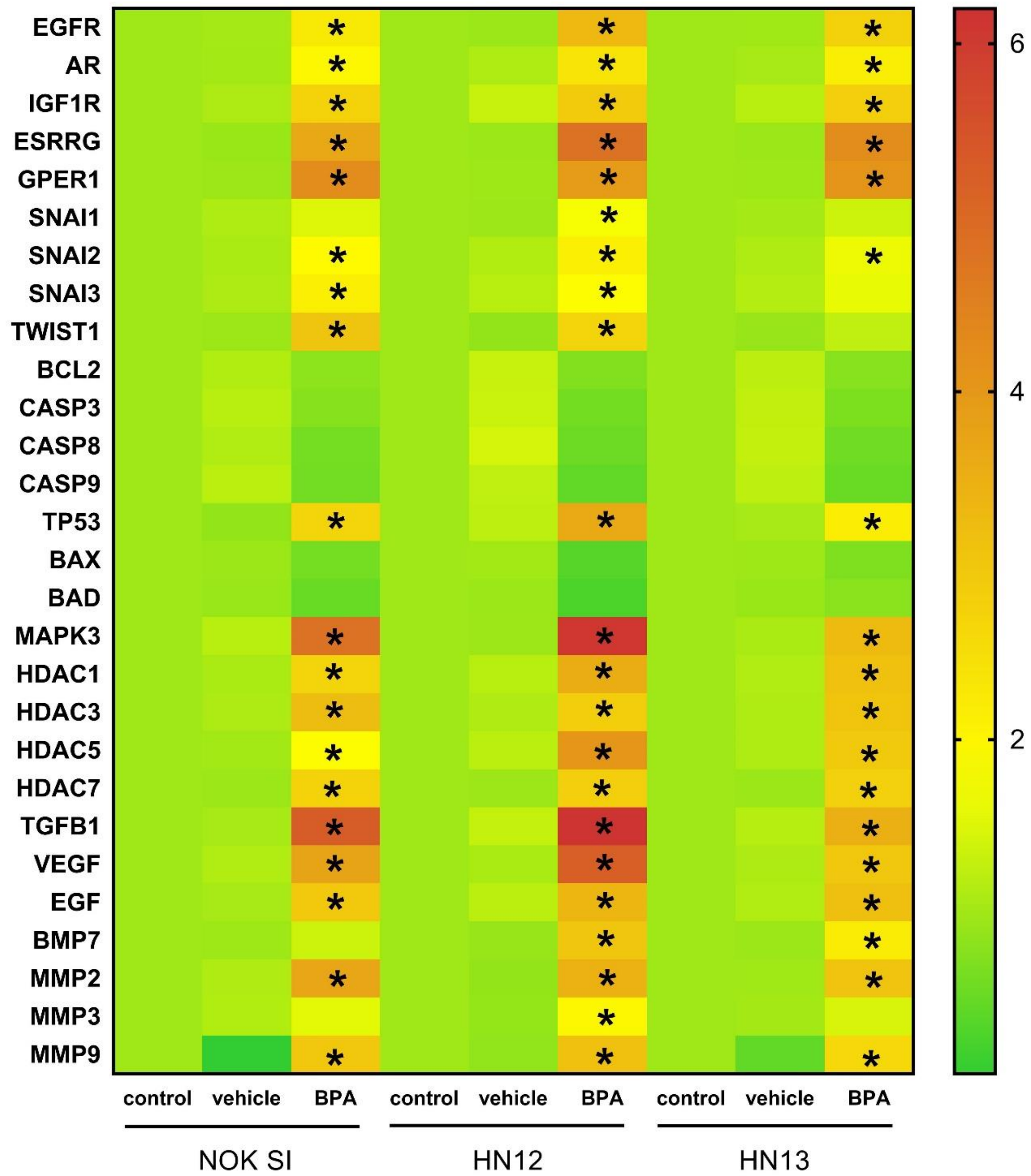
EGFR
AR
IGF1R
ESRRG
GPER1
SNAI1
SNAI2
SNAI3
TWIST1
BCL2
CASP3
CASP8
CASP9
TP53
BAX
BAD
MAPK3
HDAC1
HDAC3
HDAC5
HDAC7
TGFB1
VEGF
EGF
BMP7
MMP2
MMP3
MMP9
control
vehicle
BPA
NOK SI
HN12
HN13
6
4
2

Fig. 9: BPA modifies estrogen receptors (ER) expression and activates clonogenicity in an ER-dependent manner. ERα and ERβ expression of NOK SI (a) and HN12 (b) cells treated with BPA (10 nM) or vehicle (0.005%). Normalization was performed by untreated cells control. Mann Whitney test was used to determine statistical significance between groups. Effect of ER antagonist on colony formation assay in NOK SI and HN12 treated with Control (untreated cells) BPA (10 nM) or vehicle (DMSO 0.05%) (c, d). One-way ANOVA test followed by the Bonferroni post-hoc test was used to determine statistical significance between groups. All data are shown as means ± s.e.m. for n =2 independent biological replicates. (*): $p < 0.05$. HN12: Head and Neck 12; NOK SI: Normal Oral Keratinocyte-Spontaneously Immortalized.

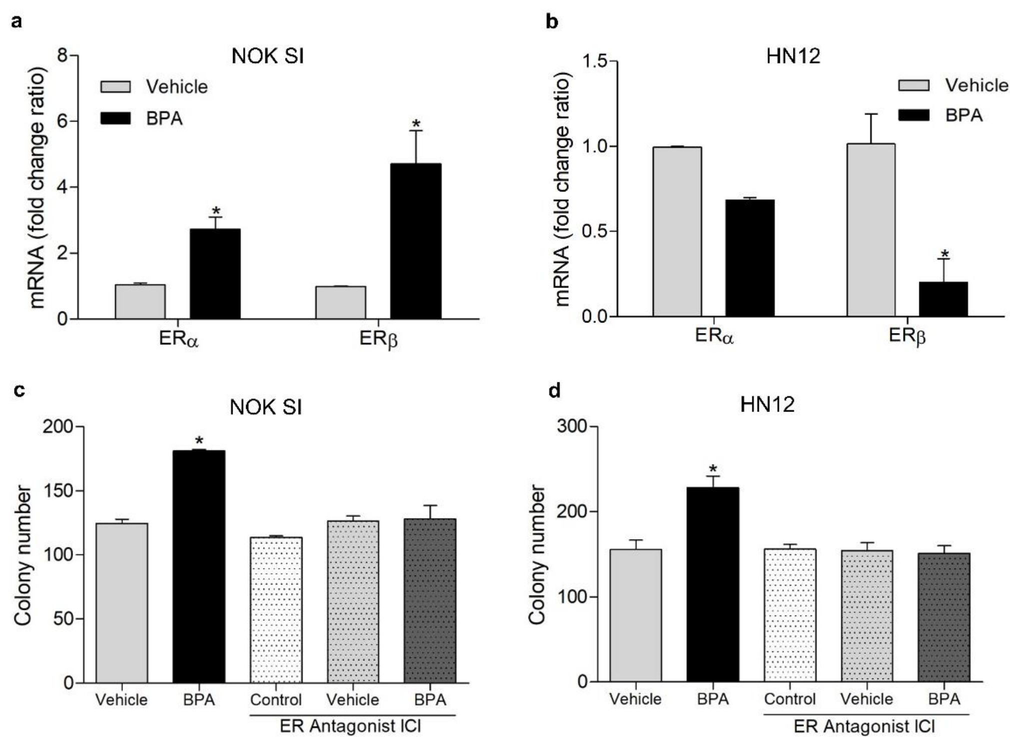

SUPPLEMENTARY DATA

Supplementary 1: Frequency of lesions observed in the mammary gland and the dorsolateral prostate. Frequency of mammary lesions (a) and prostate lesions (b). Histopathology of dorsolateral prostate in animals treated with BPA (c). The arrow in the magnified image (insert) represents nuclear atypia with hypertrophic nuclei and evident nucleolus. Thickening of the muscular layer (trait) involving acini with Prostatic Intraepithelial Neoplasia (PIN) lesions (*). N= 20. A one-way ANOVA test followed by the Bonferroni posthoc test was used to determine statistical significance between groups. All data are shown as means ± s.e.m. p < 0.05 (*): intragroup (#): intergroup. Ne: normal epithelium. Scale bars means 50 μm.

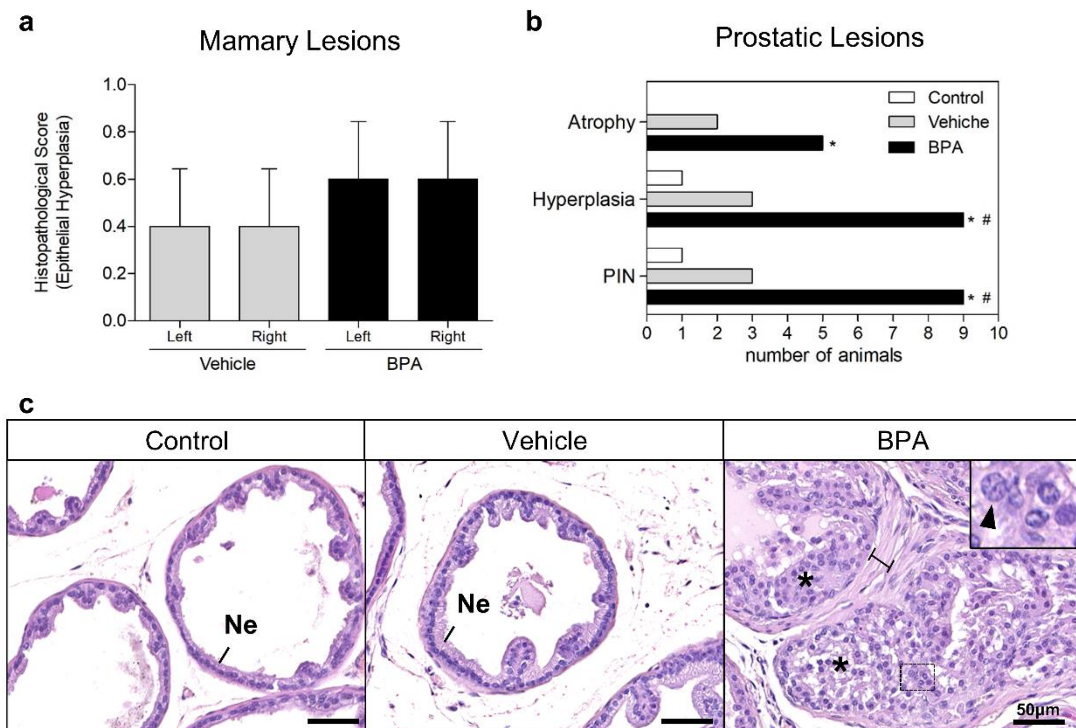

Supplementary 2: Relative cell viability by rezasurin in NOK SI (a-c), HN12 (d-f) and HN13 (g-i), UM HMC1 (j-l) and UM HMC3a (m-o), at 48, 72 and 120 hours. All data are shown as means ± s.e.m. for n =2 independent biological replicates. (*): $p < 0.05$. One-way ANOVA test followed by the Bonferroni post-hoc test was used to determine statistical significance between groups. HN12: Head and Neck 12; HN13: Head and Neck 13; NOK SI: Normal Oral Keratinocytes-Spontaneously Immortalized; UM HMC1: Human mucoepidermoid carcinoma cells 1; UM HMC3a: Human mucoepidermoid carcinoma cells 3a.

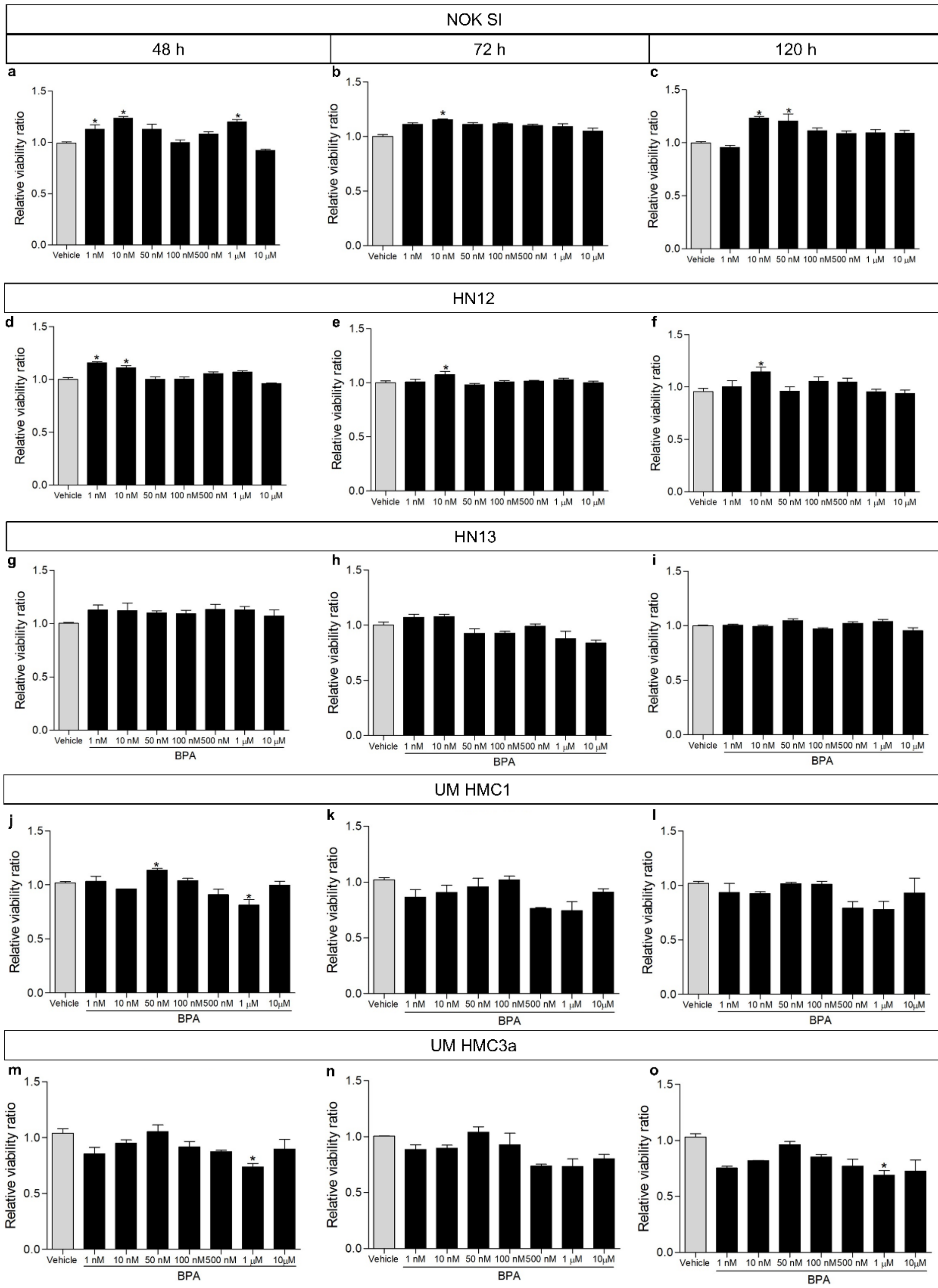
NOK SI
48 h
72 h
120 h
HN12
HN13
UM HMC1
UM HMC3a
Relative viability ratio
Vehicle
1 nM
10 nM
50 nM
100 nM
500 nM
1 μM
10 μM
BPA
a
b
c
d
e
f
g
h
i
j
k
l
m
n
o

Supplementary 3: UM HMC1 and UM HMC3a immunocytochemical and immunoblotting. The relative ratio of positive Ki67 cells in UM HMC1 (a) and UM HMC3a (b). The relative ratio of positive p63 cells in UM HMC1 (c) and UM HMC3a (d). Representative immunocytochemical images of p63 stain in vehicle and BPA 50 nM groups (e). Immunoblotting analysis of UM HMC1 and UM HMC3a (f). Cells were processed after 2 and 24 hours of cell culture under BPA incubation (50 nM). Primary antibodies for protein total and phosphorylated forms of AKT, ERK and NF-κB proteins were used. GAPDH was the loading control. Equal amounts of protein (30 μg) from each sample were subjected to SDS-PAGE and Western blot. All data are shown as means ± s.e.m. for n =2 independent biological replicates. (*): $p < 0.05$. Mann Whitney test was used to determine statistical significance between groups. UM HMC1: Human mucoepidermoid carcinoma cells 1; UM HMC3a: Human mucoepidermoid carcinoma cells 3a.

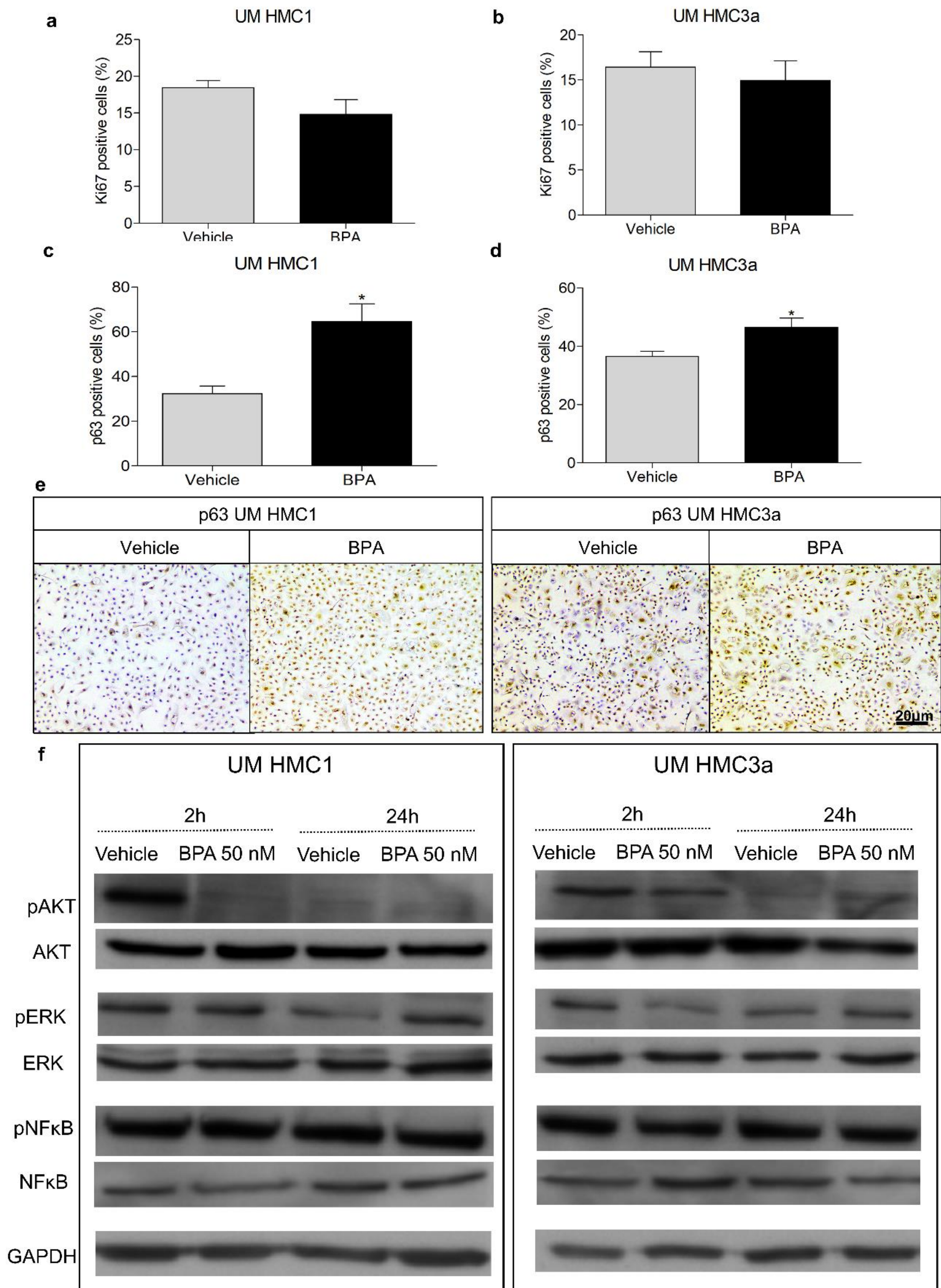
a
UM HMC1
Ki67 positive cells (%)
25
20
15
10
5
0
Vehicle
BPA
b
UM HMC3a
Ki67 positive cells (%)
20
15
10
5
0
Vehicle
BPA
c
UM HMC1
p63 positive cells (%)
80
60
40
20
0
*
Vehicle
BPA
d
UM HMC3a
p63 positive cells (%)
60
40
20
0
*
Vehicle
BPA
e
p63 UM HMC1
Vehicle
BPA
p63 UM HMC3a
Vehicle
BPA
20μm
f
UM HMC1
2h
24h
Vehicle
BPA 50 nM
Vehicle
BPA 50 nM
UM HMC3a
2h
24h
Vehicle
BPA 50 nM
Vehicle
BPA 50 nM
pAKT
AKT
pERK
ERK
pNFκB
NFκB
GAPDH

Supplementary 4: Immunocytochemical analysis of the Ki67 marker in HaCat and SCC25 cell lines. BPA increases HaCat and SCC25 relative ratio of positive Ki67 cells (a,b). All data are shown as means ± s.e.m. for n =2 independent biological replicates. (*): $p < 0.05$. A one-way ANOVA test followed by the Bonferroni posthoc test was used to determine statistical significance between groups. HaCat: human keratinocytes; SCC25: oral squamous cell carcinoma 25.

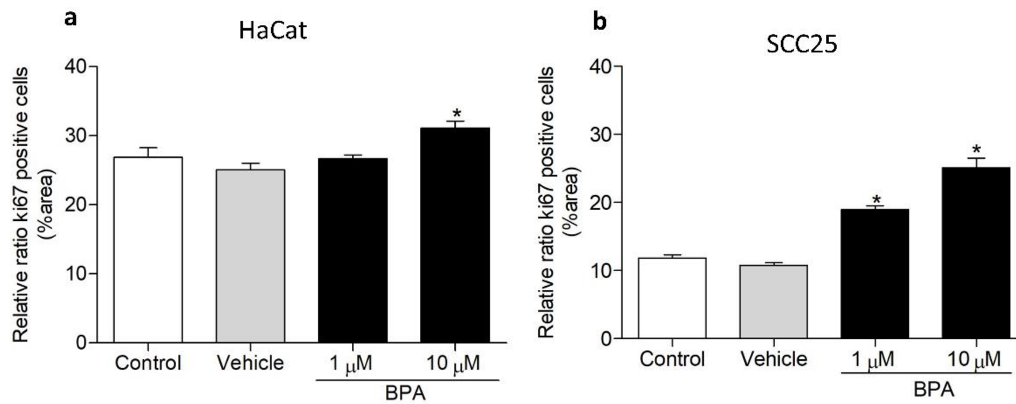

Supplementary 5: Immunoblotting analysis of HN12 cell line stimulated with BPA (10 nM, 500 nM and 1 μM) and collected after 72 hours. Vimentin primary antibodies was used. β-actin were used as a loading control. Equal amounts of protein (30 μg) from each sample were subjected to SDS-PAGE and Western blot. HN12: Head and Neck 12.

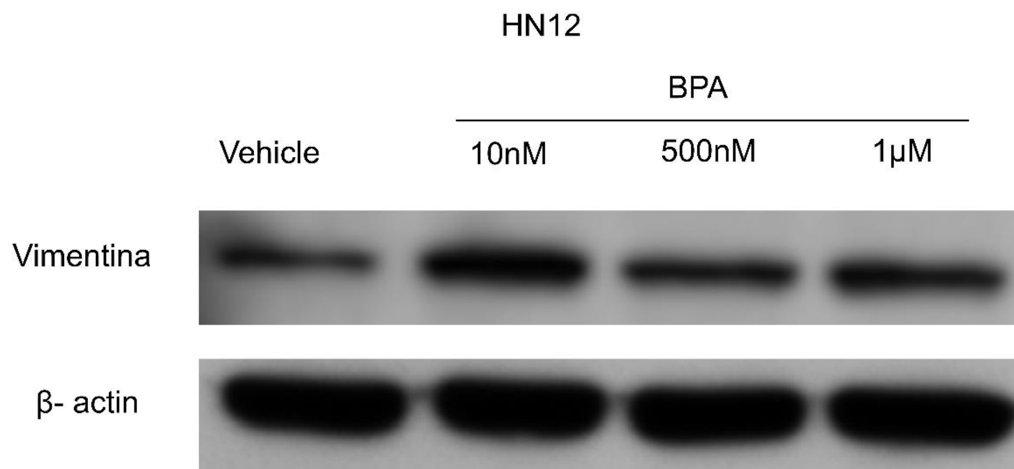

6 CONCLUSÕES

Com base nos dados obtidos, podemos concluir que:

1) A exposição crônica ao BPA resulta em alterações morfológicas dos tecidos orais de camundongos como o aumento da espessura epitelial e proliferação das células da camada basal. Na glândula salivar submandibular foi observado uma redução do número de ácinos;

2) O BPA ingerido via oral é acumulado nas mucosas de língua e na glândula salivar submandibular de camundongos;

3) O BPA induz a proliferação de queratinócitos *in vitro*, bem como alterações nas vias de sinalização ERK, STAT3, AKT e NFκB relacionadas a proliferação e sobrevivência celular;

4) Em linhagens de CCE da cavidade oral, o tratamento com BPA induziu a proliferação, invasão celular, liberação de fatores de crescimento e angiogênese;

5) Em linhagens de carcinoma mucoepidermóide de glândula salivar o BPA não induz proliferação e aumenta a expressão de p63;

6) O efeito do BPA estão possivelmente associados à interação BPA-receptores de estrógeno e à acetilação de histonas.

7 CONSIDERAÇÕES FINAIS

Baixas doses de substâncias químicas desreguladoras endócrinas foram definidas pelo National Institute of Environmental Health Sciences (NIEHS) como doses abaixo do NOAEL aceito para o produto químico (SCREENING; COMMITTEE, 1998) que, para o BPA, são doses abaixo de 5 mg / kg de peso corporal / dia. Mas, apesar disso, existem atualmente, diversos estudos descrevendo efeitos de baixas doses de BPA em animais, incluindo alterações morfológicas e tumorais em próstata, alterações neoplásicas em glândulas mamárias, infertilidade, início precoce de puberdade dentre outras (RICHTER; BIRNBAUM; FARABOLLINI; NEWBOLD *et al.*, 2007; SEACHRIST; BONK; HO; PRINS *et al.*, 2016).

A exposição humana ao BPA ocorre diariamente e de maneira constante, através da ingestão, contato com a pele ou até mesmo durante a respiração (VANDENBERG; HAUSER; MARCUS; OLEA *et al.*, 2007), sendo praticamente impossível de ser quantificada. Seus efeitos podem ser desencadeados a longo prazo, sendo até mesmo transmitido através da gestação para o feto, sem uma ação imediata, o que torna ainda mais preocupante a exposição generalizada e não quantificada a este monômero.

Corroborando com os efeitos causados pelo BPA em baixa dose já comprovados, no presente estudo observamos que o tratamento *in vitro* com baixa dose de BPA induziu a proliferação celular e alteração dos níveis de citocinas, fatores de crescimento e metaloproteinases, além de aumentar a expressão de ERα e ERβ em queratinócitos. As células neoplásicas também exibiram aumento da capacidade de invasão, produção de citocinas, alterações dos fatores de crescimento e aumento da angiogênese após o tratamento com BPA.

Já nos experimentos *in vivo* a exposição crônica ao BPA exerceu alterações nas mucosas orais, com um aumentou de espessura de mucosa bucal, língua e palato de camundongos, bem como alterações atróficas na glândula submandibular. Não foram observadas alterações displásicas e invasão das células epiteliais no tecido conjuntivo, mas comprovou-se que o BPA pode ser acumulado em mucosa oral e glândula salivar.

Recentemente foi descrita pela primeira vez uma perspectiva de delineamento de evidências, que propôs um potencial vínculo entre BPA e o câncer de boca e orofaringe com base em uma revisão da literatura das vias de ativação e

mecanismos de ação do BPA em outros órgãos e tecidos já estudados (EMFIETZOGLOU; SPYROU; MANTZOROS; DALAMAGA, 2019), enfatizando a necessidade de investigação do efeito de exposição ao BPA na carcinogênese do tecido oral.

Assim o presente estudo original, apresenta novos dados experimentais que mostram que o BPA induz alterações nos tecidos orais e tem como alvo sinais intracelulares através de vias dependentes do receptor de estrógeno. Além disso, o BPA interrompe a função normal dos queratinócitos e nas células tumorais leva a eventos epigenéticos proliferativos, invasivos e aumenta a produção de citocinas e fatores de crescimento comumente ativados no câncer de boca. Apesar de apresentar as limitações de estudos *in vitro* e *in vivo* em roedores, o presente trabalho abre perspectiva para avaliação de mais um possível fator de risco ao câncer de boca, bem como da necessidade de investigação de uma potencial relação com outros tumores de cabeça e pescoço.

REFERÊNCIAS

ACEVEDO, N.; DAVIS, B.; SCHAEBERLE, C. M.; SONNENSCHEIN, C. *et al.* Perinatally administered bisphenol a as a potential mammary gland carcinogen in rats. **Environ Health Perspect**, 121, n. 9, p. 1040-1046, Sep 2013.

AKRISH, S.; PELED, M.; BEN-IZHAK, O.; NAGLER, R. M. Malignant salivary gland tumors and cyclo-oxygenase-2: a histopathological and immunohistochemical analysis with implications on histogenesis. **Oral Oncol**, 45, n. 12, p. 1044-1050, Dec 2009.

ALAM, H.; BHATE, A. V.; GANGADARAN, P.; SAWANT, S. S. *et al.* Fascin overexpression promotes neoplastic progression in oral squamous cell carcinoma. **BMC Cancer**, 12, p. 32, 2012.

ALTAMIRANO, G. A.; MUNOZ-DE-TORO, M.; LUQUE, E. H.; GOMEZ, A. L. *et al.* Milk lipid composition is modified by perinatal exposure to bisphenol A. **Mol Cell Endocrinol**, 411, p. 258-267, Aug 15 2015.

ARANA, V.; KATCHBURIAN, E. **Histologia e embriologia oral: texto - atlas - correlações clínicas**. Guanabara, 2012. 9788527721431.

AYYANAN, A.; LARIBI, O.; SCHUEPBACH-MALLEPELL, S.; SCHRICK, C. *et al.* Perinatal exposure to bisphenol a increases adult mammary gland progesterone response and cell number. **Mol Endocrinol**, 25, n. 11, p. 1915-1923, Nov 2011.

BARNES, L.; EVERSON, J. W.; REICHART, P.; SIDRANSKY, D. **World Health Organization. Classification of tumours. Pathology and Genetics of Head and Neck Tumours**. Lyon: IARC Press, 2005. 9789283224174.

BETANCOURT, A. M.; MOBLEY, J. A.; RUSSO, J.; LAMARTINIERE, C. A. Proteomic analysis in mammary glands of rat offspring exposed in utero to bisphenol A. **J Proteomics**, 73, n. 6, p. 1241-1253, Apr 18 2010.

BRASIL. Ministério da Saúde. Instituto Nacional de Câncer José Alencar Gomes da, Silva. Estimativa 2020: incidência de câncer no Brasil. **INCA**, 2019.

BRAY, F.; FERLAY, J.; SOERJOMATARAM, I.; SIEGEL, R. L. *et al.* Global cancer statistics 2018: GLOBOCAN estimates of incidence and mortality worldwide for 36 cancers in 185 countries. **CA Cancer J Clin**, 68, n. 6, p. 394-424, Nov 2018.

CHANG, Y. L.; HSU, Y. K.; WU, T. F.; HUANG, C. M. *et al.* Regulation of estrogen receptor alpha function in oral squamous cell carcinoma cells by FAK signaling. **Endocr Relat Cancer**, 21, n. 4, p. 555-565, Aug 2014.

CHATURVEDI, A. K.; ENGELS, E. A.; ANDERSON, W. F.; GILLISON, M. L. Incidence trends for human papillomavirus-related and -unrelated oral squamous cell carcinomas in the United States. **J Clin Oncol**, 26, n. 4, p. 612-619, Feb 1 2008.

COLELLA, G.; IZZO, G.; CARINCI, F.; CAMPISI, G. *et al.* Expression of sexual hormones receptors in oral squamous cell carcinoma. **Int J Immunopathol Pharmacol**, 24, n. 2 Suppl, p. 129-132, Apr-Jun 2011.

COOPER, J. E.; KENDIG, E. L.; BELCHER, S. M. Assessment of bisphenol A released from reusable plastic, aluminium and stainless steel water bottles. **Chemosphere**, 85, n. 6, p. 943-947, Oct 2011.

CURADO, M. P.; HASHIBE, M. Recent changes in the epidemiology of head and neck cancer. **Curr Opin Oncol**, 21, n. 3, p. 194-200, May 2009.

DEKANT, W.; VOLKEL, W. Human exposure to bisphenol A by biomonitoring: methods, results and assessment of environmental exposures. **Toxicol Appl Pharmacol**, 228, n. 1, p. 114-134, Apr 1 2008.

DODDS, E. C.; LAWSON, W. Molecular structure in relation to oestrogenic activity. Compounds without a phenanthrene nucleus. **Proceedings of the Royal Society of London. Series B, Biological Sciences**, p. 222-232, 1938.

EL-NAGGAR, A. K.; CHAN, J. K. C.; GRANDIS, J. R.; TAKATA, T. *et al.* **WHO Classification of Head and Neck Tumours**. 4 ed. Lyon: IACR: 2017.

EMFIETZOGLOU, R.; SPYROU, N.; MANTZOROS, C. S.; DALAMAGA, M. Could the endocrine disruptor bisphenol-A be implicated in the pathogenesis of oral and oropharyngeal cancer? Metabolic considerations and future directions. **Metabolism**, 91, p. 61-69, Feb 2019.

EVERSOLE, L. R. Mucoepidermoid carcinoma: review of 815 reported cases. **J Oral Surg**, 28, n. 7, p. 490-494, Jul 1970.

FERGUSON, K. K.; MCELRATH, T. F.; CANTONWINE, D. E.; MUKHERJEE, B. *et al.* Phthalate metabolites and bisphenol-A in association with circulating angiogenic biomarkers across pregnancy. **Placenta**, 36, n. 6, p. 699-703, Jun 2015.

FOLIA, M.; BOUDALIA, S.; MENETRIER, F.; DECOCQ, L. *et al.* Oral homeostasis disruption by medical plasticizer component bisphenol A in adult male rats. **Laryngoscope**, 123, n. 6, p. 1405-1410, Jun 2013.

FREDERIKSEN, H.; JORGENSEN, N.; ANDERSSON, A. M. Correlations between phthalate metabolites in urine, serum, and seminal plasma from young Danish men determined by isotope dilution liquid chromatography tandem mass spectrometry. **J Anal Toxicol**, 34, n. 7, p. 400-410, Sep 2010.

GAO, H.; YANG, B. J.; LI, N.; FENG, L. M. *et al.* Bisphenol A and hormone-associated cancers: current progress and perspectives. **Medicine (Baltimore)**, 94, n. 1, p. e211, Jan 2015.

GAO, M.; HAO, Y.; HUANG, M. X.; MA, D. Q. *et al.* Salivary gland tumours in a northern Chinese population: a 50-year retrospective study of 7190 cases. **Int J Oral Maxillofac Surg**, Oct 18 2016.

GARLET, G. P.; HORWAT, R.; RAY, H. L., Jr.; GARLET, T. P. *et al.* Expression analysis of wound healing genes in human periapical granulomas of progressive and stable nature. **Journal of endodontics**, 38, n. 2, p. 185-190, 2012.

GASSMAN, N. R. Induction of oxidative stress by bisphenol A and its pleiotropic effects. **Environ Mol Mutagen**, 58, n. 2, p. 60-71, Mar 2017.

GAYRARD, V.; LACROIX, M. Z.; COLLET, S. H.; VIGUIÉ, C. *et al.* High bioavailability of bisphenol A from sublingual exposure. **Environmental health perspectives**, 121, n. 8, p. 951-956, 2013.

GE, L. C.; CHEN, Z. J.; LIU, H. Y.; ZHANG, K. S. *et al.* Involvement of activating ERK1/2 through G protein coupled receptor 30 and estrogen receptor α/β in low doses of bisphenol A promoting growth of Sertoli TM4 cells. **Toxicol Lett**, 226, n. 1, p. 81-89, Apr 7 2014.

GEENS, T.; AERTS, D.; BERTHOT, C.; BOURGUIGNON, J. P. *et al.* A review of dietary and non-dietary exposure to bisphenol-A. **Food Chem Toxicol**, 50, n. 10, p. 3725-3740, Oct 2012.

GEENS, T.; GOEYENS, L.; COVACI, A. Are potential sources for human exposure to bisphenol-A overlooked? **Int J Hyg Environ Health**, 214, n. 5, p. 339-347, Sep 2011.

GERVÁSIO, O. L.; DUTRA, R. A.; TARTAGLIA, S. M.; VASCONCELLOS, W. A. *et al.* Oral squamous cell carcinoma: a retrospective study of 740 cases in a Brazilian population. **Braz Dent J**, 12, n. 1, p. 57-61, 2001.

GIULIVO, M.; LOPEZ DE ALDA, M.; CAPRI, E.; BARCELO, D. Human exposure to endocrine disrupting compounds: Their role in reproductive systems, metabolic syndrome and breast cancer. A review. **Environ Res**, 151, p. 251-264, Nov 2016.

GLOWACKI, A. J.; YOSHIZAWA, S.; JHUNJHUNWALA, S.; VIEIRA, A. E. *et al.* Prevention of inflammation-mediated bone loss in murine and canine periodontal disease via recruitment of regulatory lymphocytes. **Proceedings of the National Academy of Sciences of the United States of America**, 110, n. 46, p. 18525-18530, 2013.

GOLAS, S. M. Trends in palatine tonsillar cancer incidence and mortality rates in the United States. **Community Dent Oral Epidemiol**, 35, n. 2, p. 98-108, Apr 2007.

GOODE, R. K.; AUCLAIR, P. L.; ELLIS, G. L. Mucoepidermoid carcinoma of the major salivary glands: clinical and histopathologic analysis of 234 cases with evaluation of grading criteria. **Cancer**, 82, n. 7, p. 1217-1224, Apr 1 1998.

GRSIC, K.; OPACIC, I. L.; SITIC, S.; MILKOVIC PERISA, M. *et al.* The prognostic significance of estrogen receptor beta in head and neck squamous cell carcinoma. **Oncol Lett**, 12, n. 5, p. 3861-3865, Nov 2016.

HASSAN, Z. K.; ELOBEID, M. A.; VIRK, P.; OMER, S. A. *et al.* Bisphenol A induces hepatotoxicity through oxidative stress in rat model. **Oxid Med Cell Longev**, 2012, p. 194829, 2012.

HUANG, D.-Y.; ZHENG, C.-C.; PAN, Q.; WU, S.-S. *et al.* Oral exposure of low-dose bisphenol A promotes proliferation of dorsolateral prostate and induces epithelial-mesenchymal transition in aged rats. **Scientific reports**, 8, n. 1, p. 490-490, 2018.

HWANG, K. A.; PARK, M. A.; KANG, N. H.; YI, B. R. *et al.* Anticancer effect of genistein on BG-1 ovarian cancer growth induced by 17 beta-estradiol or bisphenol A via the suppression of the crosstalk between estrogen receptor alpha and insulin-like growth factor-1 receptor signaling pathways. **Toxicol Appl Pharmacol**, 272, n. 3, p. 637-646, Nov 1 2013.

IKEZUKI, Y.; TSUTSUMI, O.; TAKAI, Y.; KAMEI, Y. *et al.* Determination of bisphenol A concentrations in human biological fluids reveals significant early prenatal exposure. **Hum Reprod**, 17, n. 11, p. 2839-2841, Nov 2002.

INCA. Instituto Nacional do Câncer. Tumores das glândulas salivares. Rio de Janeiro, 2002.

JASO, J.; MALHOTRA, R. Adenoid cystic carcinoma. **Arch Pathol Lab Med**, 135, n. 4, p. 511-515, Apr 2011.

KANG, J. H.; KONDO, F.; KATAYAMA, Y. Human exposure to bisphenol A. **Toxicology**, 226, n. 2-3, p. 79-89, Sep 21 2006.

KANUGA, S. Bisphenol A (BPA) may be released in the oral cavity after sealant placement. **J Am Dent Assoc**, 145, n. 12, p. 1272-1273, Dec 2014.

KERI, R. A.; HO, S. M.; HUNT, P. A.; KNUDSEN, K. E. *et al.* An evaluation of evidence for the carcinogenic activity of bisphenol A. **Reprod Toxicol**, 24, n. 2, p. 240-252, Aug-Sep 2007.

KOLUDE, B.; ADISA, A.; ADEYEMI, B.; LAWAL, A. Immunohistochemical expression of oestrogen receptor-alpha and progesterone receptor in salivary gland tumours. **J Oral Pathol Med**, 42, n. 9, p. 716-719, Oct 2013.

LUZ, F. A. C. d.; SILVA, M. J. B. **Estudos in vitro das alterações causadas por duas drogas ubíquas: estudo da ação do bisfenol a, associado a medroxiprogesterona, em células mamárias não-transformadas e em tumorais de mama**. 2016. 98 f. (Mestrado) - Instituto de ciências biomédicas, Universidade Federal de Uberlândia.

MAJCHRZAK, E.; SZYBIAK, B.; WEGNER, A.; PIENKOWSKI, P. *et al.* Oral cavity and oropharyngeal squamous cell carcinoma in young adults: a review of the literature. **Radiol Oncol**, 48, n. 1, p. 1-10, Mar 2014.

MALLOZZI, M.; LEONE, C.; MANURITA, F.; BELLATI, F. *et al.* Endocrine Disrupting Chemicals and Endometrial Cancer: An Overview of Recent Laboratory Evidence and Epidemiological Studies. **Int J Environ Res Public Health**, 14, n. 3, Mar 22 2017.

MICHAL, M.; SKALOVA, A.; SIMPSON, R. H.; RASLAN, W. F. *et al.* Cribriform adenocarcinoma of the tongue: a hitherto unrecognized type of adenocarcinoma characteristically occurring in the tongue. **Histopathology**, 35, n. 6, p. 495-501, Dec 1999.

MICHALOWICZ, J. Bisphenol A--sources, toxicity and biotransformation. **Environ Toxicol Pharmacol**, 37, n. 2, p. 738-758, Mar 2014.

MOREIRA, M. A.; ANDRE, L. C.; CARDEAL ZDE, L. Analysis of plasticiser migration to meat roasted in plastic bags by SPME-GC/MS. **Food Chem**, 178, p. 195-200, Jul 1 2015.

MORIYAMA, K.; TAGAMI, T.; AKAMIZU, T.; USUI, T. *et al.* Thyroid hormone action is disrupted by bisphenol A as an antagonist. **J Clin Endocrinol Metab**, 87, n. 11, p. 5185-5190, Nov 2002.

MURASE, R.; SUMIDA, T.; ISHIKAWA, A.; MURASE, R. *et al.* Novel therapeutic strategies for malignant salivary gland tumors: lessons learned from breast cancer. **International journal of otolaryngology**, 2011, p. 187623-187623, 2011.

MURATA, M.; KANG, J. H. Bisphenol A (BPA) and cell signaling pathways. **Biotechnol Adv**, 36, n. 1, p. 311-327, Jan - Feb 2018.

NANJAPPA, M. K.; SIMON, L.; AKINGBEMI, B. T. The industrial chemical bisphenol A (BPA) interferes with proliferative activity and development of steroidogenic capacity in rat Leydig cells. **Biology of reproduction**, 86, n. 5, p. 135-112, 2012.

NEVILLE, B. W. **Oral and Maxillofacial Pathology**. Saunders/Elsevier, 2009. 9781416034353.

NEVILLE, B. W.; DAMM, D. D.; ALLEN, C. M.; BOUQUOT, J. **Oral and Maxillofacial Pathology**. Third ed. Saunders, St. Louis: Elsevier Health Sciences, 2009. 972 p. 9781437721973.

NEWBOLD, R. R.; JEFFERSON, W. N.; PADILLA-BANKS, E. Prenatal exposure to bisphenol a at environmentally relevant doses adversely affects the murine female reproductive tract later in life. **Environ Health Perspect**, 117, n. 6, p. 879-885, Jun 2009.

NOWAK-SLIWINSKA, P.; BALLINI, J. P.; WAGNIERES, G.; VAN DEN BERGH, H. Processing of fluorescence angiograms for the quantification of vascular effects induced by anti-angiogenic agents in the CAM model. **Microvasc Res**, 79, n. 1, p. 21-28, Jan 2010.

PISAPIA, L.; DEL POZZO, G.; BARBA, P.; CAPUTO, L. *et al.* Effects of some endocrine disruptors on cell cycle progression and murine dendritic cell differentiation. **Gen Comp Endocrinol**, 178, n. 1, p. 54-63, Aug 1 2012.

PRINS, G. S.; YE, S. H.; BIRCH, L.; HO, S. M. *et al.* Serum bisphenol A pharmacokinetics and prostate neoplastic responses following oral and subcutaneous exposures in neonatal Sprague-Dawley rats. **Reprod Toxicol**, 31, n. 1, p. 1-9, Jan 2011.

PUPO, M.; PISANO, A.; LAPPANO, R.; SANTOLLA, M. F. *et al.* Bisphenol A induces gene expression changes and proliferative effects through GPER in breast cancer cells and cancer-associated fibroblasts. **Environ Health Perspect**, 120, n. 8, p. 1177-1182, Aug 2012.

PYRIOCHOU, A.; TSIGKOS, S.; VASSILAKOPOULOS, T.; COTTIN, T. *et al.* Anti-angiogenic properties of a sulindac analogue. **Br J Pharmacol**, 152, n. 8, p. 1207-1214, Dec 2007.

REGEZI, J. A.; SCIUBBA, J. J.; JORDAN, R. C. K. **Oral Pathology: Clinical Pathologic Correlations**. Elsevier Health Sciences, 2012. 9781455702695.

RICHTER, C. A.; BIRNBAUM, L. S.; FARABOLLINI, F.; NEWBOLD, R. R. *et al.* In vivo effects of bisphenol A in laboratory rodent studies. **Reprod Toxicol**, 24, n. 2, p. 199-224, Aug-Sep 2007.

ROUTLEDGE, E. J.; WHITE, R.; PARKER, M. G.; SUMPTER, J. P. Differential effects of xenoestrogens on coactivator recruitment by estrogen receptor (ER) alpha and ERbeta. **J Biol Chem**, 275, n. 46, p. 35986-35993, Nov 17 2000.

SCREENING, U. S. E. P. A. E. D.; COMMITTEE, T. A. **Endocrine Disruptor Screening and Testing Advisory Committee (EDSTAC): final report**. Environmental Protection Agency, 1998. v. vol. 2).

SCULLY, C.; BAGAN, J. Oral squamous cell carcinoma: overview of current understanding of aetiopathogenesis and clinical implications. **Oral Dis**, 15, n. 6, p. 388-399, Sep 2009.

SEACHRIST, D. D.; BONK, K. W.; HO, S. M.; PRINS, G. S. *et al.* A review of the carcinogenic potential of bisphenol A. **Reprod Toxicol**, 59, p. 167-182, Jan 2016.

SHAFEI, A.; RAMZY, M. M.; HEGAZY, A. I.; HUSSENY, A. K. *et al.* The molecular mechanisms of action of the endocrine disrupting chemical bisphenol A in the development of cancer. **Gene**, 647, p. 235-243, Mar 20 2018.

SHEELER, C. Q.; DUDLEY, M. W.; KHAN, S. A. Environmental estrogens induce transcriptionally active estrogen receptor dimers in yeast: activity potentiated by the coactivator RIP140. **Environ Health Perspect**, 108, n. 2, p. 97-103, Feb 2000.

SIMPSON, R. H.; SKALOVA, A.; DI PALMA, S.; LEIVO, I. Recent advances in the diagnostic pathology of salivary carcinomas. **Virchows Arch**, 465, n. 4, p. 371-384, Oct 2014.

SPIRO, R. H. Salivary neoplasms: overview of a 35-year experience with 2,807 patients. **Head Neck Surg**, 8, n. 3, p. 177-184, Jan-Feb 1986.

SPRAGUE, B. L.; TRENTHAM-DIETZ, A.; HEDMAN, C. J.; WANG, J. *et al.* Circulating serum xenoestrogens and mammographic breast density. **Breast Cancer Res**, 15, n. 3, p. R45, May 27 2013.

SULTAN, I.; RODRIGUEZ-GALINDO, C.; AL-SHARABATI, S.; GUZZO, M. *et al.* Salivary gland carcinomas in children and adolescents: a population-based study, with comparison to adult cases. **Head Neck**, 33, n. 10, p. 1476-1481, Oct 2011.

TAKAHASHI, O.; OISHI, S. Disposition of orally administered 2,2-Bis(4-hydroxyphenyl)propane (Bisphenol A) in pregnant rats and the placental transfer to fetuses. **Environmental Health Perspectives**, 108, n. 10, p. 931-935, 2000.

TARAPORE, P.; YING, J.; OUYANG, B.; BURKE, B. *et al.* Exposure to bisphenol A correlates with early-onset prostate cancer and promotes centrosome amplification and anchorage-independent growth in vitro. **PLoS One**, 9, n. 3, p. e90332, 2014.

TRIANTAFILLIDOU, K.; DIMITRAKOPOULOS, J.; IORDANIDIS, F.; KOUFOGIANNIS, D. Mucoepidermoid carcinoma of minor salivary glands: a clinical study of 16 cases and review of the literature. **Oral Dis**, 12, n. 4, p. 364-370, Jul 2006.

VÄLIMAA, H.; SAVOLAINEN, S.; SOUKKA, T.; SILVONIEMI, P. *et al.* Estrogen receptor-beta is the predominant estrogen receptor subtype in human oral epithelium and salivary glands. **J Endocrinol**, 180, n. 1, p. 55-62, Jan 2004.

VANDENBERG, L. N.; HAUSER, R.; MARCUS, M.; OLEA, N. *et al.* Human exposure to bisphenol A (BPA). **Reprod Toxicol**, 24, n. 2, p. 139-177, Aug-Sep 2007.

VANDER POORTEN, V.; HUNT, J.; BRADLEY, P. J.; HAIGENTZ, M., Jr. *et al.* Recent trends in the management of minor salivary gland carcinoma. **Head Neck**, 36, n. 3, p. 444-455, Mar 2014.

WARNER, K. A.; ADAMS, A.; BERNARDI, L.; NOR, C. *et al.* Characterization of tumorigenic cell lines from the recurrence and lymph node metastasis of a human salivary mucoepidermoid carcinoma. **Oral Oncol**, 49, n. 11, p. 1059-1066, Nov 2013.

WETHERILL, Y. B.; FISHER, N. L.; STAUBACH, A.; DANIELSEN, M. *et al.* Xenoestrogen action in prostate cancer: pleiotropic effects dependent on androgen receptor status. **Cancer Res**, 65, n. 1, p. 54-65, Jan 1 2005.

ZALKO, D.; SOTO, A. M.; DOLO, L.; DORIO, C. *et al.* Biotransformations of bisphenol A in a mammalian model: answers and new questions raised by low-dose metabolic fate studies in pregnant CD1 mice. **Environ Health Perspect**, 111, n. 3, p. 309-319, Mar 2003.

ZHANG, K.-S.; CHEN, H.-Q.; CHEN, Y.-S.; QIU, K.-F. *et al.* Bisphenol A stimulates human lung cancer cell migration via upregulation of matrix metalloproteinases by

GPER/EGFR/ERK1/2 signal pathway. **Biomedicine & Pharmacotherapy**, 68, n. 8, p. 1037-1043, 2014/10/01/ 2014.

ZHANG, K. S.; CHEN, H. Q.; CHEN, Y. S.; QIU, K. F. *et al.* Bisphenol A stimulates human lung cancer cell migration via upregulation of matrix metalloproteinases by GPER/EGFR/ERK1/2 signal pathway. **Biomed Pharmacother**, 68, n. 8, p. 1037-1043, Oct 2014.

ZIV-GAL, A.; CRAIG, Z. R.; WANG, W.; FLAWS, J. A. Bisphenol A inhibits cultured mouse ovarian follicle growth partially via the aryl hydrocarbon receptor signaling pathway. **Reprod Toxicol**, 42, p. 58-67, Dec 2013.

ZOELLER, R. T. Environmental chemicals as thyroid hormone analogues: new studies indicate that thyroid hormone receptors are targets of industrial chemicals? **Mol Cell Endocrinol**, 242, n. 1-2, p. 10-15, Oct 20 2005.